

# **Interpretation of Long-Term Grande Ronde Aquifer Testing in the Palouse Basin of Idaho and Washington**

A Thesis

Presented in Partial Fulfillment of the Requirements for the

Degree of Master of Science

with a

Major in Hydrology

in the

College of Graduate Studies

University of Idaho

by

Kathryn Moran

August 2011

Major Professor: Dr. Gary S. Johnson, Ph.D.

## Authorization to Submit Thesis

This thesis of Kathryn Moran, submitted for the degree of Master of Science with a major in Hydrology and titled "Interpretation of Long-term Grande Ronde Aquifer Testing in the Palouse Basin of Idaho and Washington" has been reviewed in final form. Permission, as indicated by the signatures and dates given below, is now granted to submit final copies to the College of Graduate Studies for approval.

Major Professor \_\_\_\_\_ Date \_\_\_\_\_  
Gary S. Johnson, Ph.D.

Committee  
Members \_\_\_\_\_ Date \_\_\_\_\_  
Mickey Gunter, Ph.D.

\_\_\_\_\_  
Stanley M. Miller, Ph.D.

Department  
Administrator \_\_\_\_\_ Date \_\_\_\_\_  
Mickey E. Gunter, Ph.D.

Discipline's  
College Dean \_\_\_\_\_ Date \_\_\_\_\_  
Scott A. Wood, Ph.D.

Final Approval and Acceptance by the College of Graduate Studies

\_\_\_\_\_  
Jerry R. McMurtry, Ph.D.

## Abstract

Water levels in the Grande Ronde aquifer of the Palouse Basin have been declining since the initial development of the system in the early 1900s. This decline is of particular concern to local water suppliers and citizens because groundwater is the only significant water resource in this area. Historical data and continuing research have helped to characterize the area hydrogeology to a large extent, but several important features of the aquifer are unknown or uncertain, including aquifer boundaries, the source and quantity of recharge, and average storativity of the aquifer.

A long-term, basin-wide aquifer test was conducted in the Palouse Basin from November 2009 to December 2010, with the primary goals of assessing connections between wells, evaluating the leaky-aquifer conceptual model for the Grande Ronde aquifer, and estimating average aquifer storativity. A total of 19 pumping wells and 13 observation wells completed in the Grande Ronde aquifer were monitored to provide a comprehensive, long-term dataset for the Palouse Basin.

Direct examination of water level data and pumping data, as well as the results of analytical modeling, indicated direct hydraulic connection among wells in Pullman, Moscow, and Palouse. Analytical modeling was conducted using the full dataset for two observation wells; visual curve matching suggested that the Hantush-Jacob (1955) leaky-confined aquifer solution is appropriate for approximating observed water level drawdown on daily, weekly, and annual time scales. The average storativity of the Grande Ronde aquifer is estimated to be within the range of  $3 \times 10^{-5}$  to  $3 \times 10^{-4}$ , based on aquifer test results from previous investigations, analytical modeling of this test data, and interpretation of barometric effects on well water levels.

## Acknowledgements

Completion of this research would not have been possible without the support and guidance of many individuals. I would like to thank the Palouse Basin Aquifer Committee for funding this project and allowing me to use its equipment, and for providing an example of inter-governmental cooperation at its finest. The continual support of the water and public works departments of the cities of Moscow, Pullman, Colfax, and Palouse, as well as those of Washington State University and the University of Idaho, was incredible; thanks especially for accommodating my requests for changes to the normal pump operating routines, and allowing me to install additional equipment in your pump houses. Mike Dimmick, Terry Schierman, Andy Rogers, Bill Heiser, Don Myott, Tim Leachman, and Mike Holthaus: you all were amazingly helpful throughout the entire data collection process, and I wouldn't have been able to do any of this without your assistance. Thanks to Scotty Cornelius for allowing access to your domestic well, and to Guy Gregory for loaning equipment and helpful advice.

Thanks to Jim Osiensky for providing me with the opportunity to work on this project. Special thanks to Gary Johnson and my committee members, Mickey Gunter and Stan Miller, for your support. Additional appreciation goes out to Jerry Fairley for his insight in data analysis, and especially to Steve Robischon for his much-needed advice and support. Thanks to my fellow graduate students: Attila Felnagy for all of your time and effort working with me to collect and process the large quantities of data, and to Lauren Carey for your perspective and commiseration.

I would also like to thank Brian, for your constant encouragement and support.

## Table of Contents

<b>AUTHORIZATION TO SUBMIT THESIS.....</b>	<b>ii</b>
<b>ABSTRACT.....</b>	<b>iii</b>
<b>ACKNOWLEDGEMENTS .....</b>	<b>iv</b>
<b>TABLE OF CONTENTS.....</b>	<b>v</b>
<b>LIST OF TABLES.....</b>	<b>viii</b>
<b>LIST OF FIGURES.....</b>	<b>ix</b>
<b>CHAPTER 1 - BACKGROUND.....</b>	<b>1</b>
1.1 INTRODUCTION.....	1
1.2 DESCRIPTION OF STUDY AREA.....	1
Hydrologic history and groundwater monitoring.....	2
Geology.....	6
Hydrogeology .....	8
1.3 CONCEPTUAL MODELS .....	11
Boundaries and Basin Size.....	12
Regional Flow .....	13
Recharge.....	13
1.4 RESEARCH OBJECTIVES .....	14
<b>CHAPTER 2 - MATERIALS AND METHODS.....</b>	<b>16</b>
2.1 INTRODUCTION.....	16
2.2 MONITORING NETWORK AND EQUIPMENT.....	16
Water level data .....	16
Pumping data.....	18
Well location information.....	19
2.3 WATER LEVEL DATA PREPROCESSING .....	20
2.4 BAROMETRIC CORRECTION OF WATER LEVELS.....	20
Introduction to barometric pressure effects.....	21
Barometric efficiency vs. barometric response.....	22
BE estimation methods .....	23
Methodology for selection of BE estimation technique .....	27
Results of BE estimation for Grande Ronde monitoring wells .....	28

<b>CHAPTER 3 - CHARACTERIZATION OF BASIN WATER LEVELS .....</b>	<b>31</b>
3.1 INTRODUCTION.....	31
3.2 LOCAL GRADIENTS .....	31
3.3 SHORT-TERM BEHAVIOR AND WELL CONNECTIONS.....	33
Pullman-area wells .....	34
Moscow-area wells.....	37
Palouse-area wells.....	39
Colfax-area wells .....	39
Discussion of short-term responses .....	39
3.4 LARGE-SCALE FEATURES AND SEASONAL TRENDS.....	42
Investigation of water level fluctuations in WSU 5 .....	46
3.5 SUMMARY OF BASIN WATER LEVEL ANALYSIS RESULTS.....	51
<b>CHAPTER 4 - ANALYTICAL MODELING OF AQUIFER TEST DATA .....</b>	<b>52</b>
4.1 INTRODUCTION.....	52
4.2 DATASET PREPARATION FOR ANALYTICAL MODELING.....	52
4.3 ANALYTICAL MODELING OF THE 372-DAY TEST PERIOD.....	56
Palouse 3 .....	59
IDWR 4.....	62
Discussion of analytical modeling of 372-day period.....	65
4.4 INVESTIGATION OF LOW-LEVEL WATER LEVEL FEATURES IN DOE, IDWR 4, AND PALOUSE 3 .....	65
<b>CHAPTER 5 - ESTIMATION OF BASIN STORATIVITY.....</b>	<b>72</b>
5.1 INTRODUCTION.....	72
5.2 PREVIOUS RESEARCH.....	72
5.3 ESTIMATION OF AQUIFER STORATIVITY (S) FROM BAROMETRIC EFFICIENCY (BE) ..	74
5.4 ANALYTICAL MODELING STORATIVITY (S) ESTIMATES .....	75
5.5 IMPLICATIONS OF ESTIMATED STORATIVITY (S) VALUES.....	77
<b>CHAPTER 6 - CONCLUSIONS AND RECOMMENDATIONS.....</b>	<b>79</b>
6.1 INTRODUCTION.....	79
6.2 SPECIFIC CONCLUSIONS.....	79
Barometric efficiency.....	79
Well connections .....	79
Aquifer storativity.....	80
6.3 GENERAL CONCLUSIONS.....	80

6.4 REVIEW OF METHODOLOGY AND RECOMMENDATIONS FOR FUTURE WORK.....	81
Evaluation of methodology .....	81
Recommendations for further study.....	82
<b>REFERENCES.....</b>	<b>84</b>
<b>APPENDIX A: Water level data.....</b>	<b>89</b>
<b>APPENDIX B: HOBO data and other pumping data.....</b>	<b>89</b>
<b>APPENDIX C: Well location data.....</b>	<b>89</b>
<b>APPENDIX D: Recovery trend estimation and removal.....</b>	<b>90</b>
<b>APPENDIX E: Aqtesolv methods and solution description.....</b>	<b>94</b>

## List of Tables

Table 2.1 Monitoring wells and periods of data collection .....	17
Table 2.2 Basin pumping wells and pumping rates .....	19
Table 2.3. Estimated barometric efficiencies for Grande Ronde monitoring wells .....	29
Table 2.4. Compiled BE estimates .....	30
Table 4.1 Early-test pumping periods, through 1.6 days elapsed time .....	68
Table 4.2. Estimated aquifer parameters .....	70
Table 5.1. Grande Ronde aquifer storativity estimates from previous investigations .....	73
Table 5.2. Sample Grande Ronde aquifer S estimated from BE .....	75
Table 5.3. Aquifer test estimated S values .....	77

## List of Figures

Figure 1.1. Map of Palouse Basin.....	2
Figure 1.2. Plot of historical declines in WSU Test well water levels .....	3
Figure 1.3. Pullman-area wells. ....	4
Figure 1.4. Moscow-area wells and the DOE well. ....	5
Figure 1.5. Palouse-area wells. ....	5
Figure 1.6. Colfax-area wells.....	6
Figure 1.7. General stratigraphic column of the Palouse Basin .....	7
Figure 1.8 East-west geologic cross section. ....	9
Figure 2.1. Barometric pressure (relative scale) measured at the WSU Test well.....	21
Figure 2.2. Example plot of relative water levels vs. BE-corrected water levels .....	24
Figure 2.3. Example BETCO user interface .....	27
Figure 3.1. Groundwater elevations for selected Palouse Basin wells .....	32
Figure 3.2. WSU 7 well connections .....	35
Figure 3.3. Pullman 4 well connections .....	35
Figure 3.4. WSU Test well connections .....	36
Figure 3.5. WSU 8 well connections .....	37
Figure 3.6. IDWR 4 well connections .....	38
Figure 3.7. DOE well connections .....	38
Figure 3.8. Comparison of well completion zones and subsurface geology .....	42
Figure 3.9. Plot of relative water levels for selected Palouse Basin wells.....	43
Figure 3.10. Winter/Spring relative water levels for selected wells .....	44
Figure 3.11. Clay Street groundwater elevations .....	45
Figure 3.12. Basin pumping over time (through 300 days elapsed time) .....	47
Figure 3.13. Changes in Moscow-Pullman pumping relative to offseason pumping.....	48
Figure 3.14. WSU 5 water level fluctuations vs. changes in pumping.....	49
Figure 3.15. Changes in pumping vs. WSU 5 water levels for the first 200 days .....	50
Figure 4.1. Removal of water level recovery trend from Palouse 1 water levels .....	54
Figure 4.2. Simulated basin boundaries for AQTESOLV .....	57

Figure 4.3. Palouse 3 adjusted drawdown vs. model-predicted drawdown.....	60
Figure 4.4. IDWR 4 adjusted drawdown vs. model-predicted drawdown .....	63
Figure 4.5. Examination of low-magnitude features in observed well water levels.....	66
Figure 4.6. Early adjusted drawdown in Palouse 3 and IDWR 4 .....	68
Figure 4.7. Early-time adjusted drawdown in Palouse 3, Palouse 1, and IDWR 4 .....	69

## Chapter 1 - Background

### 1.1 Introduction

The Palouse region of northwestern Idaho and eastern Washington includes the cities of Moscow, ID; Pullman, WA; Colfax, WA; Palouse, WA; and surrounding rural areas, as well as Washington State University (WSU) and the University of Idaho (UI). Due to limited rainfall and surface water, groundwater is the primary water resource in the area, with the Grande Ronde aquifer providing the majority of municipal supplies. Potentiometric heads in production wells and observation wells have consistently declined at rates up to 0.5 meters/year following the initial development of the aquifer. The continuing groundwater declines due to pumping withdrawals have prompted numerous studies to investigate aquifer characteristics and provide information for water resource management and planning.

### 1.2 Description of study area

The Palouse Basin (Figure 1.1) is a groundwater basin located within the larger Palouse region of eastern Washington and adjoining areas of Idaho. The Palouse is an important dryland agricultural region, with a semi-arid climate (approximately 75 cm of annual precipitation) and topography dominated by rolling hills composed predominantly of windblown glacial silt (loess). A larger amount of precipitation (approx 100 cm a year) falls in the mountainous terrain which bounds the study area to the east, southeast, and north. The Palouse River, its tributaries, and other local streams drain the area and flow towards the northwest to eventually join the Snake River. The study area encompasses the cities of Pullman, Colfax, Palouse, and Moscow, and multiple smaller communities and rural areas, as well as two large universities, with an estimated total population of approximately 60,000 (PBAC, 2010).

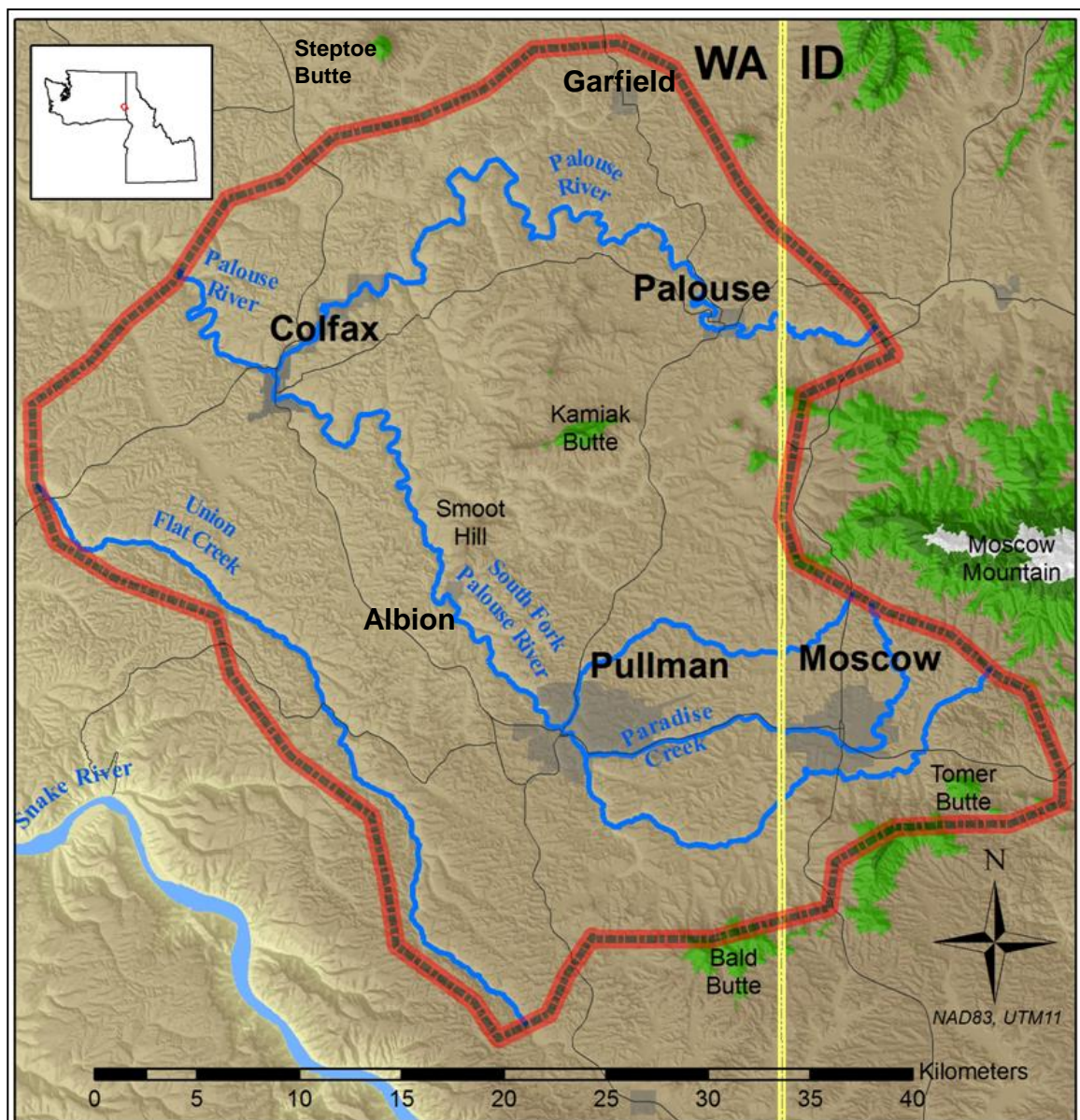


Figure 1.1. Map of Palouse Basin (modified from Bush, 2006).

### Hydrologic history and groundwater monitoring

The first wells in the Moscow-Pullman area were constructed in the 1890s. Many of the original wells were initially flowing, but water levels soon began to decline, and by the 1950s and 60s water levels in the Wanapum aquifer had declined by over 15 m (PBAC, 2010). At this time, additional, deeper wells were drilled into the Grande Ronde aquifer. Water levels in the Grande Ronde aquifer fell as development of the aquifer

continued, while Wanapum levels rebounded somewhat due to reduced pumping of that aquifer in favor of increased dependence on the Grande Ronde aquifer as the primary source of water. Records from a basin monitoring well indicate that Grande Ronde water levels have declined at rates between 0.9 and 1.5 ft (0.3 and 0.5 m) per year from 1935 to 2010 (Figure 1.2). Water level declines exhibit a seasonal pattern, based on changes in water demand. Water levels in both the Wanapum and Grande Ronde fall during the summer, and typically recover somewhat throughout the autumn, winter, and spring seasons (offseason). Large-volume groundwater pumping for municipal supplies is conducted by water utilities in Pullman, Moscow, Colfax, and Palouse, and by the University of Idaho (UI) and Washington State University (WSU). A total of 2.38 billion gallons of water were pumped from the Grande Ronde aquifer in 2009 by these entities, with an additional 302 million gallons pumped from the Wanapum aquifer by two Moscow wells (PBAC, 2010).

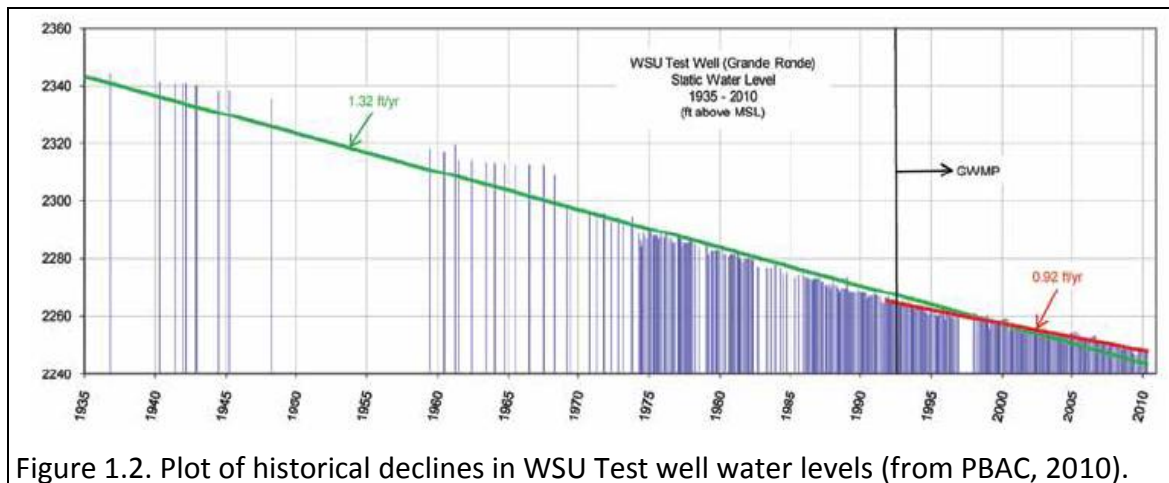
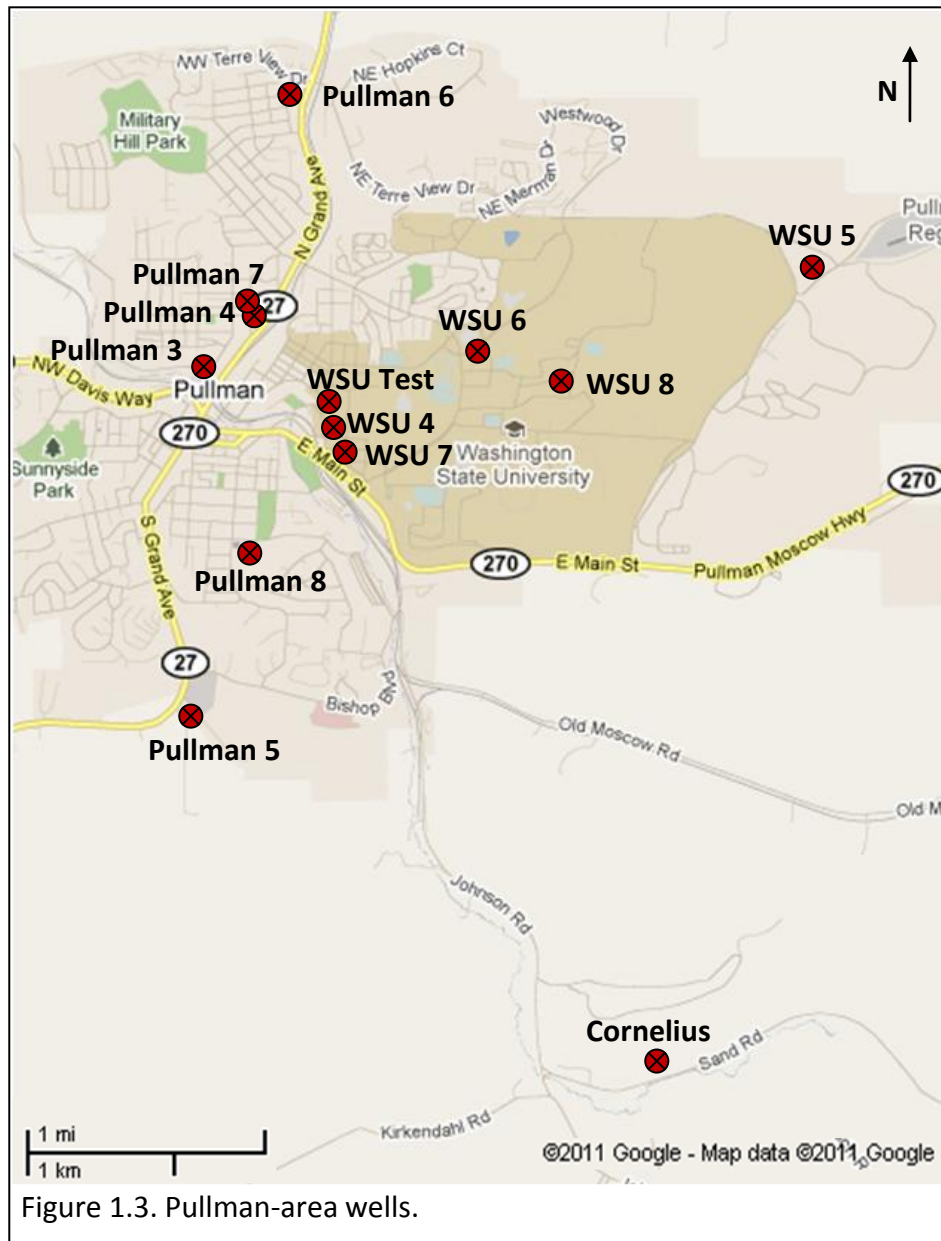


Figure 1.2. Plot of historical declines in WSU Test well water levels (from PBAC, 2010).

The Palouse Basin Aquifer Committee (PBAC) is an organization composed of representatives from the municipalities, universities, and counties (Latah County, ID and Whitman County, WA) located within the Palouse Basin. PBAC facilitates collaborative water resource planning, organizes and funds hydrologic research, maintains groundwater monitoring networks, and compiles groundwater and pumping data for the entire basin. Many of the observation wells and pumping wells included in this thesis investigation are part of the PBAC groundwater monitoring network. Specific locations

of the Pullman, Moscow, and Palouse groundwater wells monitored during this investigation are shown in Figures 1.3, 1.4, and 1.5, respectively.



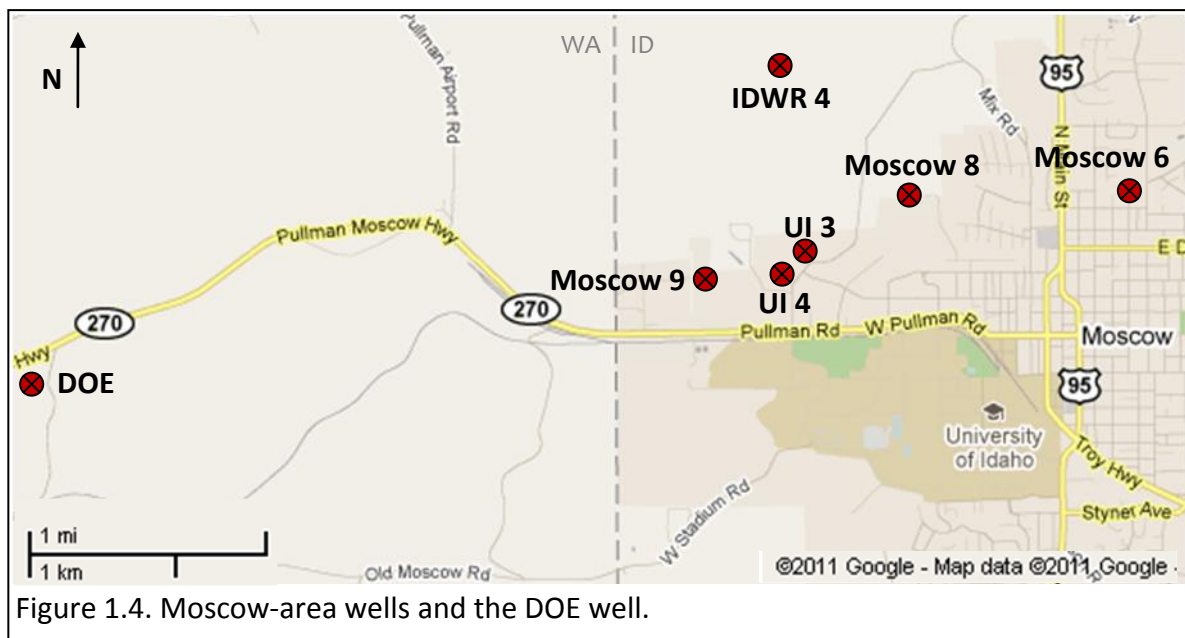


Figure 1.4. Moscow-area wells and the DOE well.

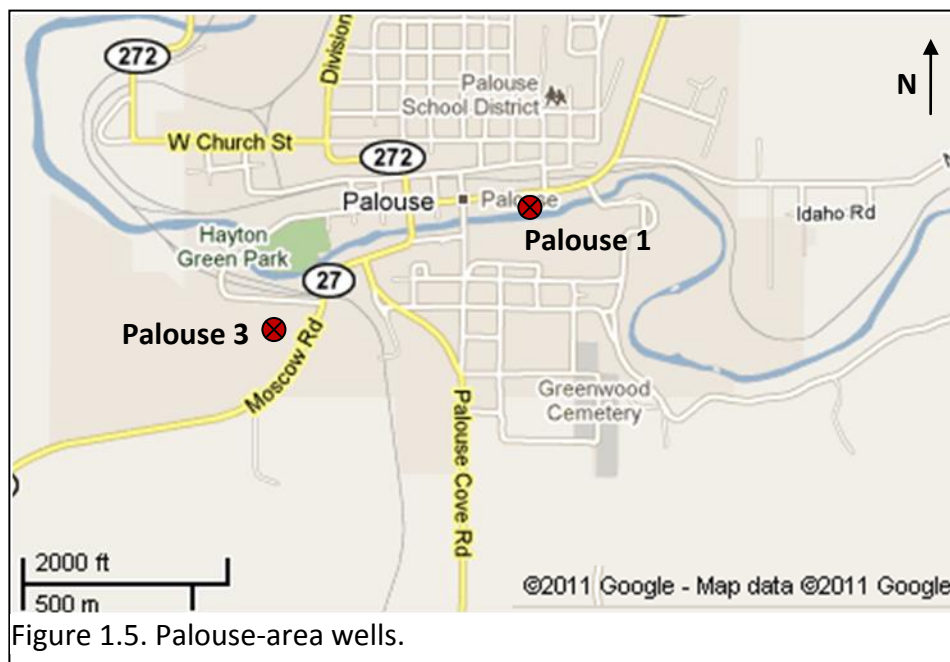


Figure 1.5. Palouse-area wells.

Groundwater monitoring data for the vicinity of Colfax, WA, were collected during this study. The city of Colfax is located approximately 24 km northwest of Pullman, WA, at an elevation of approximately 600 m AMSL. Two wells located ten kilometers northeast of Colfax, Glenwood 1 and Glenwood 2, provide the majority of the city's water (Figure 1.6). The Glenwood wells were constructed in 1915 and 1927 to depths of approximately 34 m bgs; these wells currently are free-flowing artesian wells that flow

directly into underground supply pipes located 1.5-2.5 m bgs. Two pumped wells within the city limits supplement the Glenwood supply during periods of high summertime demand. The Clay Street and Fairview wells were completed in 1949 and 1954, respectively. New access ports were drilled into the foundations of these turbine pumps in 2009 by the city of Colfax to allow manual measurement of water levels. A dedicated transducer was also installed in the Clay Street well at that time.

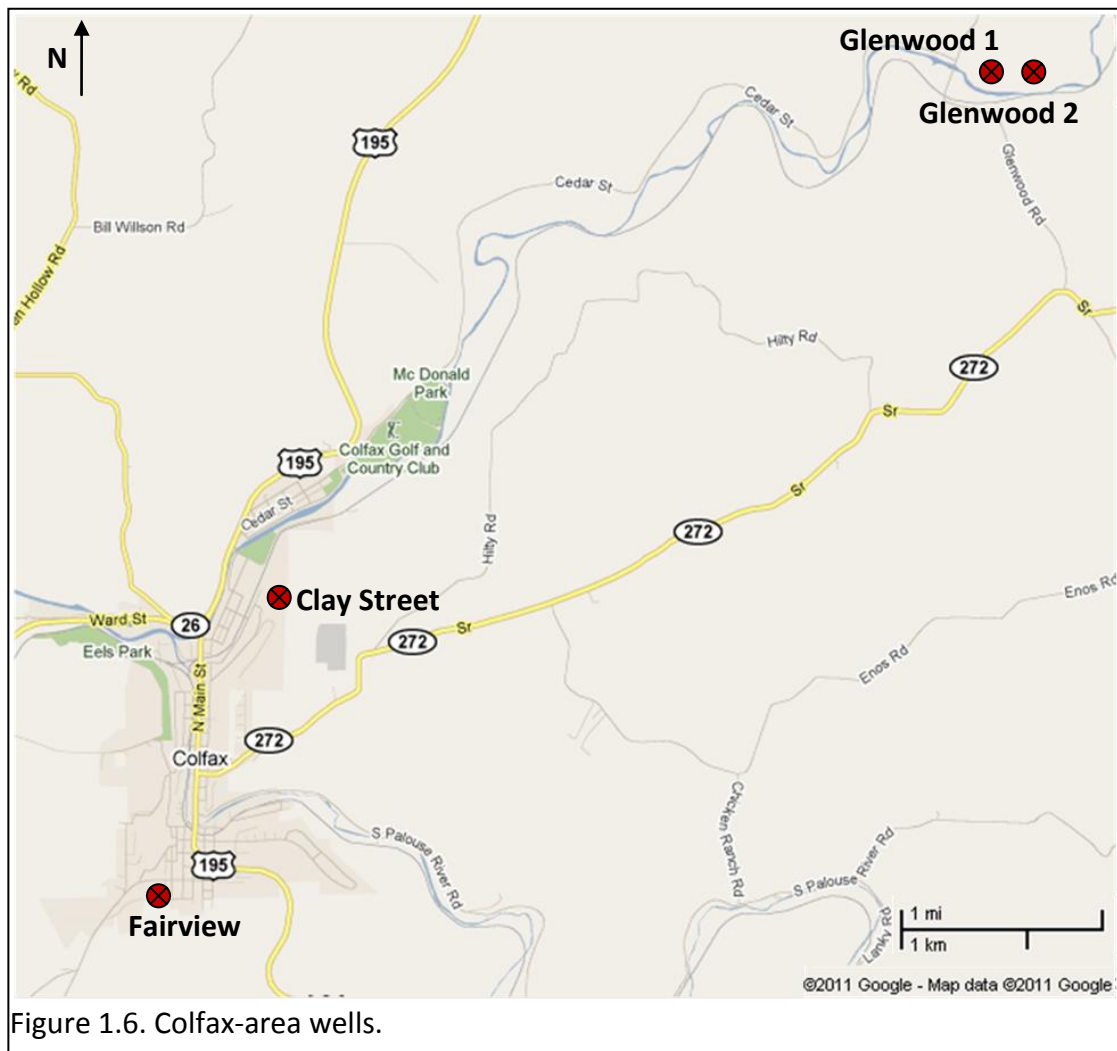


Figure 1.6. Colfax-area wells.

### Geology

The geology of the Palouse region is generally comprised of flood basalts and associated interbedded fluvial sediments which overlie older crystalline basement rocks. The area is overlain by windblown glacial silt (loess) of the Palouse Formation, except

where it has been removed by erosion. The Palouse Basin is located on the eastern margin of the Columbia Plateau, which is dominated geologically by the Columbia River Basalt Group (CRBG), a series of Miocene flood basalts that originated from fissures and/or dikes primarily in southeast Washington and northeast Oregon. Four formations of the CRBG have been identified in the Palouse Basin: the Imnaha, Grande Ronde, Wanapum, and Saddle Mountains. The Imnaha is the oldest of the basalts, and was encountered during the drilling of the WSU 7 well borehole at approximately 1882 ft (574 m) below ground surface (bgs) (Ralston, 1987). Most of the basalt found in the Palouse Basin is from the Grande Ronde Formation and Wanapum Formation. The Saddle Mountains basalts are the youngest of the CRBG, but are locally discontinuous and not believed to be significant relative to the hydrogeology of the basin. Evidence for post-emplacement structural deformation has been identified in basalts within the Palouse Basin, with the primary features comprised of northwest-trending folds (Bush, 2005).

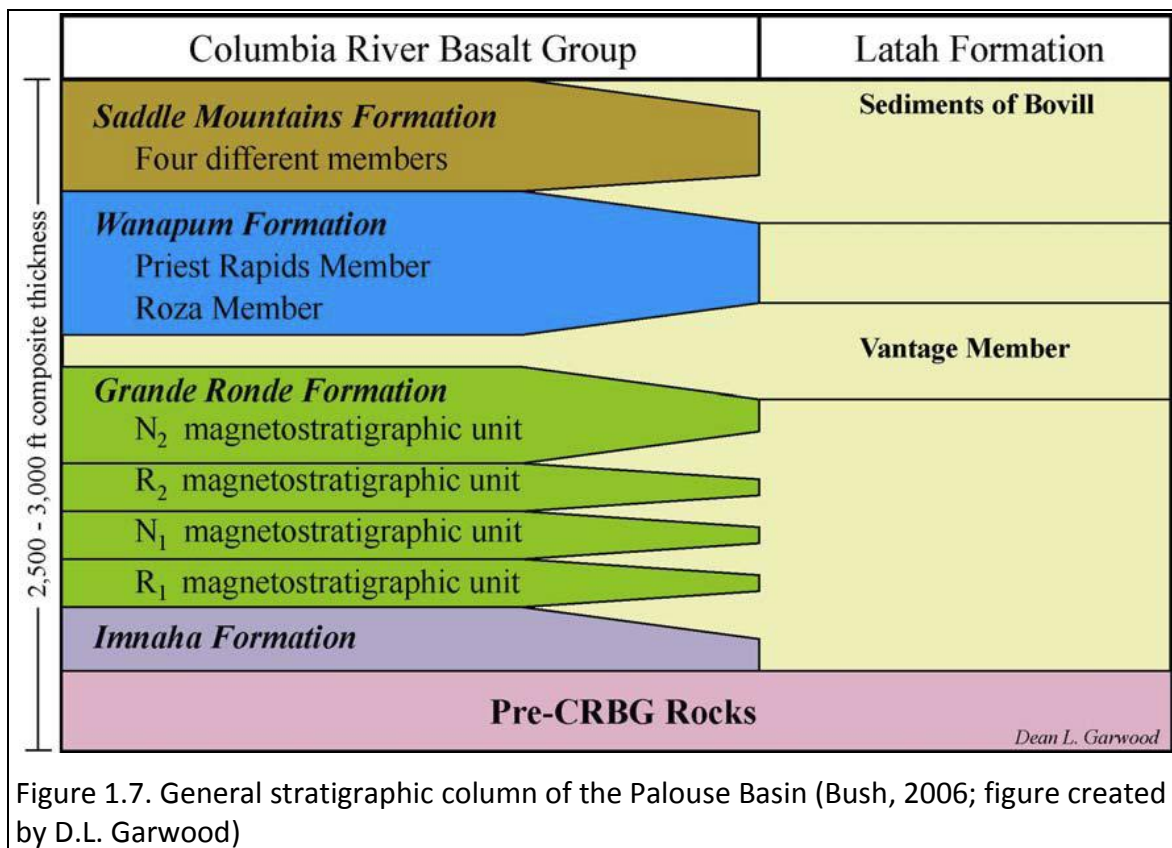


Figure 1.7. General stratigraphic column of the Palouse Basin (Bush, 2006; figure created by D.L. Garwood)

Basalt flows in the Palouse Basin are not horizontal, but dip slightly to the east between Pullman and Moscow (Bush, 2005).

The Grande Ronde was emplaced as a series of individual flows, with fluvial and/or lacustrine sediments and paleosols deposited between layers of basalt in places. These sediments were derived from erosion of the basalts themselves as well as from the crystalline rocks which form the topographic high points. Grain sizes vary from cobbles to clays. The thicknesses of these sediment interbeds are variable, with thickness increasing with proximity to the source basement rocks. In Moscow, these sediments are mapped as the Latah Formation; in the Moscow and Palouse areas, the thickest section is known as the Vantage Equivalent (corresponds to the Vantage Member of the Ellensburg Formation in central Washington), and is located stratigraphically between the uppermost Grande Ronde flow and the bottom of the Wanapum Formation (Bush, 2005; Bush and Garwood, 2006). Figure 1.8 presents an east-west cross-section illustrating differences in subsurface geology across the basin.

### Hydrogeology

The two primary aquifer systems in the Palouse Basin are the Grande Ronde aquifer and the Wanapum aquifer, which loosely correspond stratigraphically to the basalt formations of the same name. Wells completed into the Sediments of Bovill, the Palouse Formation, or the older crystalline rocks are not very productive and these aquifers are not significant on a regional scale. Both the Wanapum and Grande Ronde aquifers are considered to be confined. The Grande Ronde aquifer system is often referenced as the Grande Ronde aquifer due to the hydraulic connection between its discrete producing zones, or as the lower aquifer; however, in this thesis it will be referred to as the Grande Ronde aquifer, or simply as the Grande Ronde. Accordingly, the upper aquifer system will be referred to as the Wanapum aquifer instead of the Wanapum aquifer system.

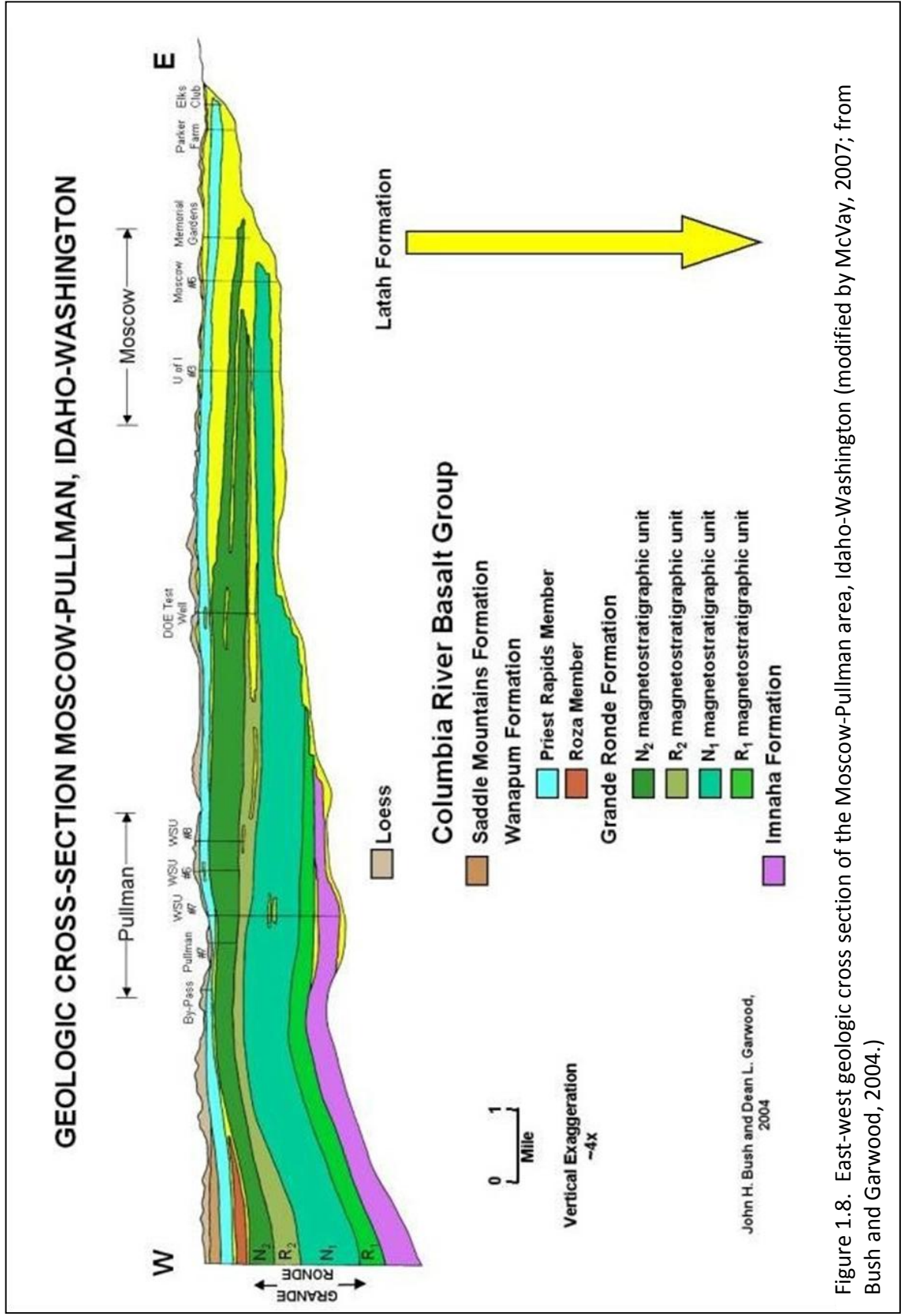


Figure 1.8. East-west geologic cross section of the Moscow-Pullman area, Idaho-Washington (modified by McVay, 2007; from Bush and Garwood, 2004.)

In the Moscow area, the Wanapum aquifer was developed first due to its shallower depth, but it is thinner, less productive overall, and contains water of lower quality than the Grande Ronde aquifer. Also in the Moscow area, hydraulic connection between the Wanapum basalt and the substantial Vantage Member of the Latah Formation makes the Wanapum aquifer an important groundwater resource, with two city of Moscow municipal wells currently producing from the aquifer; however, the thickness of the Vantage sediments decreases significantly westward and limits the Wanapum aquifer's utility in Washington as a productive water source. The Vantage is also vertically extensive in the vicinity of Palouse (Bush et al., 2001). Recent head measurements within the Wanapum aquifer indicate a potentiometric surface elevation of approximately 756 m above mean sea level (AMSL) in the Moscow area.

The vertical extent of the Grande Ronde aquifer has been established based on information obtained during well drilling (Figure 1.7). The top of the aquifer occurs at the base of the uppermost Grande Ronde basalt flow, where significant head declines were documented in well construction reports (Ralston, 1987; Brown, 1976). The dense interior of the uppermost Grande Ronde basalt flow, along with the overlying fine-grained sediments of the Vantage equivalent and a weathered saprolitic surface, are presumed to form the aquitard that separates the Wanapum and Grande Ronde aquifers (Bush, 2005). The bottom of the Grande Ronde aquifer is thought to coincide with the base of the Grande Ronde Formation; a 1.5 m drop in head was measured between the base of the deepest Grande Ronde flow and 50 m into the Imnaha Formation during the drilling of WSU 7 (Ralston, 1987). Aquifer thickness ranges from 200 m or less below Moscow to approximately 500 m in Pullman. Current head measurements indicate that the potentiometric surface of the Grande Ronde in Moscow and Pullman is approximately 684 m AMSL.

Groundwater flow in layered basalt aquifers occurs predominantly within the permeable zones of rubbled basalt flow tops (or bottoms), and/or within interbedded sediments between individual flows, which are estimated at 5% to 10% of the vertical sequence in the CRBG; production zones within the Grande Ronde are usually vertically

separated (US DOE, 1986). Flowpaths between producing zones may be present in the form of fractures of variable extent, or occur at rubble zones along the edges of basalt flows or at intersections between flow lobes. Typically, the dense interiors of individual basalt flows are considered to form aquitards.

It is important to note the distinction between geologic features and hydrogeologic properties. The hydrogeology of the Palouse Basin is not consistently controlled by structural or stratigraphic variations. Evidence for structural folding and faulting does not always indicate the presence of either hydraulic barriers or connections; many features are ambiguous in their relation to hydraulic conductivity. Variations in the composition and extent of fluvial sediments between individual basalt flows means that in some locations, sediment interbeds are producing zones, while in other locations, they may form aquitards. Some differences in the geology of the Grande Ronde and Wanapum basalts between Moscow and Pullman have implications on the hydrogeology of both aquifers. Individual basalt flows within the Grande Ronde are less continuous in Moscow than in Pullman. In Moscow, flows are likely more irregular, with rubble zones at horizontal intersections between flow lobes, and sediment interbeds may be more heterogeneous (Brown, 1976).

### 1.3 Conceptual models

Perceptions and conceptual models for the Grande Ronde aquifer and the Palouse Basin in general have evolved considerably over time as additional hydrogeologic information has become available, and as the system has responded to continued stress from pumping. Many of the most important characteristics about the Grande Ronde aquifer are uncertain, including 1) its extent and boundaries, 2) the degree of connection between various areas, 3) the sources and magnitudes of recharge and surface water/groundwater interaction, and 4) the direction and magnitude of regional flow systems.

### Boundaries and Basin Size

The boundaries of the Grande Ronde aquifer, and its overall size, are relatively uncertain. To the east and south, the sloping contacts between basement igneous and metamorphic rocks and overlying sediments and basalts are assumed to form an irregular hydraulic boundary; however, the western and northern extents of the basin are poorly defined and/or unknown. The approximate size of the Palouse Basin (500 mi<sup>2</sup>, or 1300 km<sup>2</sup>) as depicted in Figure 1.1 is only an estimate, and is based on political and water-use demarcations as much as hydrogeologic research (Bush, 2005). It includes the surface water drainage basins of the upper Palouse River and its tributaries as well as parts of the Union Flat Creek drainage. The primary reason for a lack of definitive basin boundaries is a paucity of deep monitoring wells outside of the municipal centers. Kamiak Butte and Smoot Hill represent “islands” of low hydraulic conductivity basement rock within the basin.

Within the context of available data, hydraulic connectivity between the municipal centers has been well debated, with presentation of contradictory evidence. Hydraulic connection between Palouse and the rest of the basin through the Kamiak Gap has been investigated on a geophysical basis by several researchers. The Kamiak Gap is defined as the area between Kamiak Butte and Angel Butte. Klein et al. (1987) and Holom (2006) employed magnetics and gravity methods, respectively, to evaluate the stratigraphy within the Gap. Their results were not congruent, with Klein et al (1987) interpreting continuity of the Grande Ronde Formation, and Holom (2006) suggesting that the Grande Ronde was interrupted by a saddle of crystalline basement rock. An aquifer pump test conducted in Palouse suggested the presence of negative (no-flow) boundaries in the vicinity (Ralston, 2000). However, it is unknown if the indicated boundaries included an obstruction south of Palouse.

Previous investigators have divided the basin up into a number of sub-basins defined by geography and geologic distinctions; the discussion of sub-basins is not included in this thesis in an attempt to minimize external influence on qualifying observed hydrologic data.

### Regional Flow

Regional studies of the Columbia River Basalt Group indicate that groundwater flows from the edges of the Columbia Plateau towards the center within the Wanapum and Grande Ronde basalts. Additional regional flow may occur along structural discontinuities between aquifers or sub-basins (US DOE, 1986). In general, groundwater elevations in the Grande Ronde decrease to the south and west, but the spatially limited groundwater elevation data in the Palouse Basin make it impossible to define the direction and magnitude of outflow. Evidence of northwest-trending structural deformations in the basalts indicate that the overall direction of groundwater flow might be to the northwest (Bush, 2005); however, few data are available to confirm this hypothesis.

### Recharge

The long-term head declines measured in basin wells indicate that pumping plus natural discharge from the Grande Ronde aquifer exceeds recharge. However, the mechanisms and magnitudes of recharge to the aquifer have not been confidently delineated despite decades of research. Recharge is possible from direct infiltration of precipitation or seepage from surface water (streams). Potential pathways for recharge include vertical flux through overlying material, and seepage entering the aquifer from the sides and base by passing through Latah Formation sediments along the boundary with crystalline rocks. It is difficult to quantify vertical flux through the aquitard separating the Wanapum and Grande Ronde due to the lack of defensible hydrologic data characterizing the aquitard. Calculation of recharge based on a water-budget model is also problematic because of similar uncertainty in the quantity and locations of local and regional discharge.

Potential for seepage into the Latah Formation sediments along part of the eastern aquifer boundary was investigated by Fairley et al. (2006) through direct sampling of subsurface materials; the results of this study suggested that the potential for recharge in this area would be greatly impeded by low-hydraulic-conductivity silt and

clay layers. However, the spatial extent of the study was limited. It is certain that a significant vertical gradient exists between the Wanapum and Grande Ronde aquifers, and a recent PBAC-funded analysis of previous research reports that “the dominant source of recharge is expected to be leakage from the upper aquifer” (TerraGraphics, 2011, p. 58). Investigations of recharge based on groundwater age dates have been conducted by several researchers (Crosby and Chatters, 1965; Larson, 2000; Douglas, 2004), with generally consistent results indicating the presence of predominantly old water (up to 30,000 years old), and correspondingly long residence times associated with low annual recharge rates to the Grande Ronde aquifer.

#### 1.4 Research objectives

This study involved conducting a basin-wide aquifer test of the Grande Ronde aquifer starting at 21:50 on 11/24/2009, and continuing for 372 days. The primary objective was to investigate the comprehensive data set to glean new information on the behavior and hydraulic properties of the system. A secondary aim was to provide an estimate of the storativity of the Grande Ronde, and to improve on previous estimates by compiling more detailed pumping and water level data over a longer time period. Analysis of aquifer test data was focused towards providing preliminary responses to the following questions:

- How do water levels respond to individual pumping episodes as well as long-term stresses?
- Do water levels in Palouse respond to pumping in Pullman and Moscow?
- Do water levels in Colfax respond to pumping in Pullman and Moscow?
- What is the overall storativity of the Grande Ronde aquifer? What implications does this have for estimating basin size?
- What is the source and magnitude of recharge to the Grande Ronde aquifer?

This thesis is organized into several chapters. Chapter 2, Materials and Methods, describes the monitoring network and procedures followed for compiling water level data and pumping data, and accounting for barometric responses. Chapter 3, Characterization of Basin Water Levels, identifies connections between individual wells, and assesses long-term and seasonal trends within water level data. Chapter 4, Analytical Modeling of Aquifer Test Data, outlines the procedure for processing observation well drawdown data to prepare them for analytical modeling input, develops the leaky-aquifer conceptual model, and includes estimates of aquifer parameters based on interpretation of the aquifer test data. Approaches to estimating the aquifer storativity of the Grande Ronde are described in Chapter 5, Estimation of Basin Storativity. Chapter 6, Conclusions, summarizes observations from the previous sections and relates the conclusions of this study to the larger context of research on the Palouse Basin.

## Chapter 2 - Materials and Methods

### 2.1 Introduction

This chapter introduces the types of data used in this study, describes the data collection network, and delineates the time periods of data collection. Procedures followed for processing and compiling water levels and pumping data, and the step-by-step details for removing barometric effects from water level data, are also discussed.

### 2.2 Monitoring network and equipment

Groundwater levels and municipal pumping schedules were recorded for wells within the Palouse Basin from November 2009 through November 2010. Existing information on well locations and wellhead elevations was required to convert well water levels to groundwater elevations; municipal pumping schedules and well pumping rates were also used to confirm the accuracy of independently-collected information on well pumping on/off times.

#### Water level data

Thirteen wells completed within the Grande Ronde aquifer were instrumented for continuous water level monitoring (Table 2.1). These wells were selected based on availability, access and location. Non-vented Solinst pressure transducers (Levelloggers®) were deployed below the static water level at known depths in ten wells to measure absolute head on 5-minute time increments. Water levels in Palouse 1 were recorded at the same frequency by a Schlumberger Micro-Diver® direct read data logger. A Druck vented pressure transducer was deployed in the city of Colfax Clay Street well with data recorded by a Campbell Scientific PST 8/3 Pump and Slug Test System® data logger; water levels measured in this well were collected and recorded on an irregular time interval of approximately 2.5 hours.

Barometric pressure was recorded on 5-minute time intervals by three Solinst Barologgers<sup>®</sup> located in a well house (Palouse 1)(Figure 1.5) or suspended in well casings above the water level (WSU Test and IDWR 1)(Figure 1.3 and Figure 1.4, respectively). Levelogger and Barologger pressures were recorded in units of feet of water. Manual depth-to-water measurements were collected with a steel tape or electronic sounder. The same electric sounder, an In-Situ<sup>®</sup> Inc. meter with 400 ft of tape, was used for all manual measurements in Palouse, Pullman, and Moscow, to ensure consistency. Recorded water level data and manual measurements are presented in Appendix A.

Additional water level data (airline and pressure transducer) were collected by each pumping entity, typically on a daily basis, and compiled by PBAC. These levels were rarely used with the exception of the Clay Street bubbler (airline) levels compiled by the city of Colfax. The Clay Street airline data were used to corroborate the data collected by the Druck transducer and “fill in” the period of missing measurements from May and June 2009, when the initial transducer failed and was subsequently replaced (Table 2.1).

Table 2.1 Monitoring wells and periods of data collection

Well ID	Start	End	Gaps	Explanation for reduced period of monitoring
Clay Street	11/20/09 10:40	12/7/10 4:44	5/6/10: 6/29/10	transducer failure
Cornelius	11/10/09 16:30	12/3/10 8:35		
DOE	11/11/09 11:45	12/3/10 8:00		
IDWR 4	11/16/09 13:00	12/2/10 9:30		
Palouse 1	11/10/09 9:00	10/1/10 7:45		access tube obstructed following pump maintenance
Palouse 3	11/10/09 9:00	12/2/10 8:15		
Pullman 4	12/17/09 8:50	2/23/10 8:45		obstructed access tube
Pullman 6	11/10/09 15:00	3/26/10 12:15		replacement of pump
Pullman 8	11/11/09 11:00	2/23/10 9:30		installation of pump
WSU 5	11/11/09 9:45	12/3/10 10:25		
WSU 7	11/23/09 8:50	12/3/10 11:20	12/17/09: 1/29/10	pump maintenance
WSU 8	11/23/09 10:05	12/3/10 10:50		
WSU Test	11/11/09 8:35	12/3/10 12:00		

### Pumping data

Researchers conducting previous aquifer tests in the Palouse Basin have emphasized the need to collect more accurate pump on/off timing data for municipal pumping. The large scope and duration of this aquifer test, and the subsequent need for compatible data formatting among the different water utilities, necessitated the use of external pump monitors operating independently of in-place monitoring systems. HOBO® U9 Motor On/Off Data Loggers (HOBOs®), manufactured by Onset Computer Corporation, were tested and installed on each of the municipal pumps within the Palouse Basin, with the exception of smaller pumps in the towns of Albion, WA, and Garfield, WA (Table 2.2). These devices sense the presence or absence of the electromagnetic field generated by a turbine pump motor or the electrical wiring leading to a down-hole submersible pump, and record periods of pump activity accurate to a time increment of one second (HOBO® product manual, 2010). Simultaneous monitoring of each of the municipal wells completed in the Grande Ronde aquifer precluded problems encountered in previous pump test interpretations that resulted from incomplete knowledge of pumping activity in non-targeted wells.

Additional pumping data were recorded by municipal well operators and compiled by PBAC. Monthly pumping totals provided by each agency were used along with HOBO® data to calculate pumping rates for each well (Calculated Average Rate column in Table 2.2), along with the standard pumping rates estimated by operators for each well. Comparison of total pumping durations recorded by the HOBO® loggers to pumping totals recorded by each municipality was also useful for revealing periods of HOBO® malfunction. Any identified “missing” periods within the HOBO® pumping record (due primarily to problems with HOBO placement) were restored using daily or monthly totals provided by each pumping agency. Motor on/off data and details of HOBO data processing are presented in Appendix B.

Table 2.2 Basin pumping wells and pumping rates

City	Well	Estimated Rate (gpm)	Calculated Average Rate (gpm)
Moscow	6	1015	1006
	8	950	944
	9	2100	2028
WSU	4	1400	1440
	6	1050	
	7	2700	
	8	2400	2392
Pullman	3	650	591
	5	1600	1683
	6	600	631
	7	1750	1752
	8	1900	1921
UI	4	2000	
Palouse	1	725	719
	3	800	734
Colfax	Fairview	625	650
	Clay Street	500	453
	Glenwood 1	555	
	Glenwood 2	555	

Colfax city wells Glenwood 1 and 2 are flowing wells without pumps. HOBOS<sup>®</sup> were installed on two booster pumps in the Clay Street well house which distribute water from a gravity line (from the Glenwood wells) into the city water system. Therefore, Glenwood HOBOS<sup>®</sup> data are only an approximate measure of groundwater withdrawals at the Glenwood wells. Leaks are known to occur in the 10 km pipeline between the Clay Street well house and the Glenwood wells. The amount of this leakage has not been quantified, but it is probable that calculations based on the Glenwood HOBOS<sup>®</sup> data may be underestimating the total withdrawals from groundwater.

#### Well location information

Existing surveyed coordinates and elevations were compiled for each pumping well and monitoring well (Appendix C). No new position data were collected during this

study. The original source (or best available source) of survey data is noted, with a secondary source substituted in cases where the primary citation was unknown or unavailable. Eastings (x) and northings (y) were confirmed for each well within several meters using Google Earth® to visually identify the positions of existing well houses.

### 2.3 Water level data preprocessing

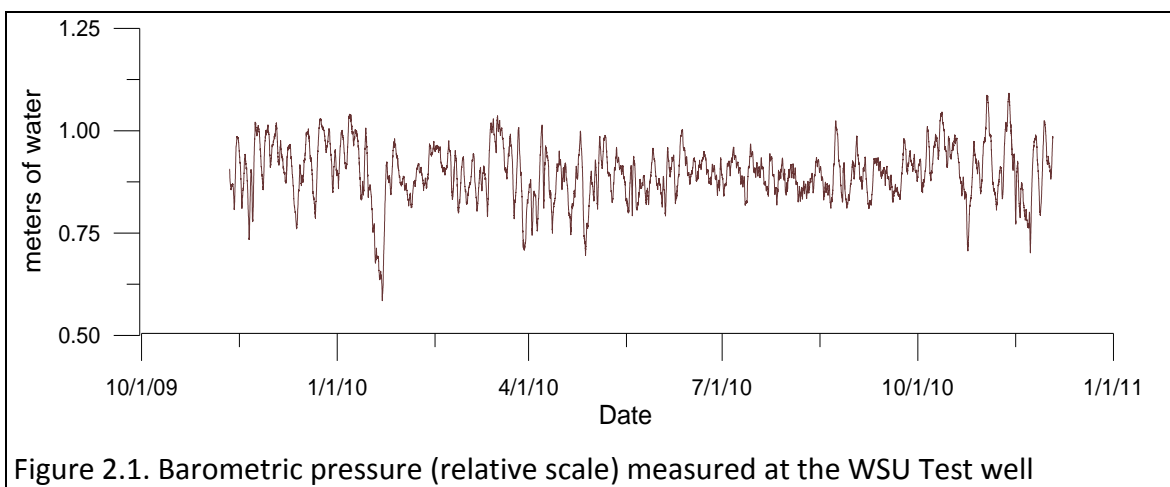
Some preprocessing was required to produce an accurate, continuous groundwater elevation series from the raw Levellogger data. The absolute pressures recorded by the Levelloggers were first converted to gage pressures by subtracting the barometric pressures from the absolute pressures for each time increment. Barometric correction methods rely on relative changes in barometric pressure instead of absolute magnitudes; Levellogger data were paired with barometric readings from the closest available Barologger. The Clay Street transducer is vented (records gage pressure), so conversion to gage pressure was unnecessary for this well.

Levellogger deployment depths were determined through comparison of the recorded gage pressures to the manual depth-to-water measurements recorded during data downloads. Water levels were converted to depths-to-water using a reference point on the well casing, and then converted to ground water elevations using surveyed top-of-casing elevation data. Any discrepancies between the measured depths and the corresponding converted Levellogger water levels (e.g., differences between the manual depths measured before and after each Levellogger deployment period) were minimized by choosing the depth that was most consistent with the preceding and subsequent manual measurements for each individual deployment period.

### 2.4 Barometric correction of water levels

Fluctuations in well water levels resulting from barometric pressure variations complicate hydrologic analyses by concealing water level changes caused by pumping, recharge, and long-term water level trends. Water level fluctuations in Grande Ronde

wells due to barometric pressure changes are measurable and typically occur on the order of about 0.03 m, with occasional changes approaching 0.3 m (Figure 2.1), creating difficulties in interpretation of pump test data and fluctuations in groundwater levels. Several methods for evaluating and removing barometric effects on water levels have been described in the literature; three of the most prominent techniques were applied to a three-month time period of Grande Ronde monitoring well data. Barometric efficiencies calculated by each method were compared to evaluate each method's suitability for Grande Ronde wells and to provide the best possible estimate of barometric efficiency for each observation well.



### Introduction to barometric pressure effects

The movement of water on and below the earth's surface is controlled by the hydraulic head at any given point in space, calculated as:

$$\text{total head} = \text{pressure head} + \text{elevation head} + \text{velocity head}$$

In ground water aquifers, velocity head is usually too small to have any appreciable effect, so that total head is a sum of the elevation of the measurement point above the datum and the pressure head, often expressed in feet or meters of water. Pressure head in a well can be evaluated in two ways: as gage pressure, which corresponds to the pressure exerted by the height of the water column in a well above the measurement point; or as absolute pressure, which is a sum of the water pressure exerted by the

column of water in the well and the air pressure acting on the surface of the water. Atmospheric or barometric pressure is defined as the force exerted on the earth's surface by the weight of the atmosphere. Temporal variations in barometric pressure generated by surface fronts may reach magnitudes of approximately 0.3 m over time scales as short as a few hours.

#### Barometric efficiency vs. barometric response

In a confined aquifer system, well water levels (WL) theoretically respond instantly to changes in atmospheric pressure ( $\Delta B$ ). This instantaneous ratio of change in water level (due to barometric effects) to barometric change is constant for any given well, and designated as its barometric efficiency (BE).

$$BE = \frac{\Delta WL}{\Delta B}$$

eq. 2.1

In order to calculate BE from well data, the dataset must include water levels and barometric measurements collected simultaneously (or within a justifiably short time span). Barometric efficiency can vary between zero and one. BE=1 describes confined aquifers with incompressible skeletons, and BE=0 represents shallow unconfined aquifers with direct connection between the water table and the atmosphere through pore spaces. Equation 2.2 was developed by Jacob (1940), and defines BE explicitly in terms of physical properties of the aquifer, specifically aquifer matrix compressibility ( $\alpha$  [1/Pa]), and the compressibility of water ( $\beta$  [1/Pa]).

$$BE = \frac{1}{1 + \left(\frac{\alpha}{n\beta}\right)}$$

eq. 2.2

Unconfined aquifers often exhibit complicated responses to barometric effects, due to the amount of time it takes for atmospheric pressure changes to propagate through pore spaces in the vadose zone to the water table at depth. This time lag is proportional to the pneumatic resistance of the unsaturated porous medium above the

water table (determined by the degree of consolidation and pore throat diameter of the material), but is constant for each well (Price, 2009). BE on its own is a poor measure of the total barometric effects over time under these conditions because it only defines the instantaneous effect on water level; a better descriptor for time-lagged phenomena is *barometric response*, which describes the full effect of a change in barometric pressure over time, from the initial perturbation through equilibrium (Rasmussen and Crawford, 1997).

Confined aquifers exhibit a representative constant barometric response, and barometric effects on wells in confined aquifers such as the Grande Ronde can be successfully characterized by BE alone. Because BE and barometric response are constant in each well, estimation of these parameters allows for the removal of the barometric effects on water levels. “Barometric correction” of water levels can be performed with eq. 2.3, where WL<sub>corr</sub> is the corrected water level, WL is the original (gage) water level, BE is the barometric efficiency, B is the barometric pressure, and B<sub>1</sub> is the initial barometric pressure for the series being corrected.

$$WL_{corr} = WL + [BE * B] - [BE * B_1]$$

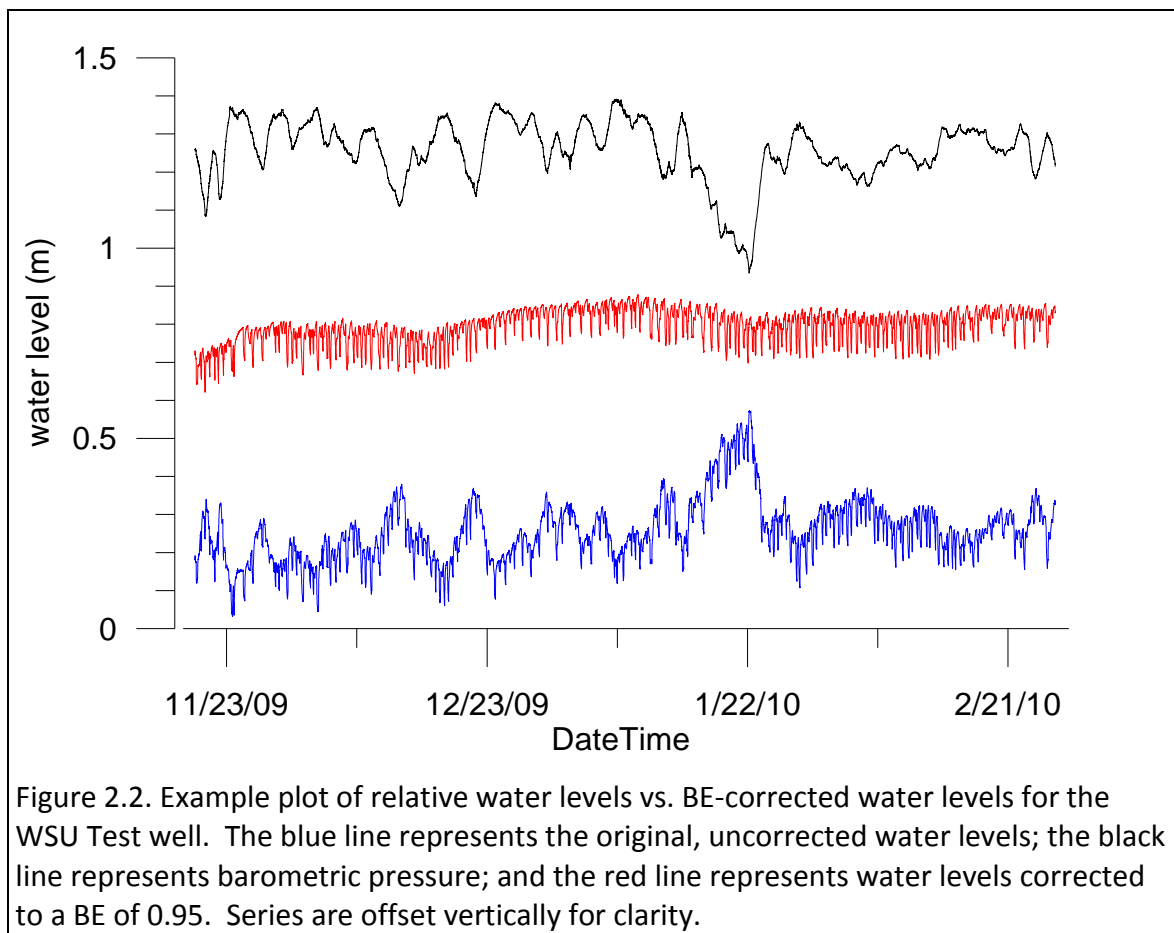
eq. 2.3

Removal of barometric effects is necessary to delineate water level changes caused by pumping or other sources, as illustrated in Figure 2.2.

### BE estimation methods

In practice, it is difficult to identify the changes in water levels caused by barometric pressure fluctuations alone because few well water levels are truly static due to the effects of temporally-variable recharge or ground water withdrawal. Several methods for estimating BE have been published over the past 50 years, with recent research primarily focused on delineating time-lagged barometric response. Some of these techniques are more robust than others in dealing with non-barometric effects on

water level. Three methods for estimating barometric response are outlined below; each represents a different approach to solving the same problem.



#### *Trial-and-Error (TE) Method*

The trial-and-error, or graphical, method for estimating BE was mentioned by Clark (1967), and further described by Merritt (2004) as a fallback technique if other methods produce unreasonable results. This method involves several steps. First, several reasonable values of BE based on aquifer characteristics are selected by the investigator, and a series of water levels corrected to each BE are plotted together, along with the uncorrected (BE=0) water levels and corresponding barometric measurements. Next, the corrected water levels are compared visually to each other and the uncorrected levels; the most appropriate BE value will correspond to the “smoothest” record. Once the “best” BE correction level has been identified, the process is repeated

(choosing new BEs based upon the best of the previous group) as necessary to select a final estimate. In wells exhibiting strong barometric response and limited pumping effects, the uncorrected water levels will appear to mirror (i.e. oppose) the barometric record; the correct BE will produce a plot that appears to be intermediate between the two. Overestimation of BE will result in the corrected water levels that mimic (follow) highs and lows observed in the barometric record.

This method is subjective, relying on visual clues in the record which could potentially be misleading. However, it is quick and relatively simple to execute. Error is minimized by increasing the length of the water level record to average out barometric highs and lows and make long-term barometric trends apparent, and by preferentially analyzing periods of the record in which pumping or other transient effects are known to be absent or small.

#### *The Clark Method*

Clark (1967) developed a method for determining the BE for a well from simultaneous water level measurements and barometric pressure measurements. Use of the Clark (1967) method relies on the assumption that changes in water level resulting from non-barometric influences will average to zero over time with respect to the sign (+/-) of corresponding incremental barometric changes. The Clark method is commonly used, and is identified by Spane (2002) and Merritt (2004) as one of the few BE-estimation tools that will approximate BE for water level records which exhibit fluctuations due to non-barometric influences such as pumping, recharge, and long-term trends.

BE is approximated from the slope of a best-fit linear regression line through an arithmetic plot of paired, and summed, incremental water levels and barometric pressure measurements. The procedure is as follows:

- 1) For each time step, calculate the incremental change in barometric pressure ( $B_i - B_{i-1} = \Delta B$ ) and the corresponding change in water level ( $W_i - W_{i-1} = \Delta W$ ).  $\Sigma \Delta B$  is represented on the x-axis,  $\Sigma \Delta W$  on the y-axis. For each time increment,  $\Sigma \Delta B_i = \Sigma \Delta B_{i-1} + |\Delta B_i|$ .
- 2) If  $\Delta B$  and  $\Delta W$  have opposite signs (corresponding to a potential barometric response),  $\Sigma \Delta W_i = \Sigma \Delta W_{i-1} - |\Delta W_i|$ .
- 3) If  $\Delta B$  and  $\Delta W$  have the same sign,  $\Sigma \Delta W_i = \Sigma \Delta W_{i-1} + |\Delta W_i|$ .
- 4) Plot  $\Delta B$  vs.  $\Delta W$  and fit a linear regression line through the data. The slope of this line is equal to the BE.

#### *Regression Deconvolution and BETCO*

Application of regression deconvolution techniques to determine time-lagged barometric response has been examined by Rasmussen and Crawford (1997), Spane (2002), and recently by Rasmussen and Toll (2007). Regression deconvolution involves two steps: first, estimating the response function through ordinary least-squares linear regression; and second, subtracting this response function from water level data to create a smoothed record. The response function follows the form:

$$\Delta W(t) = \sum_{i=0}^n \gamma(i) \Delta B(t-i)$$

eq. 2.4

in which  $\gamma$  is the unit response, unique for each time lag  $i$ ;  $\Delta W$  is the incremental change in water level at each time step (time increment between measurements) up to the maximum lag of  $n$ ;  $t$  is time; and  $\Delta B$  is the incremental change in barometric pressure. The first term in the summation, at  $t=0$ , represents the instantaneous response to a barometric change, for which  $\gamma$  is equal to the BE of the well. Each subsequent time lag  $i$  delineates the continued response to lagged incremental changes in barometric pressure.

Rasmussen and Toll (2007) developed the freeware software program BETCO, Barometric and Earth-Tide Correction, as a user-friendly tool to calculate the barometric

response function and create a corrected head series for user-input water levels and barometric measurements (Toll, 2005). The maximum time lag to be considered ( $n$ ) can be adjusted by the user, up to 48 time steps. As suggested by the program name, BETCO will also identify and remove earth-tide effects, which result from elastic deformation of the aquifer matrix due to gravitational and centripetal forces. Required data inputs for BETCO include two weeks or more of paired water level measurements and barometric measurements recorded at evenly-spaced time intervals. Figure 2.3 illustrates the BETCO user interface.

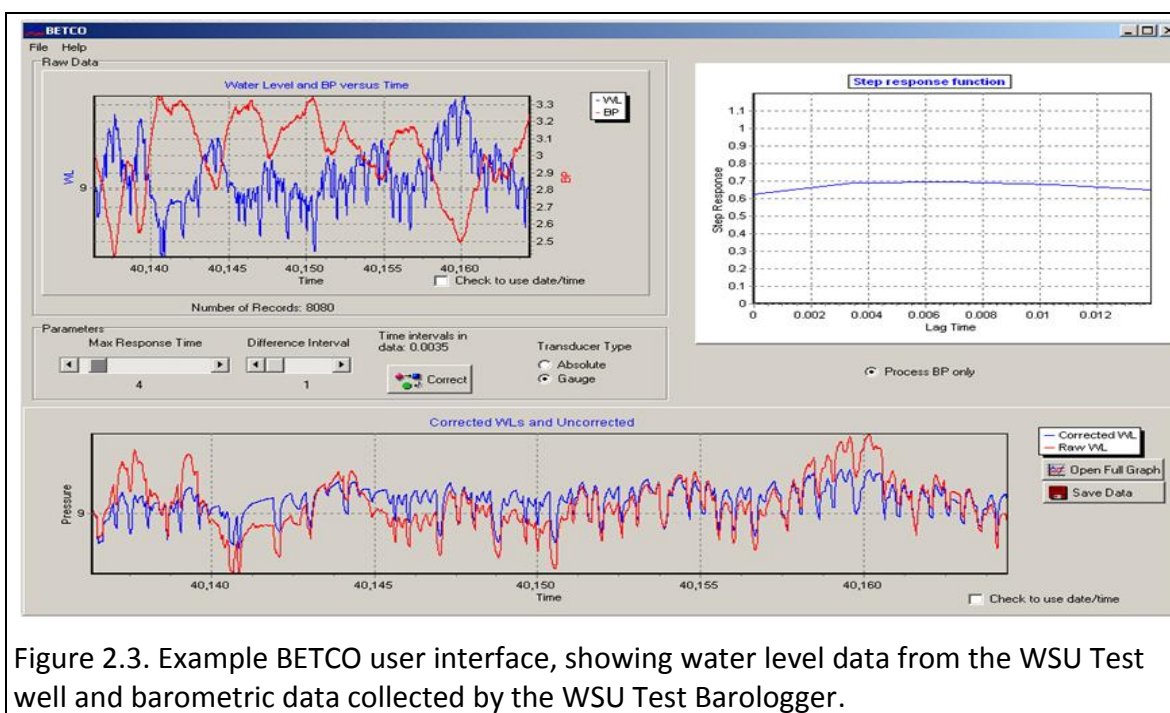


Figure 2.3. Example BETCO user interface, showing water level data from the WSU Test well and barometric data collected by the WSU Test Barologger.

### Methodology for selection of BE estimation technique

After water level elevations were compiled for each well, BE was estimated using the Clark method. The result of the Clark method provided a starting point for graphical trial-and-error comparison. The goal of trial-and-error BE correction was to identify the most appropriate BE to within 0.05. A threshold of 0.05 was selected because it is challenging to visually identify differences in water levels with a BE tolerance of less than 0.05, especially in wells with large pumping influences. In addition, an error of 0.05 in the BE estimate will not introduce a significant amount of noise to the dataset. For

example, with a barometric change of 0.05 m of water, an error in BE of 0.05 would only offset water elevation by 0.0025 m, which is below the precision reasonable for water level measurements. If the Clark method yielded a BE estimate which appeared to represent the best water level correction within 0.05 through visual comparison, the BE from the Clark method was selected as the “best” BE. After graphical comparison, BETCO was used to estimate the barometric response. A maximum time of 12 intervals (60 minutes) was initially specified to characterize the time-lagged barometric response. The maximum time step interval was then decreased to one (5 minutes), in order to produce two estimates for (for  $t=0$  and  $t=1$ , eq. 2.4) for ready comparison to the BE estimates derived by the Clark method and the trial-and-error method.

#### Results of BE estimation for Grande Ronde monitoring wells

Estimated BE values for each well are presented in Table 2.3. As shown, agreement between the BE values predicted by the Clark method, BETCO, and trial-and-error method best estimates are inconsistent among wells. BE for wells WSU 5, Pullman 8, Pullman 6, and DOE were accurately predicted by the Clark method and corroborated by BETCO. With the exception of wells WSU 7 and Palouse 3, BETCO and Clark BE estimates were within 0.07 of each other, regardless of the BE estimated by the trial-and-error method. However, in some cases both the Clark method and BETCO predicted unreasonable BE values, outside of the  $BE=0$  to  $BE=1$  range. As expected considering the physical attributes of the Grande Ronde aquifer, the BETCO-generated response functions were comparable to the idealized confined aquifer response illustrated by Rasmussen and Crawford (1997), with minimal changes from the instantaneous response at longer time lags (Figure 2.3).

Trial-and-error estimation yielded BE values between 0.9 and 1.0 for each Grande Ronde well. Barometric efficiencies were also estimated for IDWR 2 (0.5) and IDWR 3 (0.4), two Wanapum aquifer monitoring wells (completed in the Vantage interbed) located near Moscow, from water level data collected by PBAC. Trial-and-error BE

estimates corresponded to the BETCO-generated values for these two wells, with the BETCO response functions displaying confined-aquifer signatures for these wells.

Table 2.3. Estimated barometric efficiencies for Grande Ronde monitoring wells

Well ID	Final		Clark	BETCO	
	BE	Method	BE	t=0	t=1 (5 min)
WSU 5	0.98	Clark/TE	0.98	0.97	0.98
WSU 7	1.0	TE	0.91	1.00	1.01
WSU 8	0.98	TE	unreasonable	1.58	0.54
IDWR 4	1.0	TE	0.77	0.68	0.63
WSU Test	0.95	TE	0.63	0.63	0.63
Cornelius	0.97	TE	unreasonable	3.28	3.85
Pullman 8	0.95	Clark/TE	0.95	0.92	0.98
Pullman 6	0.91	Clark/TE	0.91	0.88	0.92
Pullman 4	0.97	TE	0.84	0.77	0.85
Palouse 3	0.95	TE	0.70	0.27	-0.22
Palouse 1	0.95	TE	0.32	0.29	0.58
DOE	0.94	Clark/TE	0.94	1.00	0.81

Neither the Clark method nor BETCO was able to accurately predict the BE for actively-pumped wells (WSU 8, Palouse 1, Palouse 3, and Cornelius), most likely due to characteristic large jumps in water level resulting from the initial well pump start. The Clark method and BETCO produced reasonable estimates for BE for WSU 5, Pullman 8, Pullman 6, and WSU 7, wells less affected by other area pumping wells. Failure of the Clark method for other basin wells is consistent with a critique by Merritt (2004) that this method “does not appear to be entirely robust” for data sets with noise from frequent pumping.

Barometric efficiencies estimated for selected basin wells (monitored during this investigation) by previous researchers are presented in Table 2.4 along with the estimates obtained during this investigation. This table does not include the BE estimates presented by Sokol (1966), which were the first estimates for Grande Ronde wells in the Palouse Basin, because those wells were not monitored as a part of this

project; however, it is important to note that his original estimates for BE for two Grande Ronde wells (UI 3 and Moscow 8) ranged between 0.9 and 0.91.

Table 2.4. Compiled BE estimates

Well ID	McVay 2007	Fiedler 2009	Robischon 2007	Moran 2011*
Palouse 1	0.35	0.99		0.95
	TE	Clark (<48 hr record)		TE
Pullman 6		0.99		0.91
		Clark		Clark
Cornelius		0.99	0.23	0.97
		Clark (filtered data)	Clark	TE
WSU 5		0.99		0.98
		Clark		Clark
DOE	0.20			0.94
	TE			Clark
WSU Test	0		0.12	0.95
	TE		Clark	TE
IDWR 4		no correction (0)	0.37	1.0
			Clark	TE

\*Moran 2011 column identifies BE values estimated during this thesis investigation

In summary, accurate estimation of BE for Grande Ronde monitoring wells is essential for 1) removal of barometric effects from water level records, 2) correct interpretation of aquifer pumping test results, and 3) identification of intermediate-scale trends. The Clark method and BETCO provide acceptable estimates for BE in basin wells showing minimal responses to pumping. These methods are not suitable for identifying the level of barometric response in wells with significant, nearly-instantaneous responses to pumping. Trial-and-error visual interpretation predicted BE values between 0.9 and 1 for all Grande Ronde wells; these high BE values are consistent with the physical properties of the confined Grande Ronde aquifer.

## Chapter 3 - Characterization of Basin Water Levels

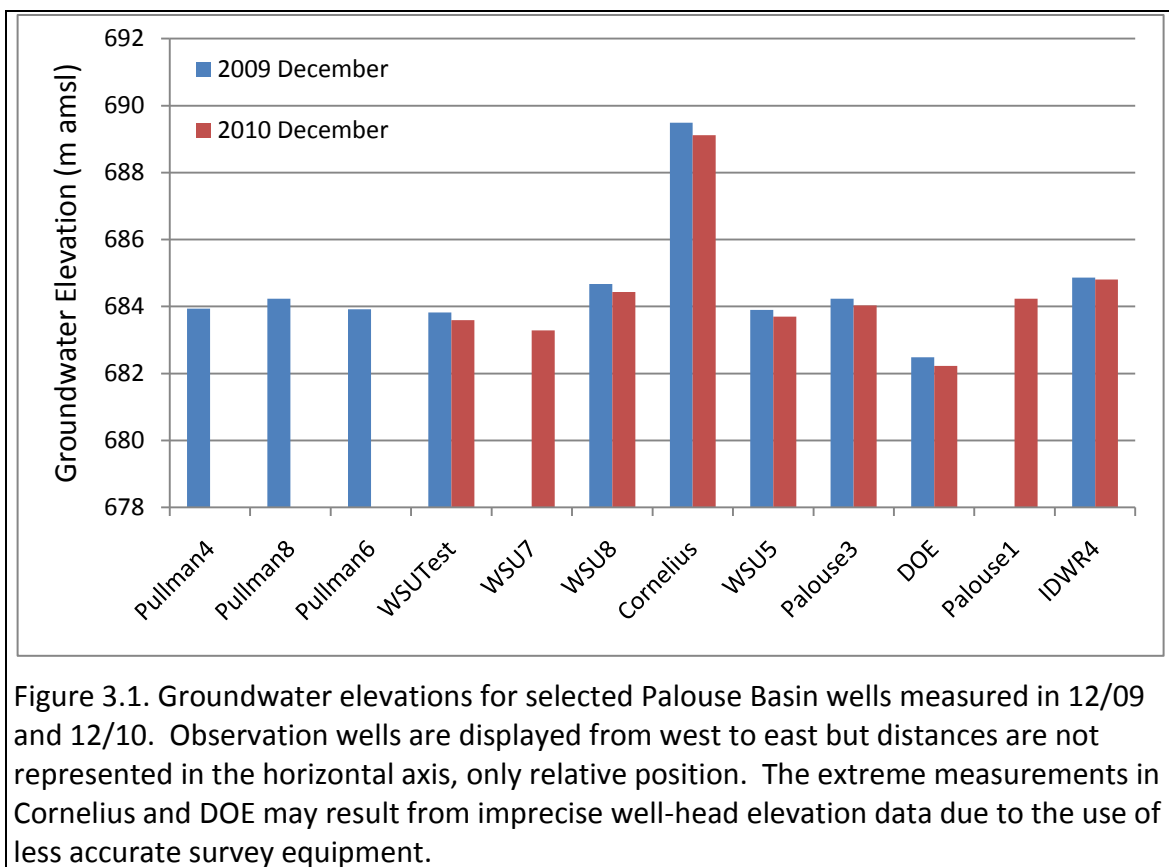
### 3.1 Introduction

Observation well water levels were analyzed together with comprehensive pumping data to investigate the behavior of the Grande Ronde aquifer. Water levels in a complex system such as the Grande Ronde exhibit different patterns on daily, weekly, and annual time scales with respect to influences from pumping, boundaries, regional flow patterns, and recharge. Groundwater elevations and gradients in the study area are discussed in section 3.2. Section 3.3 of this chapter identifies hydraulic connections among basin wells by focusing on selected short time periods from within the complete, year-long dataset. Long-term and seasonal trends, and their significance relative to evaluation of basin properties and boundaries, are discussed in section 3.4; water levels in wells which do not appear to respond to stresses from individual pumping events are also evaluated in that section.

### 3.2 Local gradients

Accurate calculation of underlying local and regional groundwater gradients is problematic in the Palouse basin due to the relative paucity of piezometers, imprecise measurement of well-head elevations, and constantly-moving water levels due to pumping. An additional source of error in measured heads collected from pumping wells is that the reference point for the original survey data may not be the same as the reference point used for water level measurements; for example, the difference between a surveyed elevation of the top of the steel casing of a well and a water level reference point at the top of an access tube port may be as much as several decimeters. Measured groundwater elevations for two periods of data collection are shown in Figure 3.1. Grande Ronde aquifer groundwater elevations measured in Pullman, Moscow, and Palouse are similar, especially considering the magnitudes of the potential sources of

error listed above, and do not indicate a unified direction of regional flow. Measured groundwater depths and surveyed well-head elevations are presented in Appendix A and Appendix C, respectively.



Groundwater elevation data indicate that a large drop (approximately 142 m) in the potentiometric surface of the Grande Ronde exists between Pullman and Colfax, corresponding to a horizontal gradient of 0.0066 m/m between the WSU Test well and the Clay Street well (water levels in Colfax are lower). Water levels in the Colfax area also show a significant local gradient. The Glenwood wells, located about 6.8 km northeast of the Clay Street well, are currently flowing into a distribution pipeline just below ground surface. The Clay Street well water level is approximately 57 m bgs; the horizontal gradient between water levels in Glenwood and those measured in the Clay Street well is approximately 0.013 m/m, due to a change in head of approximately 88 m between the wells. However, it is important to note that precise measurements of head in the

Glenwood wells are not available; it is possible that groundwater heads in these wells rise higher than ground surface, which would indicate a larger gradient between these wells and the Clay Street well. Water levels measured in the IDWR wells also indicate a substantial downward gradient of 0.19 m/m between the Wanapum aquifer (IDWR 3) and the Grande Ronde aquifer (IDWR 4) in Moscow.

### 3.3 Short-term behavior and well connections

Pumping rate data for discrete Grande Ronde pumping periods were compared to compiled water levels in order to identify short-term hydraulic connections between pumping wells and observation wells. A comprehensive pumping dataset that included detailed pumping records for all of the Grande Ronde pumping wells was compiled for this investigation. Data for numerous pumping periods for each well over the course of an entire year were evaluated to minimize well interference effects that have plagued previous aquifer test analyses. To identify short-term hydraulic connections, plots of groundwater levels for each monitoring well were inspected for short-term water level drawdown and changes in slope. These water levels were then compared to specific well pumping records within the full pumping dataset to isolate individual responses. Analysis of water level measurements on five-minute increments was beneficial for delineating changes in slope between drawdown and recovery in water level plots.

Interpretations of individual well responses to short-term pumping events are discussed below, with observation wells grouped by geographical location for presentation purposes. Previously-identified well connections from well construction reports and aquifer test reports are included where relevant. A full list of basin pumping wells and pumping rates is presented in Table 2.2.

Water level records analyzed herein have been corrected to remove barometric effects using the procedure outlined in section 2.4. Time is represented as days elapsed from the start of the aquifer test ( $t=0$ ) at 21:50 on 11/24/2009.

### Pullman-area wells

Eight observation wells were monitored in and near Pullman: Pullman 4, Pullman 6, Pullman 8, WSU Test, WSU 5, WSU 7, WSU 8, and Cornelius (Figure 1.3). Two city of Pullman pumping wells, Pullman 6 and Pullman 8, were instrumented for water level monitoring for less than the full year period. Pullman 6 levels were recorded from November 2009 through March 2010 while the pump was removed for maintenance. Pullman 8 levels were monitored from November 2009 through February 2010, for the period after construction of the well and before installation of the pump. Water levels were monitored in Pullman 4 for three months; however, the Levellogger was not replaced after downloading due to an obstruction in the access tube. Water levels were monitored in WSU 7, a WSU pumping well, for the majority of the year, with a data gap in December and January corresponding to work being conducted in the well to replace the pump. Continuous, year-long water levels were recorded for WSU 8, a WSU pumping well; the WSU Test well, a non-pumping well within one kilometer of several pumping wells; WSU 5, a non-pumping well east of Pullman; and the Cornelius well, a domestic well south of Pullman.

Short-term drawdown from specific pumping wells was observed in the WSU Test well, Pullman 4, WSU 7, and WSU 8. No observable responses to specific pumping episodes were identified in Cornelius, WSU 5, Pullman 6, or Pullman 8. Pullman 6 and Pullman 8 water levels exhibited frequent low-magnitude fluctuations (less than 0.005 m) which may have been caused by nearby pumping; however, visual inspection was unable to delineate responses from any specific pumping wells. Hydraulic connections between Pullman 6 and Pullman 8 were identified by Fielder (2008) and Golder (2008). Neither of these wells was actively pumping during the periods in which the other well was monitored during this test, so this connection could not be confirmed. Cornelius and WSU 5 both exhibited smoothed water levels with very little noise in the data; however, water levels measured in the Cornelius well do reflect daily water level drawdowns derived from domestic pumping of the well itself.

As shown in Figure 3.2, water levels in WSU 7 respond to pumping in WSU 4 (0.15 km distant), WSU 8 (1.56 km), and Pullman 7 (0.91 km). Pullman 4 water levels show drawdown in response to pumping in Pullman 7 (0.02 km) and WSU 7 (0.89 km) (Figure 3.3). Water levels in the WSU Test well (Figure 3.4) respond to pumping in WSU 4 (0.02 km), WSU 7 (0.17 km), possibly WSU 8 (1.63 km), Pullman 7 (0.74 km), and Pullman 8 (0.95 km). Connections between the WSU Test well and WSU 7, Pullman 6, and Pullman 7 were identified previously by McVay (2007). Water levels in WSU 8 (Figure 3.5) respond to pumping in WSU 4 (1.63 km), WSU 6 (0.59 km), and WSU 7 (1.56 km).

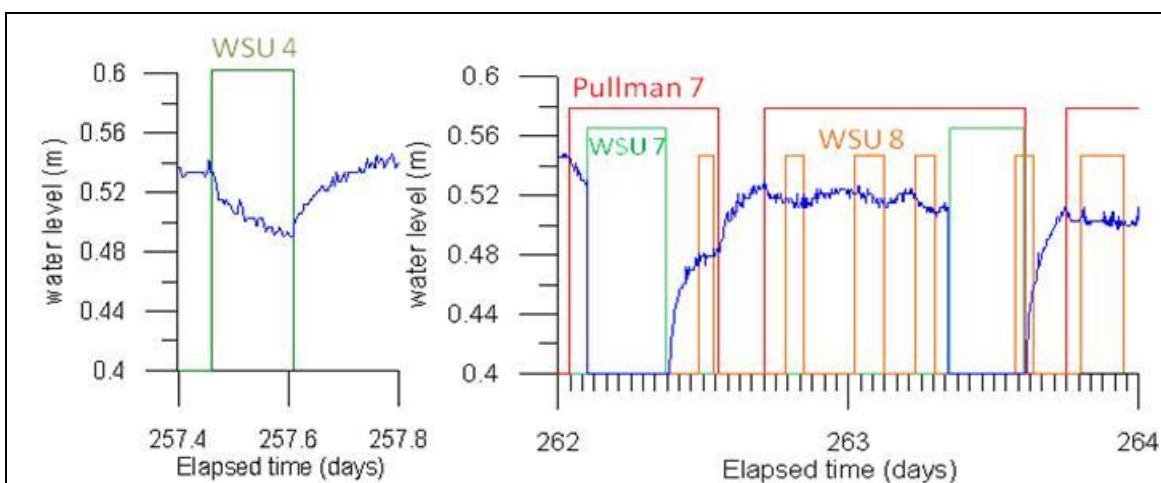


Figure 3.2. WSU 7 well connections. Water level in WSU 7 is represented by the blue line; periods of active pumping are designated by the vertical rectangles with labels identifying individual pumping wells. Relative water levels are shown in meters above an arbitrary datum.

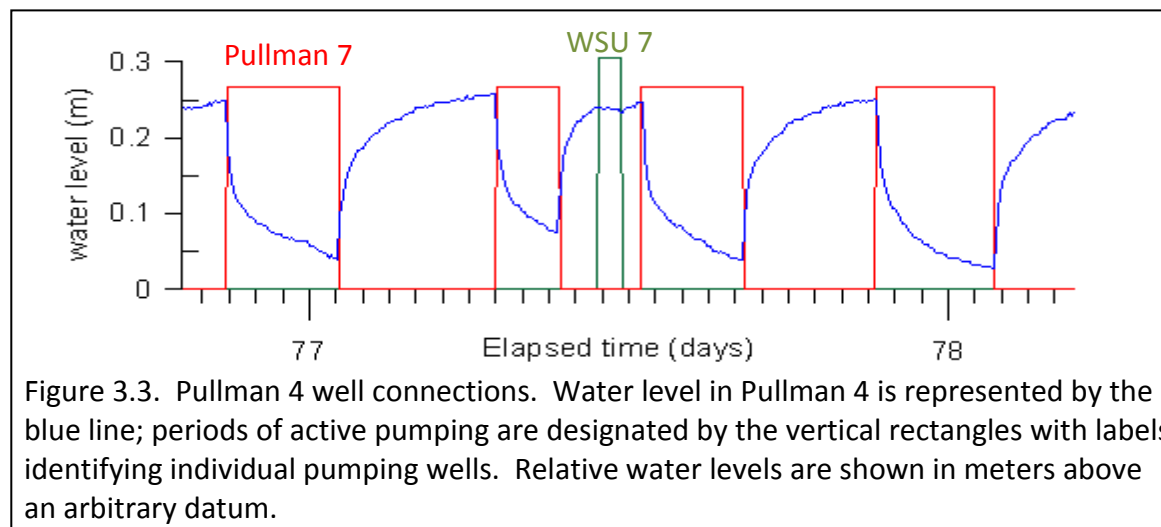
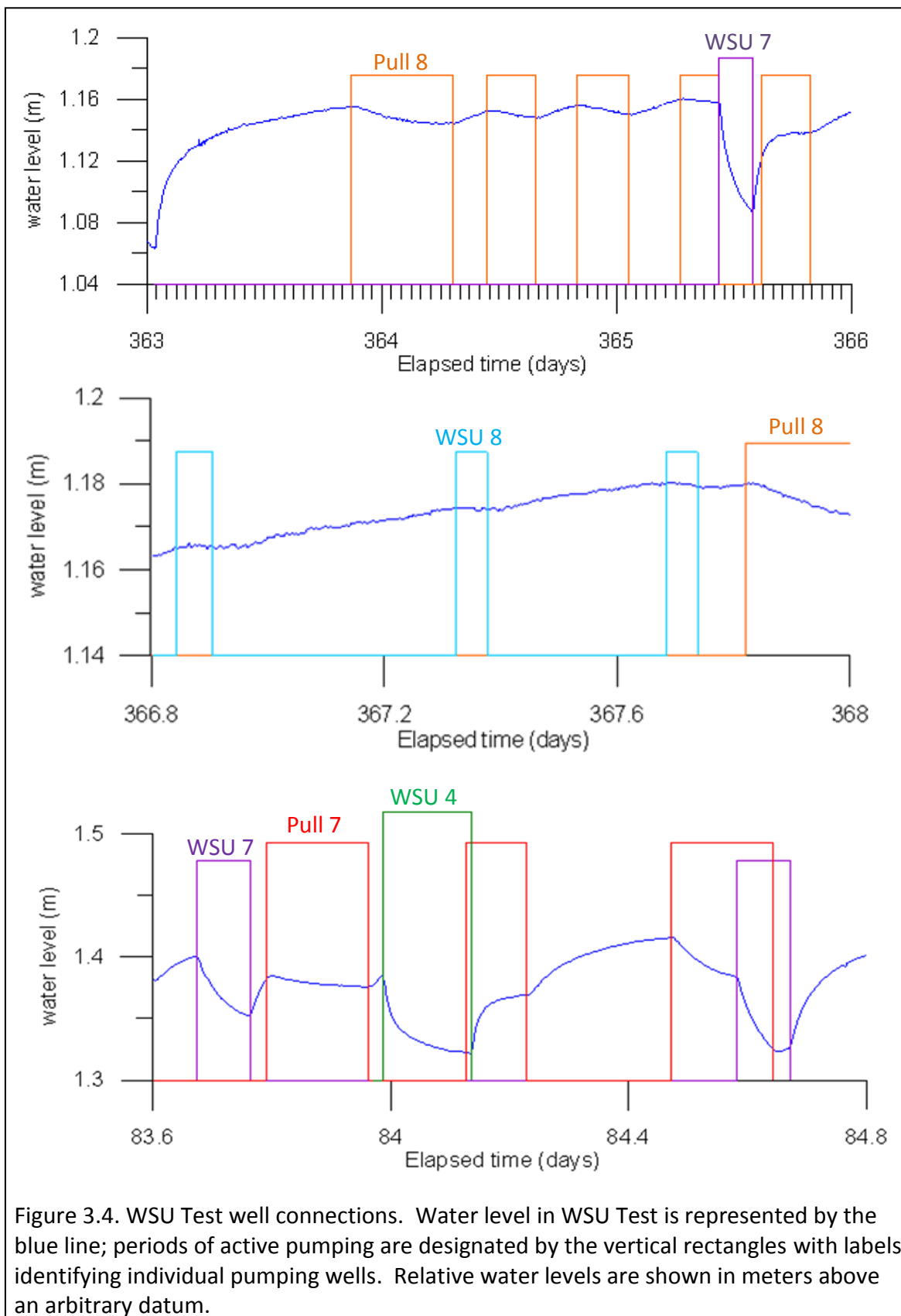


Figure 3.3. Pullman 4 well connections. Water level in Pullman 4 is represented by the blue line; periods of active pumping are designated by the vertical rectangles with labels identifying individual pumping wells. Relative water levels are shown in meters above an arbitrary datum.



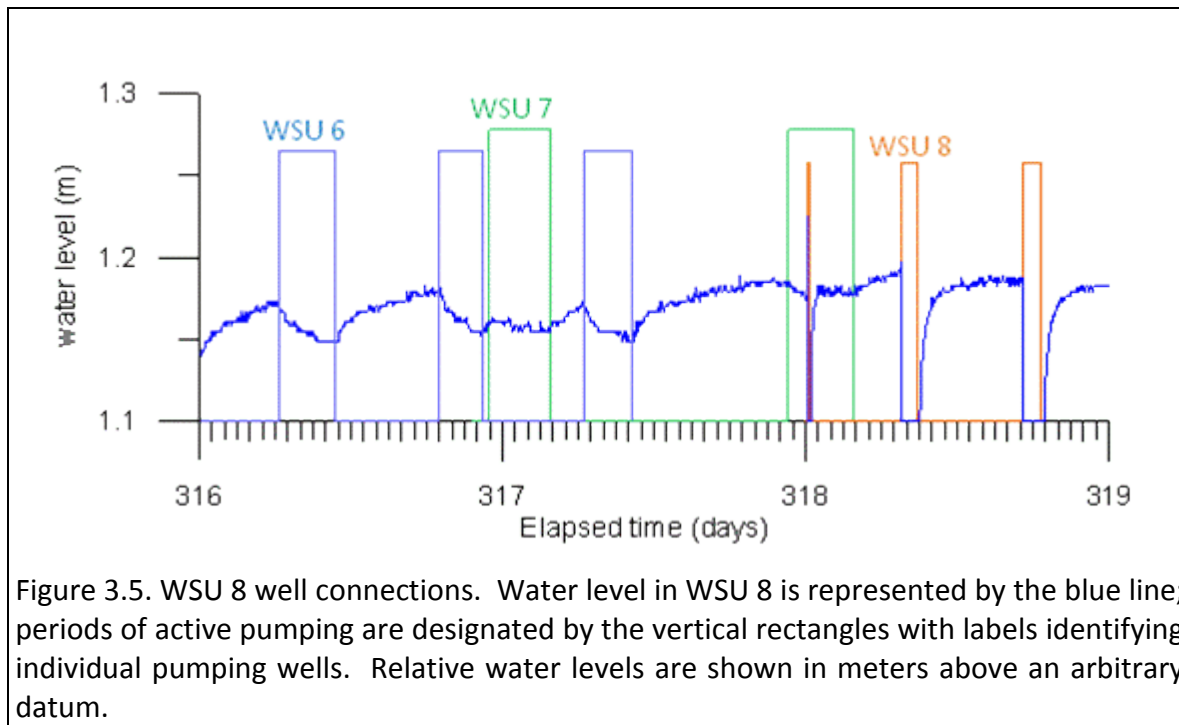


Figure 3.5. WSU 8 well connections. Water level in WSU 8 is represented by the blue line; periods of active pumping are designated by the vertical rectangles with labels identifying individual pumping wells. Relative water levels are shown in meters above an arbitrary datum.

#### Moscow-area wells

The IDWR monitoring wells 1, 2, 3, and 4 are located on the north side of Moscow, with IDWR 4 completed within the Grande Ronde aquifer (Figure 1.4). Water levels in IDWR 4 show significant drawdown during pumping of UI 4 (1.35 km) and Moscow 9 (1.47 km), as shown in Figure 3.6; these connections were also observed by Fiedler (2009). No drawdown was identified in IDWR 4 in response to pumping of Moscow 6 (2.48 km) or Moscow 8 (1.28 km).

The DOE observation well is located approximately halfway between Moscow and Pullman. Like IDWR 4, DOE water levels show observable drawdown to pumping in UI 4 (4.89 km) and Moscow 9 (4.33 km), but to no other individual pumping wells for the period of this test (Figure 3.7). Previous researchers (McVay, 2007; Fielder, 2009) have noted these connections, and also suggested a possible connection between DOE and WSU 7 (6.17 km); however, a direct connection between DOE and WSU 7 was not observed during this test. A connection identified by McVay (2007) between UI 3 and DOE could not be confirmed during this test because UI 3 did not pump.

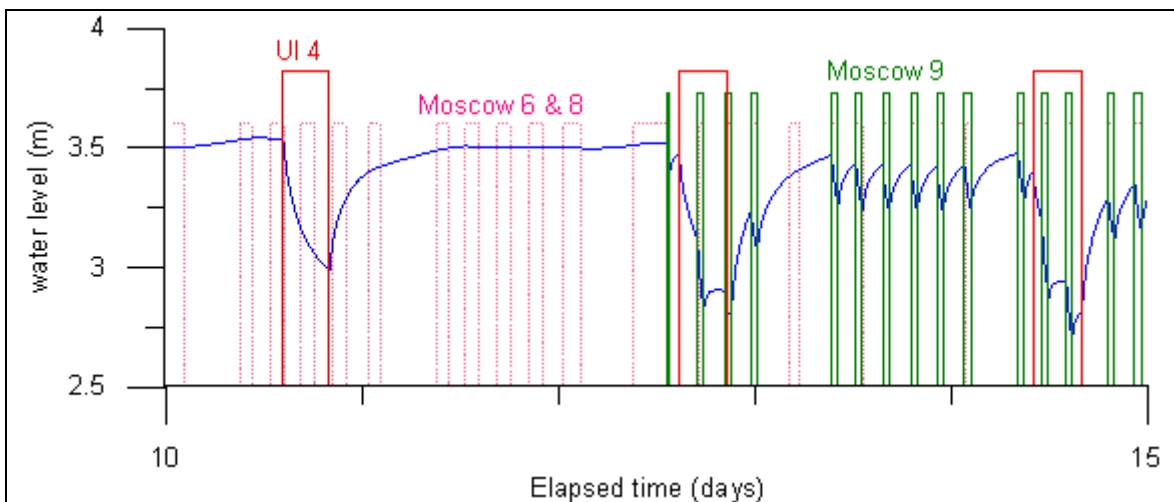


Figure 3.6. IDWR 4 well connections. Water level in IDWR 4 is represented by the blue line. The dotted pink vertical bars indicate periods of Moscow 6 and Moscow 8 pumping (they generally pump together), with UI 4 and Moscow 9 pumping indicated by the red and green bars, respectively. Relative water levels are shown in meters above an arbitrary datum.

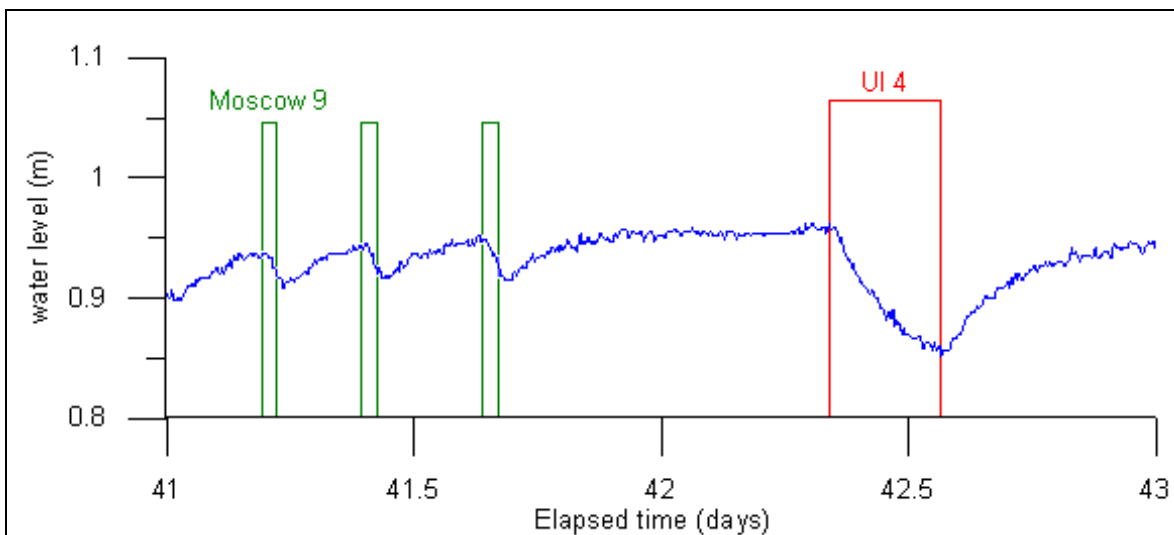


Figure 3.7. DOE well connections. Water level in the DOE well is represented by the blue line; periods of active pumping are designated by the vertical rectangles with labels identifying individual pumping wells. Relative water levels are shown in meters above an arbitrary datum.

### Palouse-area wells

The city of Palouse has two active pumping wells, Palouse 1 and Palouse 3 (Figure 1.5). Water levels and pumping data were recorded for both wells during this investigation, but the water level record for Palouse 1 is truncated due to removal of the data logger in September 2010 during well maintenance. The wells are located 0.91 km apart; water levels in both wells respond to pumping of each other. Possible drawdown in Palouse wells due to Moscow and Pullman pumping was previously reported by Owsley (2003) and McVay (2007); no measurable responses in water levels were traced to pumping of individual Moscow or Pullman wells during this test. Moscow and Pullman are both located approximately 20 km from Palouse.

### Colfax-area wells

The Clay Street and Fairview pumping wells (Figure 1.6) in the city of Colfax only actively pump during summertime peaks in demand. Water levels recorded by a dedicated transducer in Clay Street show clear drawdown from the well pumping; no clear drawdown due to any other pumping wells is identifiable in the water level records.

### Discussion of short-term responses

Based on identification of observable water level responses to specific pumping events, basin observation wells can be categorized as wells which exhibit measureable drawdown/recovery responses to specific short-term pumping (responsive), and those which do not show the expected (based on distance), identifiable responses to specific short-term pumping (unresponsive). Water level data recorded for IDWR 4, DOE, Palouse 1, Palouse 3, Pullman 4, WSU 7, WSU 8, and the WSU Test well show identifiable drawdown/recovery resulting from pumping of specific wells. The distances between specified pumping wells and the observation wells exhibiting drawdown are less than 2.0 km, except for DOE, which responded to pumping in two wells (UI 4 and Moscow 9) located more than 4.0 km away. Cornelius, WSU 5, Pullman 6, and Pullman 8 did not

exhibit identifiable drawdown/recovery due to specific pumping events (unresponsive to short-term pumping).

Drawdown in Pullman-area observation wells appears to be relatively predictable with respect to distance from pumping wells when pumping rate is also taken into account. WSU 7, WSU 8, Pullman 7, and Pullman 8 are all frequently-pumped, high-volume production wells (between 1700 and 2400 gpm). Pullman 3 only pumps 615 gpm, and although Pullman 5 pumps over 1600 gpm, it is located farther from the city center than other pumping wells and usually pumps for very short periods of time.

Obvious connections exist between DOE, IDWR 4, and pumping wells UI 4 and Moscow 9; drawdown from pumping in these wells is unexpectedly large considering the absence of measureable drawdown in these wells from Moscow 6 and Moscow 8 pumping. Although Moscow 6 and Moscow 8 pump at lower rates (1136 and 951 gpm, respectively) than Moscow 9 (2100 gpm), no drawdown response is observed in IDWR 4 or DOE even when both Moscow 6 and Moscow 8 are pumping at the same time. Based on these observations, it appears that the clear, immediate responses in DOE from Moscow 9 and UI 4 pumping are anomalous, possibly due to a high-conductivity zone connecting these wells and IDWR 4, that does not extend to other Moscow or Pullman wells.

Hydraulic connections within the basin do not appear to be ubiquitous and/or limited by the horizontal stratigraphy of the basalts and interbedded sediments, based on information on the total depths and screened intervals from well logs, and a compilation by Fiedler (2009) (Figure 3.8). In Pullman, the bottom-hole elevation in the WSU Test well is over 100 m above the uppermost screened producing zone in WSU 7, and 50 m above the uppermost producing zone in Pullman 7; however, short-term responses from these pumping wells are measured in the WSU Test well. As another example, the DOE well shows significant drawdown in response to pumping in UI 4 across 100 m of vertical separation between their completion zones; however, considerable problems were reported during placement of seals in the borehole annulus during construction of the DOE well (Osiensky, 2011).

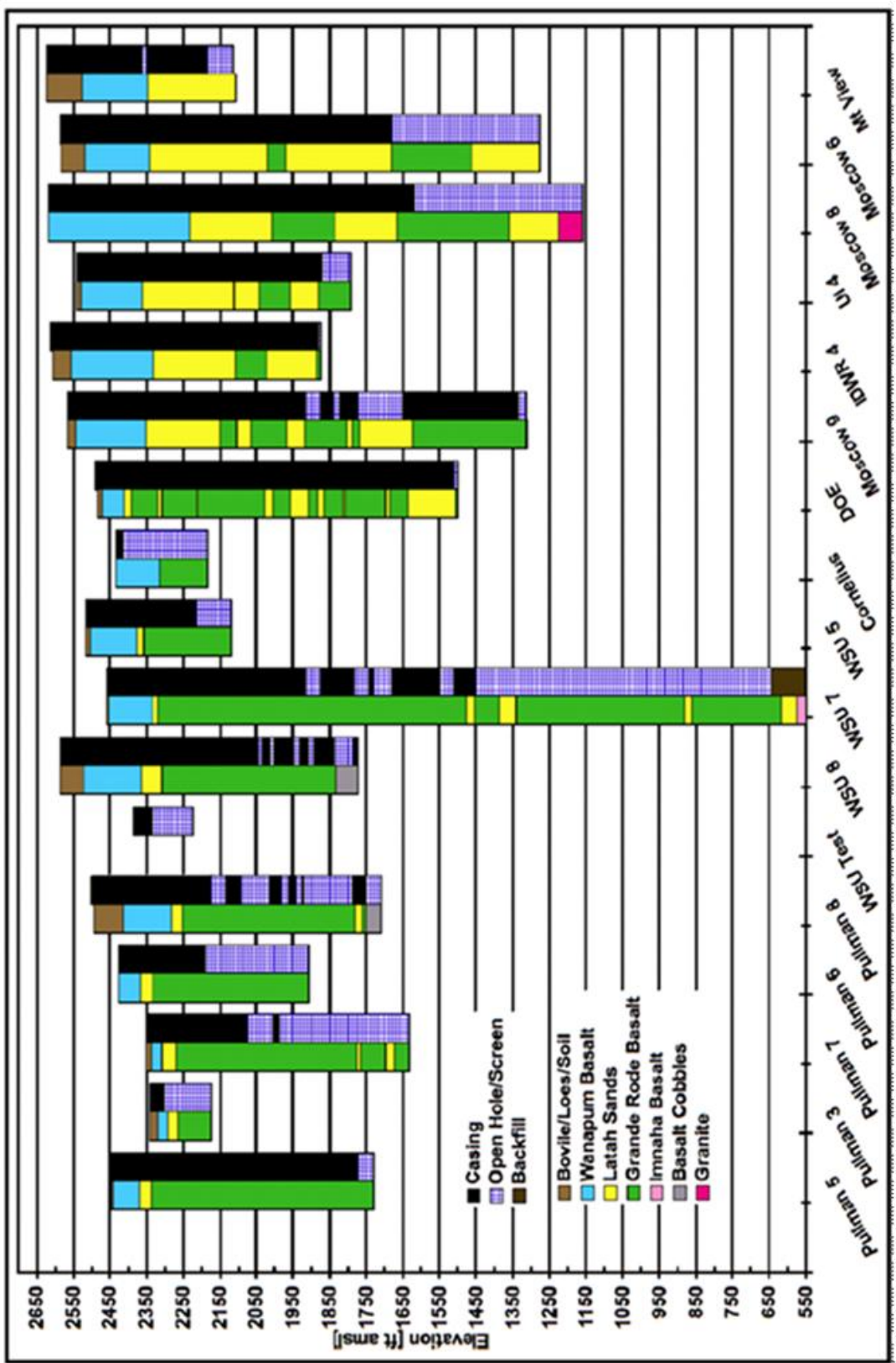
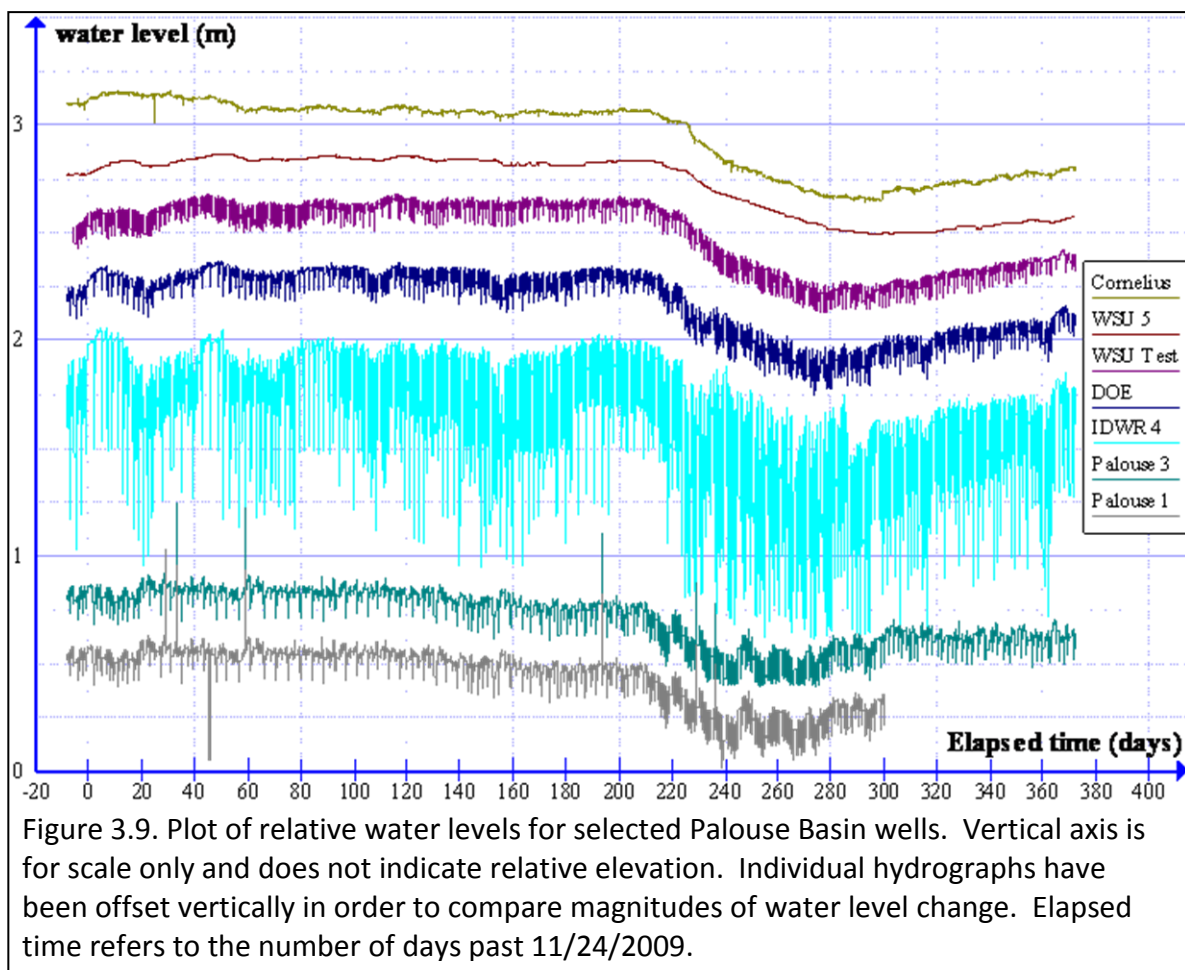


Figure 3.8. Comparison of well completion zones and subsurface geology (Fiedler, 2009).

It is important to understand that a paucity of identifiable, short-term responses to individual pumping wells does not preclude some degree of hydraulic connection between any two wells within the basin on either short-term or long-term time scales. Observation well drawdown is controlled by distance (horizontal and vertical) from the pumping well(s), rate and duration of pumping, and aquifer/aquitard properties; as noted by Fiedler (2009), drawdown in high-transmissivity settings is low enough in magnitude to be easily confounded by noise in measured water levels, especially as distances between observation wells and pumping wells increase. Traditional aquifer tests maximize drawdown by controlling pumping, whereas the methodology utilized in this study was limited to demand-controlled municipal pumping in which typical pumping durations rarely exceeded several hours. The constant cycling of pumps throughout the basin also makes it difficult to identify individual responses of low magnitude, or to distinguish a single response when multiple wells are pumping simultaneously.

#### 3.4 Large-scale features and seasonal trends

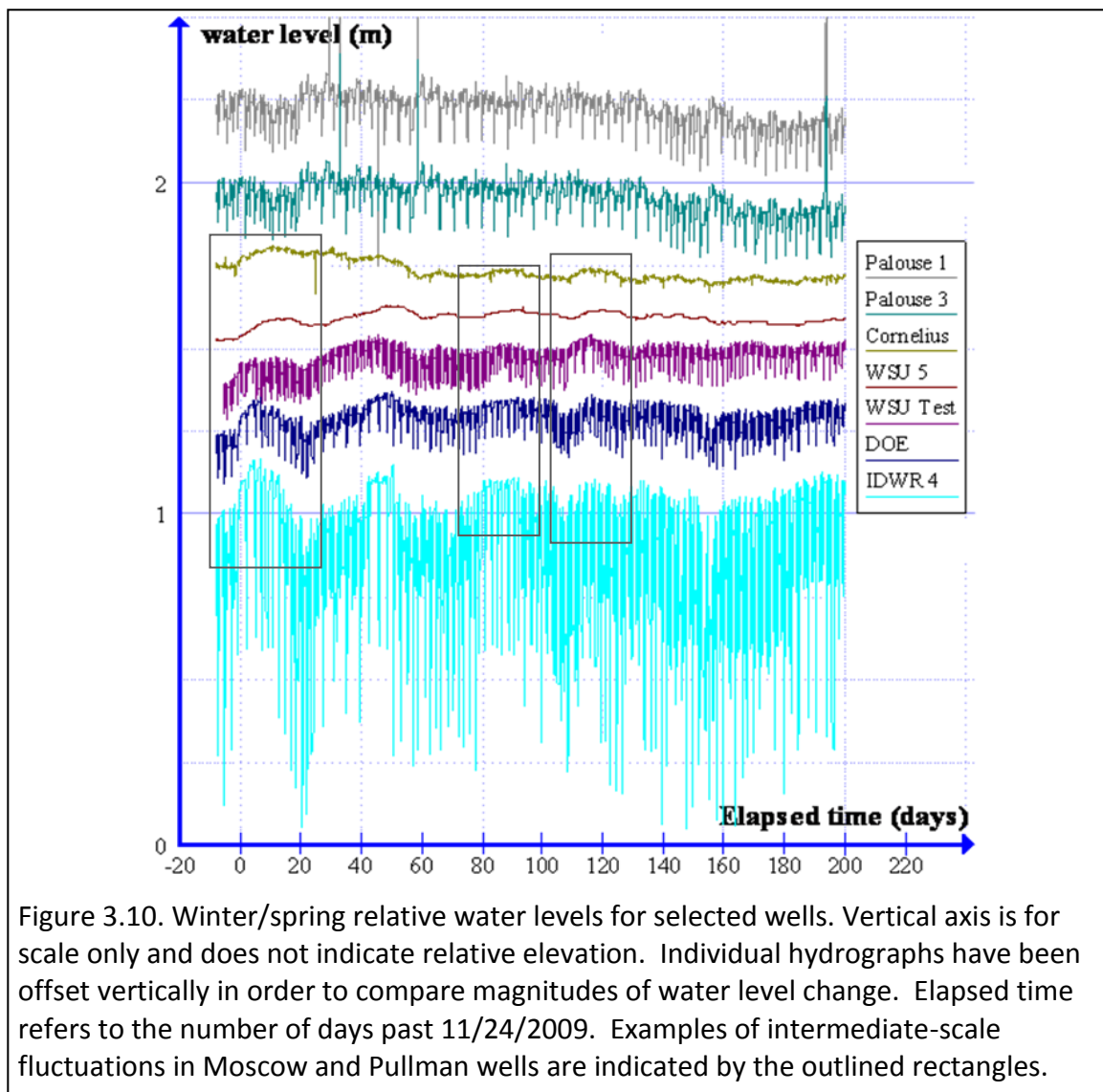
Compiled water levels were plotted for the full period of observation in order to identify seasonal and long-term trends in the data. Figure 3.9 displays water levels for several of the monitored wells. Pullman 4, Pullman 6, and Pullman 8 were omitted from this chart because of their relatively short periods of record. WSU 7 and WSU 8 were excluded due to repetitive jumps in the water levels from frequent pumping of these wells, as well as inconsistencies in the WSU 8 record related to data logger eccentricity and problems associated with the access tube. The relative water level data presented in this section have had barometric effects removed and are displayed according to elapsed time since the start ( $t=0$ ) of the aquifer test on 11/24/2009.



The most prominent features in the long-term hydrographs are the water level declines in all wells extending from late June through August, with subsequent rising water levels beginning in late August. These seasonal water level declines have been recognized as characteristic of Palouse Basin water levels, and are related to the marked increase in municipal pumping during the summer. The magnitude, timing, and shape of these features are consistent in the Pullman area wells, including those which are visually unresponsive to short-term pumping stresses (Cornelius and WSU 5), and also in DOE and IDWR 4. The shape and magnitude of the summertime declines in Palouse 1 and Palouse 3 are different from those in the Pullman wells; the Palouse wells exhibit declining water levels starting around 120 days elapsed time (about March 24), and appear to recover to a steady water level by approximately 300 days. By comparison, Pullman and Moscow well water levels do not begin declining until 200 days (about June

12), and appear to still be recovering around the end of the test. However, the annual declines observed in each of the basin water level records, including those of the Palouse wells, are of similar magnitudes. The similarities in the magnitudes of the annual declines in different wells across the basin suggest that these wells are connected on at least annual time scales.

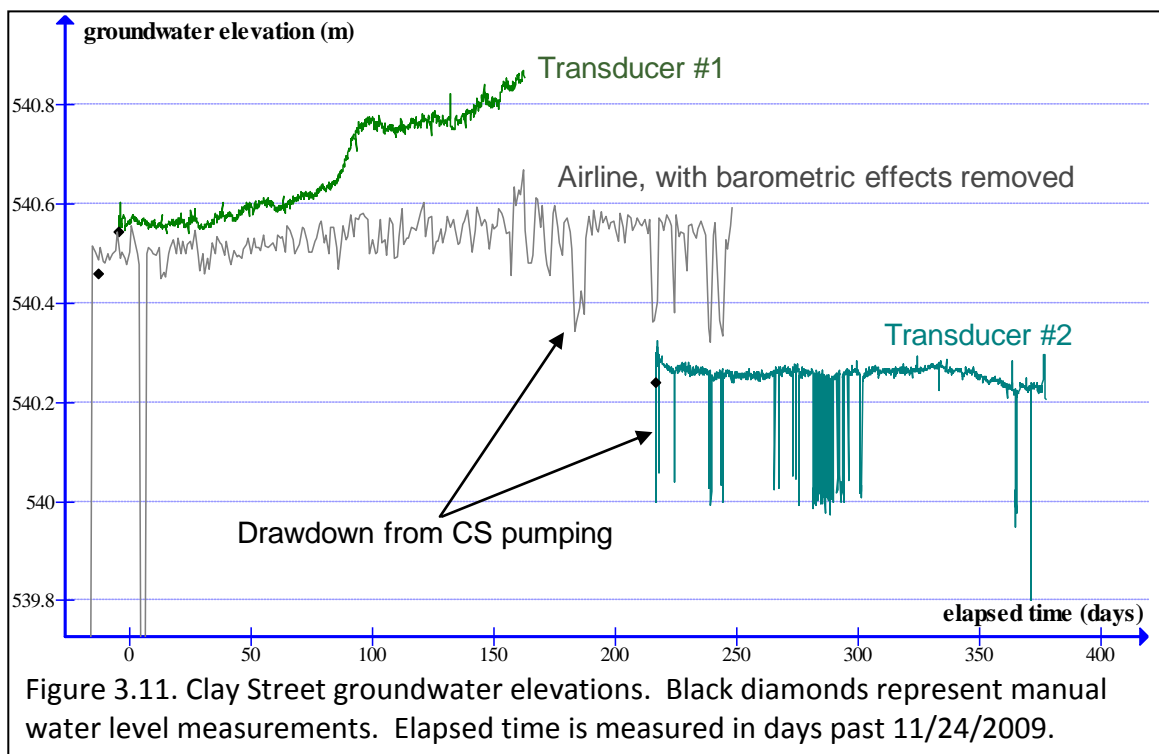
Closer inspection of water levels in the offseason reveals similarities in intermediate-scale (weeks-to-months) fluctuations among different wells (Figure 3.10).



The similarities of these shapes among the Moscow and Pullman water level fluctuations suggests that these wells are hydraulically connected, and/or subject to the same forcing

influences from recharge or cumulative pumping. Palouse 1 and Palouse 3 do not appear to exhibit the same patterns on these intermediate scales, as shown in Figure 3.10.

Several problems were encountered during monitoring of the Clay Street well in Colfax, including difficulty in measuring the static water level in the well with a steel tape, reliance on two different 25+ year-old transducers to monitor water levels, and a 50-day data gap due to transducer failure. Despite these issues, it appears that water levels in the Clay Street well do not exhibit the same seasonal trends as well water levels in Moscow, Pullman, and Palouse. Figure 3.11 displays ground water elevation versus time, measured for the Clay Street well. The green and blue lines denote groundwater elevations measured by the original and replacement Druck transducers (after barometric correction). The grey line represents adjusted airline data collected by the city of Colfax; the minimum daily value was paired with the maximum daily barometric measurement to remove barometric effects from the airline data, and produce a “best estimate” of water levels.



Barometrically-corrected airline data indicate slowly-rising water levels during the winter and spring. Water levels measured by the second (replacement) transducer

indicate a small overall declining trend after 215 days elapsed time to the end of the record. The Clay Street well does not have a dedicated access tube contained within the outer well casing, and the offset between the two transducer-recorded water level series is believed to be a result of the difficulties experienced in passing the steel tape past obstructions in the well to get “good” measurements. This offset is believed to be an artifact of measurement error and not a real displacement. The downward spikes shown in the Figure 3.11 transducer data between 215 and 300 days correspond to active pumping of the Clay Street well. The gently rising trend from zero to 80 days is consistent with rising water level trends in Moscow and Pullman wells during the same period. The steeper rising trend from 80 to 170 days was most likely caused by drift in the transducer prior to its failure at 170 days, based on comparison with the airline data, which do not indicate a corresponding increase in head.

Steel tape water level measurements indicate that annual water level declines in the Clay Street well have been much smaller than in other areas of the basin. A depth-to-water measurement of 180 ft (55 m) bgs was recorded in the Clay Street well log dated 1949. The most recent manual water level measurement for Clay Street was 57.4 m below the top of the well casing (approximately 0.15 m above the well house floor), which represents a decrease of 2.4 m since the well was completed, or an average decline of 0.04 m per year for over 60 years. This long-term rate of decline is significantly less than that measured in the WSU Test well (1.18 ft/year, or 0.36 m/year) for the same period (Robischon, 2010).

#### Investigation of water level fluctuations in WSU 5

As shown in Figure 3.9, water levels in WSU 5 do not show measureable drawdown responses to discrete pumping episodes, but do exhibit the same intermediate-scale fluctuations and seasonal trends as other wells in Moscow and Pullman (Figure 3.10). The summertime drawdowns indicate that water levels in these wells are sensitive to basinwide pumping deficits to the same degree as water levels in wells which do respond to individual pumping periods. To investigate the scale of this

phenomenon, comprehensive pumping data were plotted as cumulative volumes over time, through 300 days after the start of the test. Cumulative pumping volumes were determined from the HOBO data by first calculating the total discharge volumes for each individual pumping event, and then merging the values for each well to create a series representing total volumes pumped over time for each water utility (Figure 3.12). These data sets were summed to produce cumulative pumped volumes for Moscow and Pullman. Colfax pumping wells were not included in this analysis because of the lack of evidence for hydraulic connection between Colfax wells and those in other areas of the basin, as well as inaccuracies concerning the timing and volumes of groundwater withdrawals from the Glenwood wells.

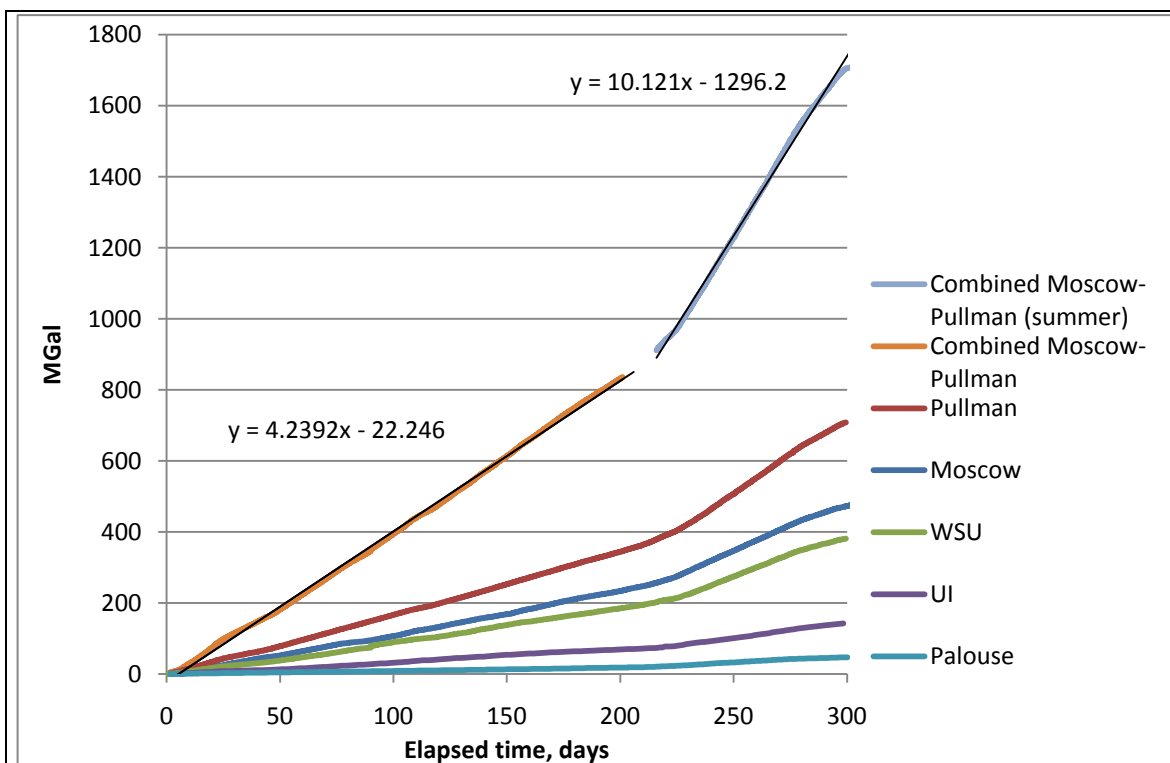


Figure 3.12. Basin pumping over time (through 300 days elapsed time). The two linear trend lines estimate the average combined Moscow-Pullman pumping rates for the winter/spring and summer.

As shown in Figure 3.12, groundwater pumping rates in the Palouse Basin are relatively constant during the winter and spring, but increase to another, higher, rate during the summer. PBAC (2010) describes the steady pumping rate observed in the

offseason as “baseline” pumping. Linear regression of the combined series shown in Figure 3.12 provided an average baseline pumping rate of 4.2 MGal/day for combined Moscow and Pullman pumping. Figure 3.13 displays the combined pumping in Moscow and Pullman over time relative to this average offseason pumping rate. Some fluctuations in pumping are visible in Figure 3.13 between 0 and 200 days elapsed time.

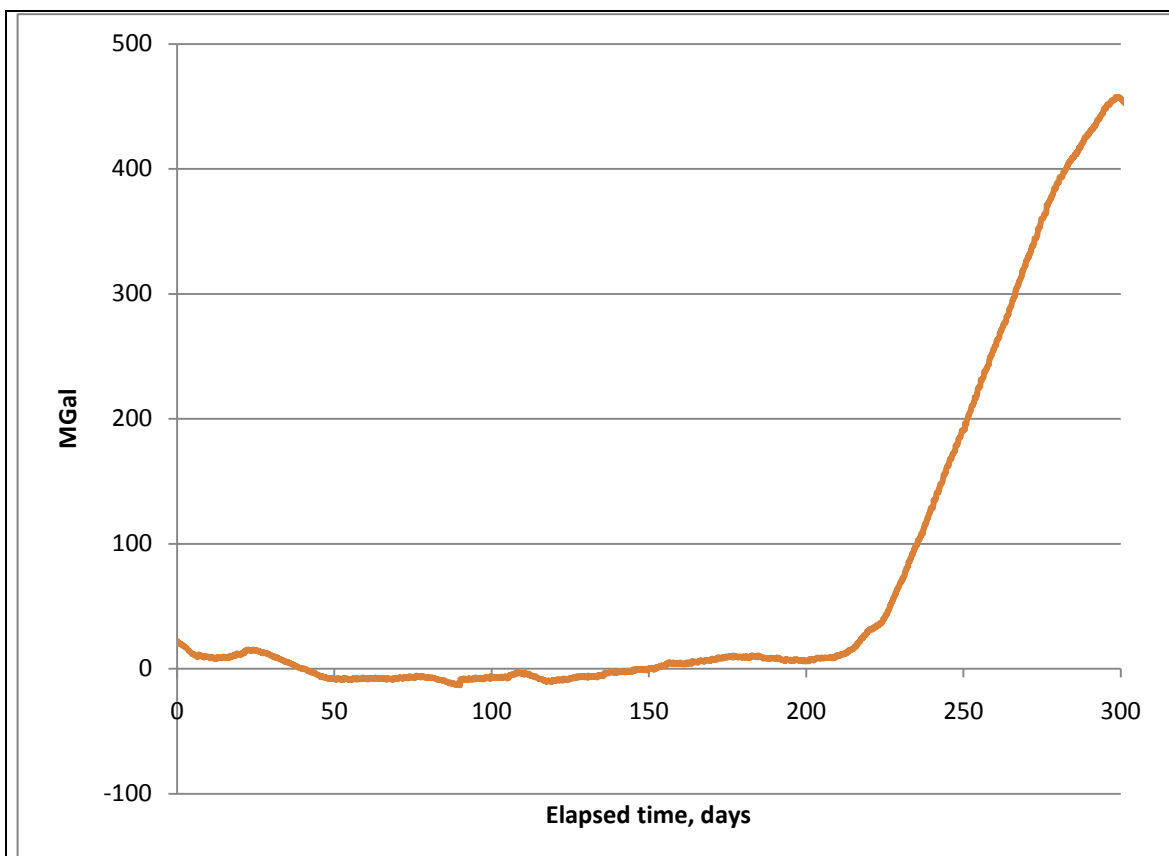


Figure 3.13. Changes in Moscow-Pullman pumping relative to average offseason pumping. This plot displays the differences between observed volumes pumped over time and the average baseline pumping rate determined by linear regression in Figure 3.12.

Fluctuations in pumping relative to average offseason pumping were plotted along with water levels in WSU 5 in order to directly compare the relative shapes of variations in basin pumping to water levels (Figure 3.14). The general shapes and timing of local extrema observed in the series of pumping volumes over time are also present in WSU 5 water levels, which suggests that the pattern of intermediate-scale offseason fluctuations in WSU 5, Cornelius, and other Moscow/Pullman wells shown in Figure 3.10

may be a function of total pumped volumes over time. It also appears that there is a short lag of a few days in the timing between the local minima and maxima in the pumping record and corresponding features in WSU 5 water levels. This analysis indicates that water levels in WSU 5 are indeed responsive to pumping stresses over relatively short time scales. It is important to note that these fluctuations in pumping reflect volumetric changes as compared to average volumes pumped over time (0 MGal in Figure 3.13 and Figure 3.14); it is more accurate to compare water levels to changes in pumped volumes than changes in pumping rate, because head responds to changes in the volume of the cone of depression over time.

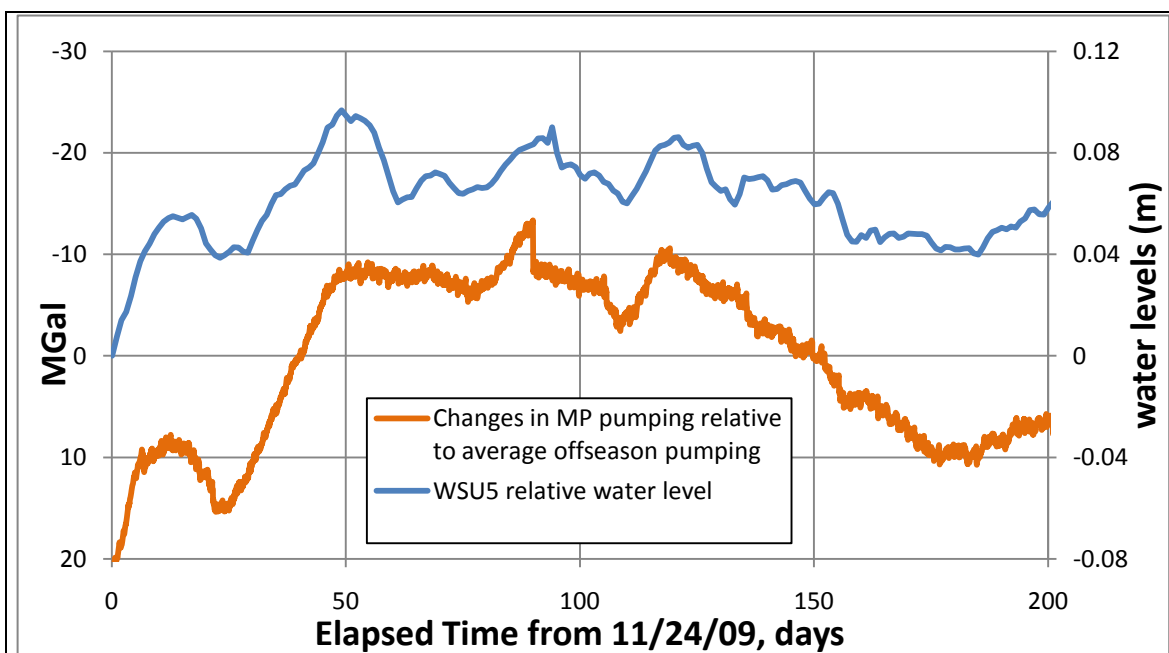


Figure 3.14. WSU 5 water level fluctuations vs. changes in pumping relative to average baseline pumping for wells in Moscow and Pullman. Note that the axis for pumping data is inverted to facilitate visual comparison between the series. Water level data are referenced to an arbitrary datum. Changes in water levels generally occur after corresponding changes in the slope (rate) of Moscow-Pullman pumping.

To further investigate the observed relationship between changes in Moscow-Pullman pumping and WSU water levels, paired water level and pumping volume (cumulative departure from average) data points were plotted. Figure 3.15 shows a strong negative relationship between changes in pumping relative to baseline pumping and WSU 5 water levels, with a coefficient of linear correlation ( $r^2$ ) of 0.79.

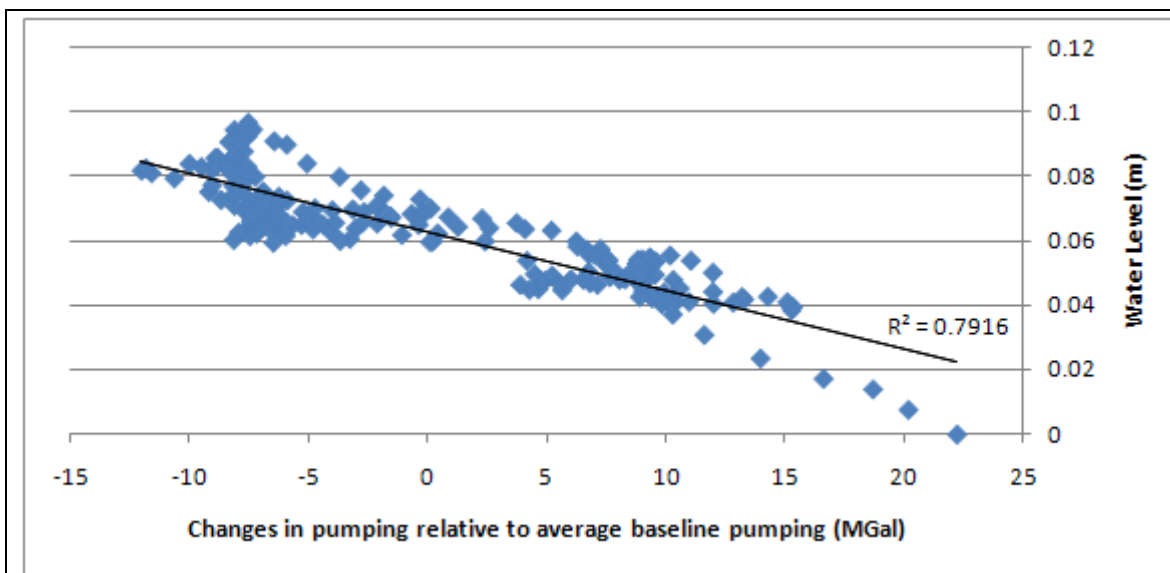


Figure 3.15. Changes in pumping relative to average baseline pumping vs. WSU 5 water levels for the first 200 days elapsed time.

It is important to note that the original pumping data used to create the pumping series for Figure 3.14 includes all Moscow and Pullman-area pumping wells. Additionally, although the correlation between fluctuations in offseason pumping and water level change in WSU 5 is acceptable, this is only a preliminary investigation of possible connection. Altering the pumping series by weighting individual pumping episodes according to the distance between WSU 5 and each pumping well may better represent theoretical response and provide a better match to observed water levels.

This comparison also should not be misinterpreted as a firm indication of connection between Moscow and Pullman. While it is likely that the intermediate-scale offseason fluctuations shown in basin water levels are generated from changes in pumping rates and volumes, both Moscow and Pullman-area pumping follows temporal patterns similar to those shown in the combined pumping rates in Figure 3.14. These fluctuations in pumping rate are determined by changes in demand, which as a function of weather and residence patterns, are comparable for both cities as well as individual pumpers, and occasionally for individual pumping wells.

### 3.5 Summary of basin water level analysis results

Analysis of basin water levels yielded the following observations:

- Many observation wells show direct hydraulic connections to nearby pumping wells, and in the case of DOE, to wells over 4.0 km distant. These hydraulic connections do not appear to depend solely on distance, pumping rate, and duration, implying the existence of varying degrees of heterogeneity, especially in the Moscow area.
- Long-term shapes and the magnitudes of summertime water level declines are very similar among wells located in Moscow and Pullman, including wells which were not found to respond to specific, short-term pumping stresses (WSU 5 and Cornelius). Palouse water levels show different seasonal characteristics, but exhibit annual declines of similar magnitudes to those measured in Moscow and Pullman wells.
- Long-term and annual declines in Clay Street are not consistent with those measured in Moscow, Pullman, and Palouse.
- Comparison of water levels in WSU 5, which does not show drawdown from short-term pumping episodes, to changes in combined pumping volumes indicates that this well does respond to basin pumping.

## Chapter 4 - Analytical Modeling of Aquifer Test Data

### 4.1 Introduction

Analytical modeling of observation well drawdown data and pumping well data was performed as part of this thesis investigation; this chapter describes this process and the results in detail. Section 4.2 describes the procedures used to estimate water level recovery from pre-test data and generate adjusted drawdown data for input into analytical modeling software. Section 4.3 presents the results of analytical modeling of aquifer test data on both short and long time scales. Section 4.4 presents an evaluation of low-magnitude water level fluctuations and investigates hydraulic connection among wells in Pullman, Moscow, and Palouse. Additional information on the analytical modeling software and the method chosen for aquifer test analysis are presented in Appendix E.

### 4.2 Dataset preparation for analytical modeling

A substantial proportion of the data analysis for this investigation was performed using AQTESOLV® (HydroSOLVE, Inc., 2007), an aquifer test analytical modeling computer program. Analytical modeling is the principal method for estimating aquifer properties from pumping test data; however, analytical solutions are limited by their reliance on certain idealized assumptions about the physical properties and temporal state of the aquifer. One of the most obvious limitations is the assumption of homogeneous and isotropic conditions within the pumped aquifer, which are both uncommon and difficult to verify empirically. Recent work by Butler (2008) and several other investigators indicates that analytical solutions are robust in averaging the effects of heterogeneities during large-scale aquifer tests; while the basalt aquifers of the Palouse Basin are vertically stratified with an unknown degree of areal variability, homogeneity is assumed for the purposes of analytical modeling, and is addressed on a case-by-case basis later in

this thesis. The irregular aquifer boundaries along the eastern, southern, and northern contacts between basalts and crystalline rock also create difficulties for classical analytical modeling. AQTESOLV uses image well theory and the principle of superposition to account for boundary effects, and relies on superposition to accurately model the extreme variable-rate pattern of pumping in the Palouse Basin over a long period of time.

Another significant issue that affects the design and implementation of aquifer tests in the Palouse Basin is related to the high frequency of large-volume groundwater withdrawals. Local water demand combined with limited storage tank capacity requires utility operators to pump for multiple episodes each day, often spread among several wells. Periods of down time rarely coincide among the four water providers in Moscow and Pullman, resulting in a constantly-evolving potentiometric surface which violates one of the key assumptions of analytical modeling. The absence of a true “static” water level, as an initial condition, complicates analysis, especially in a long-term test with numerous individual pumping episodes and multiple wells. The complex, scaled responses in water levels due to overlapping, transient cones of depression are too variable to remove using traditional pre-test antecedent trend corrections (Walton, 2007). The difficulties in estimating pre-test static water levels in the Palouse Basin have been described as a major obstacle and source of error by several previous investigators (Fiedler, 2009; McVay, 2007; Owsley, 2003).

To circumvent this potential issue, “static” water levels were approximated using a two-step process. First, at the beginning of the aquifer testing period, all of the Grande Ronde pumps in the basin (Moscow, Pullman, Colfax, Palouse, UI, and WSU) were shut off at a coordinated time with the objective of allowing water levels to recover as much as possible before pumping resumed. All Grande Ronde pumps were kept offline simultaneously for a minimum of 24 hours, with the first pump (WSU 4) resuming operation at 21:50 on 11/24/2009 (start of the aquifer test). This moment, when the first pump turned back on, became  $t=0$  for the long-term aquifer test, with elapsed time represented in days past 21:50 on 11/24/2009. The 24-hour period of water level

recovery, from  $t=-1$  day through  $t=0$ , became the basis for fitting a logarithmic curve, as shown in Figure 4.1 A. This logarithmic curve was chosen to approximate the continued recovery of water levels that would have theoretically occurred if pumping had not resumed at  $t=0$ .

For each selected observation well, the specific, logarithmic curve fit to pre-test data was subtracted from measured water levels, from  $t=0$  onward, to produce a series of “adjusted” water levels. This procedure was based on the principle of superposition, and the assumption that water level recovery would have continued unchanged throughout the test period. An example of the process of fitting a curve to the 24-hour pre-test water levels, and extrapolation at later times, is shown in Figure 4.1. Additional information related to the fitting of the logarithmic curve and process of adjusting water level data for each observation well is presented in Appendix D.

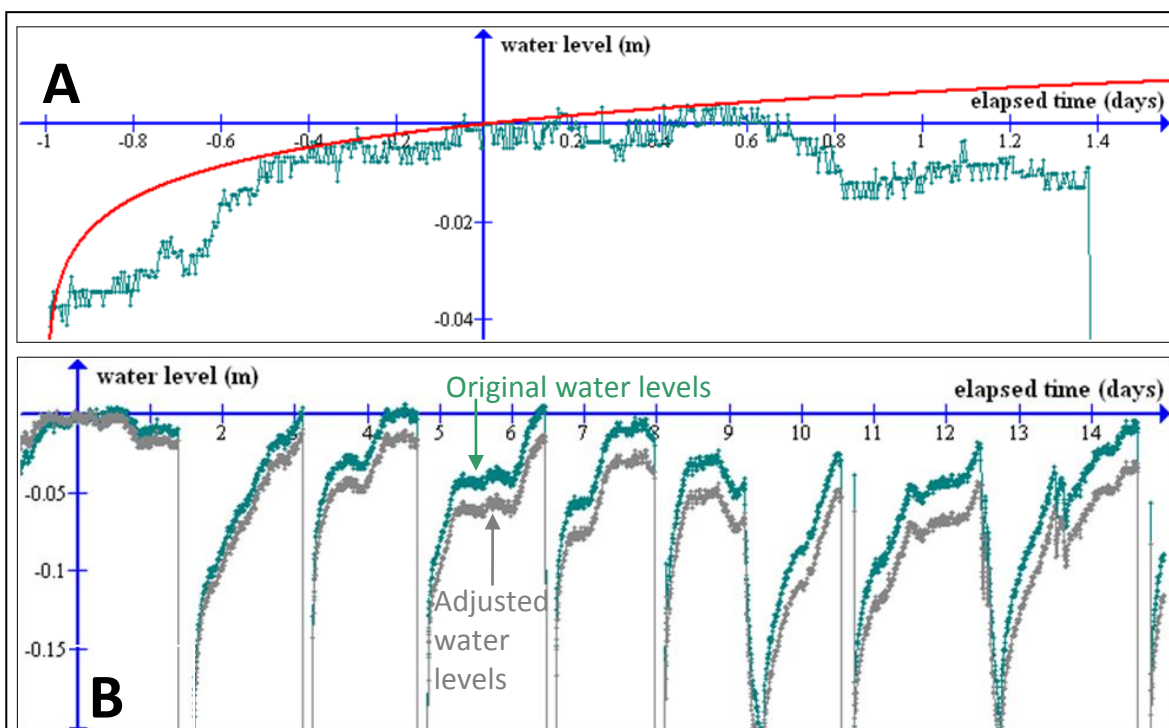


Figure 4.1. Removal of water level recovery trend from Palouse 1 observed water levels. The plots above show observed water levels in green with the logarithmic curve fit to pre-test data in red (A), and the “adjusted” water levels in grey below the observed water levels (B).

It is important to understand the limitations involved with the application of a single logarithmic equation, developed from 24 hours of recovery data, to estimate long-term static water levels. However, this method for removing a recovery trend from water level data is believed to be the most appropriate for this analysis, for several reasons:

- The trend correction is based on the observable phenomenon of water level recovery after the cessation of pumping, which theoretically continues through  $t=\infty$ . Traditional antecedent trend correction would be inappropriate for this analysis because the “background”, or “regional”, trends in Palouse Basin well water level data are derived from changes in pumping, the independent variable represented in analytical modeling; extrapolation of a seasonal trend in water levels to the entire period of the test would generate erroneous “adjusted” drawdown data.
- While a logarithmic curve will not exactly reproduce an analytical solution for recovery, it can approximate the general shape and magnitudes of both early and late time recovery.
- Some error is potentially introduced into adjusted water levels because of uncertainty in the application of the logarithmic curve approximation. However, the degree of error introduced into both early and late time adjusted data is likely less than the error that would be created by ignoring the effects of pumping which occurred before the beginning of the aquifer test. For the wells in this study, using the original, unadjusted drawdowns would result in a significant amount of negative drawdown at early times.

Due to the uncertainty involved with superposition of interpolated recovery trends, the majority of data analysis in this study was performed using the original water level data. The adjusted drawdown data are only required for the traditional aquifer tests analyses conducted using AQTESOLV. The potential magnitudes and implications of introduced errors are discussed in more detail in the following sections.

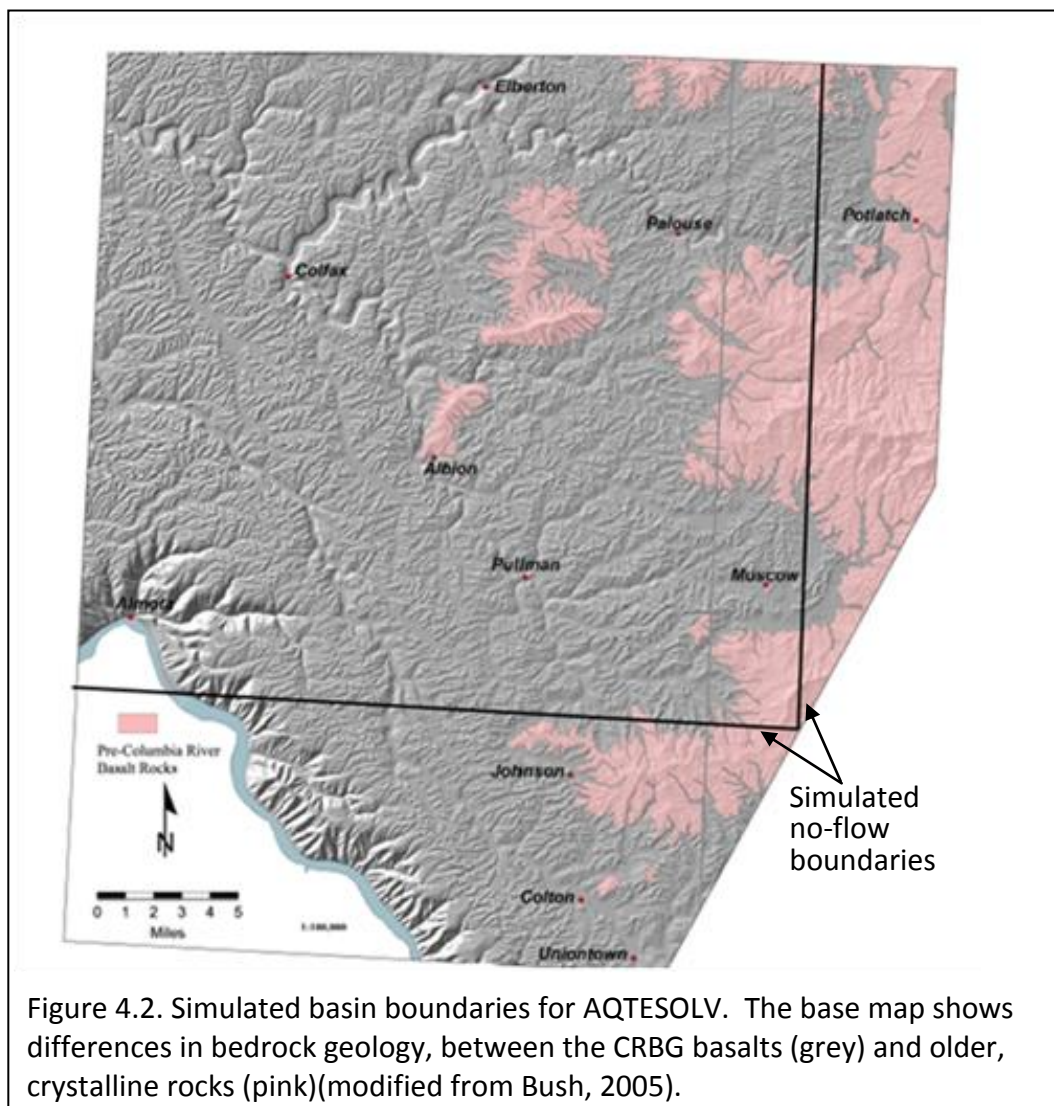
### 4.3 Analytical modeling of the 372-day test period

AQTESOLV was used to investigate the applicability of a specific analytical method for aquifer test analysis, consistent with the conceptual model for the aquifer, for simulating the magnitudes of both short-term and annual drawdown. Due to the paucity of sufficient field data to quantify geologic and hydrogeologic heterogeneities within the Grande Ronde, the layers of fractured basalt and associated interbedded sediments were treated as equivalent porous media. Aquifer tests conducted by Fiedler (2009) indicated that the Grande Ronde aquifer in the Moscow area responds to pumping as a bounded, leaky aquifer. A variation on this basic conceptual model was tested analytically using AQTESOLV.

The Hantush-Jacob (1955) method for analysis of transient drawdown within a leaky confined aquifer was selected for this investigation from among several other leaky-aquifer solutions. Most of the assumptions of this method are the same as those for other leaky methods, including an infinite homogeneous, uniformly leaky-confined aquifer; no storage within the well (infinitely small well radius); and vertical flow only within the uniformly-thick, homogeneous, overlying aquitard. The limiting assumptions of the Hantush-Jacob method are 1) no water is derived from storage in the aquitard, and 2) no head change occurs in the overlying source aquifer (i.e., infinite supply of water). The Hantush-Jacob method was selected because it is the simplest of the leaky-aquifer solutions, and uses a minimum of solved parameters to represent leakage. An advantage of the Hantush-Jacob solution for this aquifer test is that it is the least computationally-demanding leaky-aquifer method; the sheer computational requirements for the analysis of a long-term, multi-well, variable-rate data set in a leaky aquifer with multiple impermeable boundaries were a major limitation in this preliminary analysis.

AQTESOLV cannot accommodate variability in the shapes and lengths of aquifer boundaries, and is limited to linear (straight) boundaries with perpendicular intersections. The impermeable rocks bounding the Palouse Basin to the east and south

were approximated in AQTESOLV by two no-flow boundaries extending to infinity north and west from the coordinate point (503525, 5166500 UTM; Figure 4.2). Observation wells and pumping wells were modeled as fully-penetrating, with an aquifer thickness of 400 meters and a vertical/horizontal hydraulic conductivity ratio of one.



The model aquifer was unbounded to the north and west for this analysis; known partial boundaries such as Kamiak Butte, Smoot Hill, and the Snake River canyon could not be represented in the system as modeled. The unknown areal extent of the Palouse Basin, and the necessity to approximate spatially complex boundaries, are significant disadvantages for modeling the system using analytical aquifer testing software.

However, Butler and Tsou (2003) concluded that leakage in leaky-aquifer systems is controlled by pumping-induced hydraulic gradients, and as such is not dependent on aquifer size or the location of no-flow boundaries; this means that the total leakage volume in the system will be the same regardless of the size of the basin, and is a “scale-invariant” phenomenon. This condition, along with unknown aquitard thickness, would also introduce considerable variability into calculations of flux from leakage parameters derived by aquifer testing.

For each individual aquifer test analysis, pumping data were included for all municipal wells in the basin, excluding the Colfax pumping wells and Glenwood withdrawal wells due to the much lower groundwater elevations measured in the Colfax area, and the uncertainty of the connection between Colfax and the rest of the basin based on investigation of Clay Street well hydrographs. Observation well data used in AQTESOLV were generated by multiplying the adjusted water levels by (-1) to create drawdown. The AQTESOLV-generated type curve for each observation well was matched visually to the adjusted drawdowns for the full period of record, based on the best fits derived for shorter time windows selected from various sections of the data. Type curves for the Hantush-Jacob solution are defined by the aquifer parameters  $S$  (storativity),  $T$  (transmissivity) and  $B$  (leakage).  $B$  is defined as:

$$B = \sqrt{\frac{Tb'}{K'}}$$

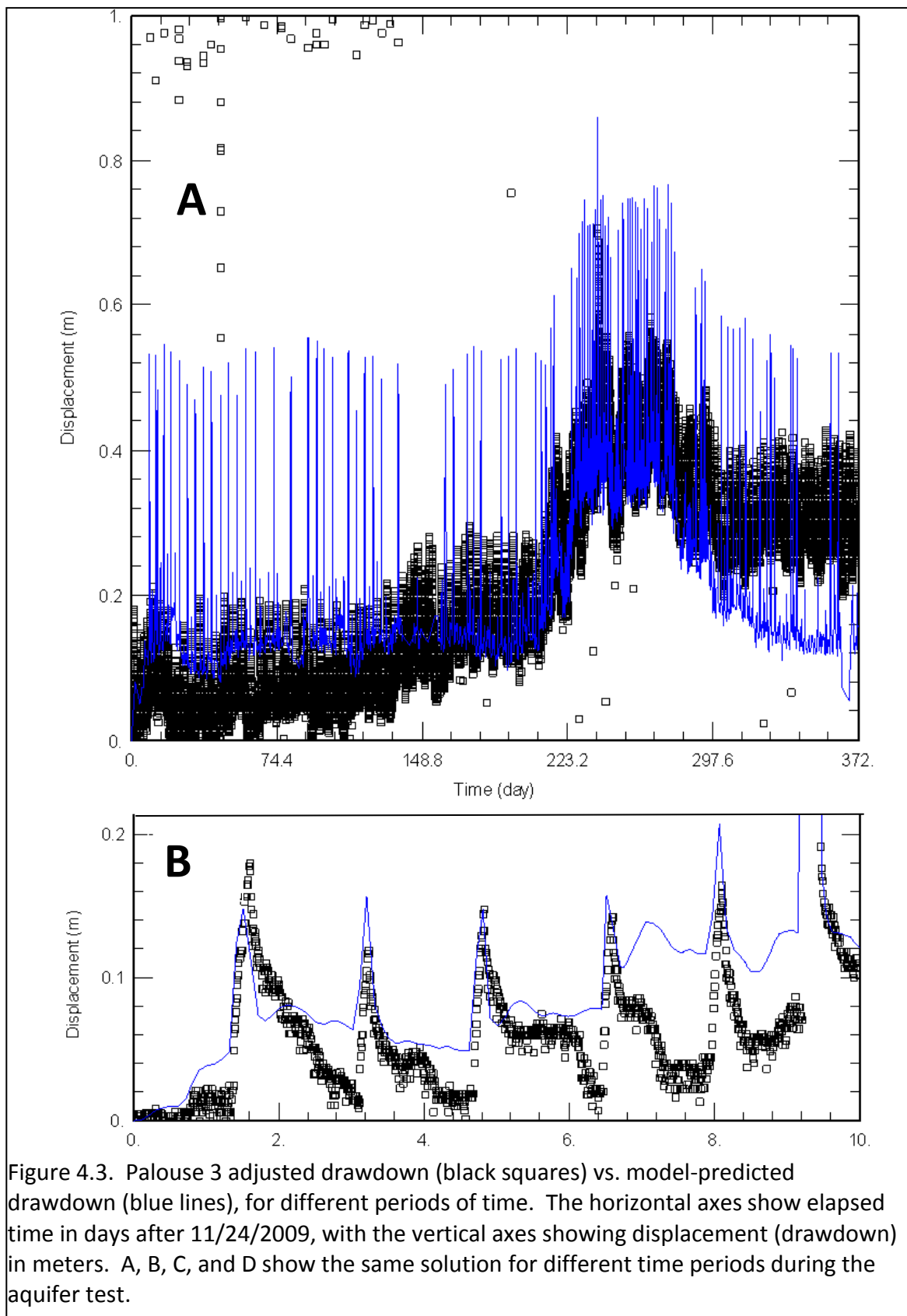
eq. 4.1

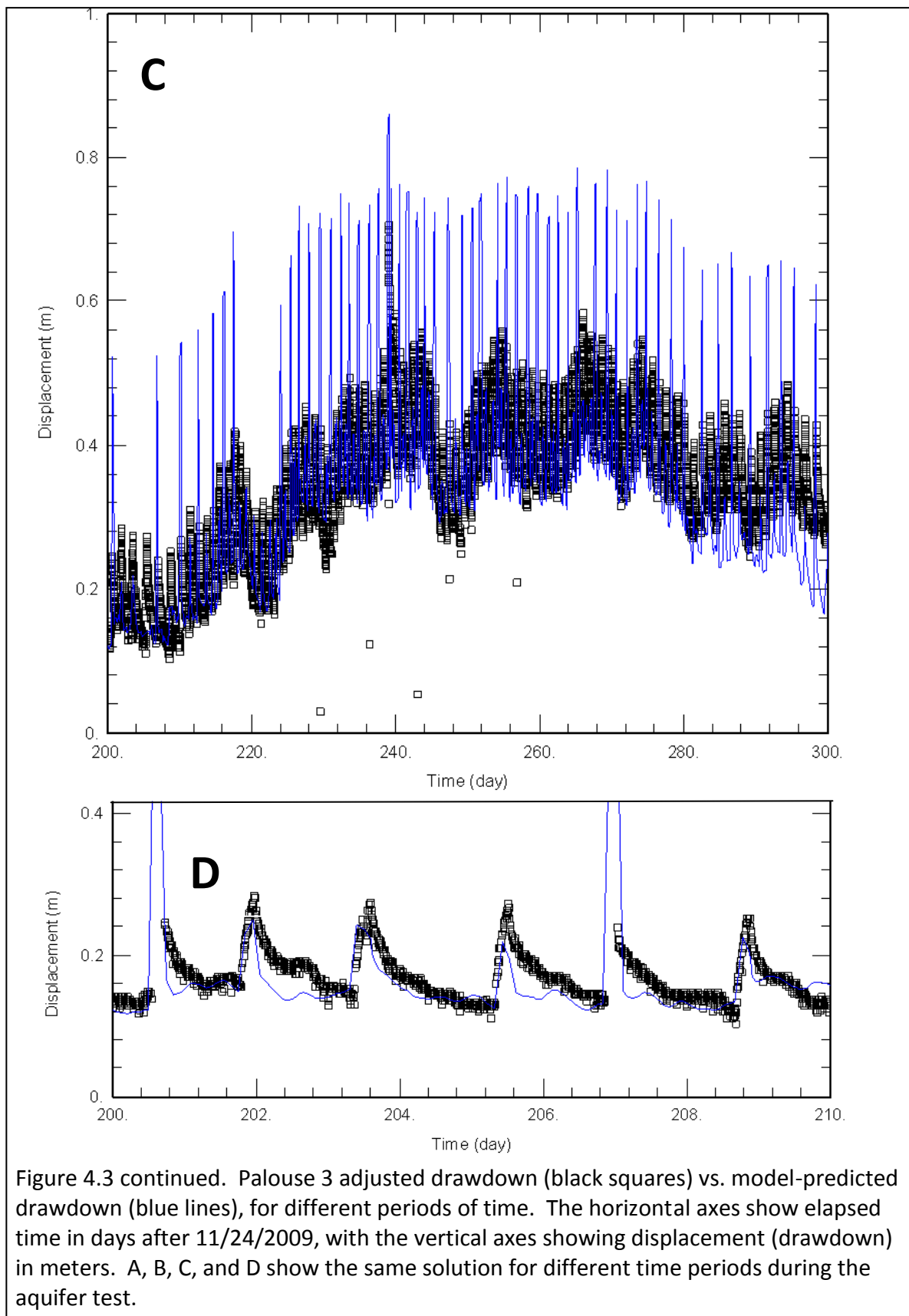
in which  $b'$  and  $K'$  represent the thickness and hydraulic conductivity, respectively, of the overlying aquitard. Although the leakage parameter  $r/B$  is traditionally presented, this parameter is different for each well in a multiple pumping-well aquifer test due to the inclusion of  $r$  (radius);  $B$  is held constant for the full, superposed, solution, and is the leakage parameter presented with the results of aquifer test analysis for this thesis. Presentation of  $B$  also allows easier comparison of different aquifer test results.

As explained in section 4.2, drawdown data used for AQTESOLV analyses have had barometric effects removed, and were also adjusted to account for the effects of continued recovery due to pumping which occurred before the start of the test. Elapsed time is presented as days past the beginning ( $t=0$ ) of the aquifer test on 11/24/2009. Two observation wells, Palouse 3 and IDWR 4, were selected for analytical modeling of the full test period. These wells were selected due to the length of the record, geographical placement within the test area, and the quality of the pre-test water level recovery trend match.

### Palouse 3

A visual curve match for the full period of record, based on examination of multiple windows from within this time period, was generated for the Palouse 3 adjusted drawdown data, with an estimated aquifer transmissivity ( $T$ ) of  $1.4 \times 10^4 \text{ m}^2/\text{day}$ , aquifer storativity ( $S$ ) of  $4.7 \times 10^{-5}$ , and leakage parameter ( $B$ ) of  $1.8 \times 10^4 \text{ m}$ . Figure 4.3 shows four plots of corrected drawdown versus elapsed time, for different periods of the record. Figure 4.3 A displays the drawdown data through 370 days. Figure 4.3 B,C, and D show different sections (windows) of the record as examples of the quality of the type curve match over both short-term and long-term time scales. Additional model runs were conducted to test other conceptual models, including several which excluded some or all Moscow and Pullman pumping wells or isolated Palouse in its own separate basin; however, the aforementioned boundary conditions appeared to yield the best visual type curve matches.



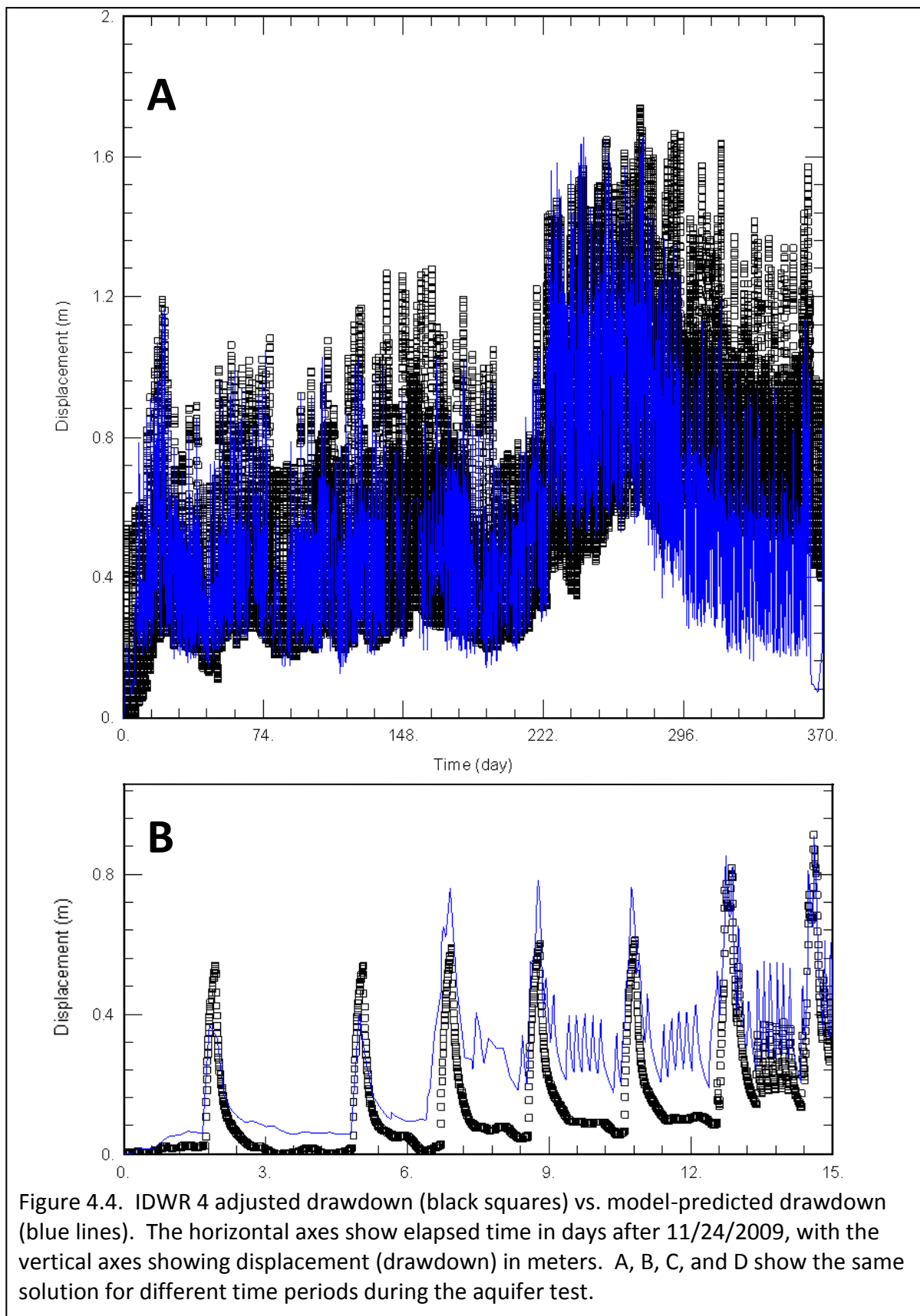


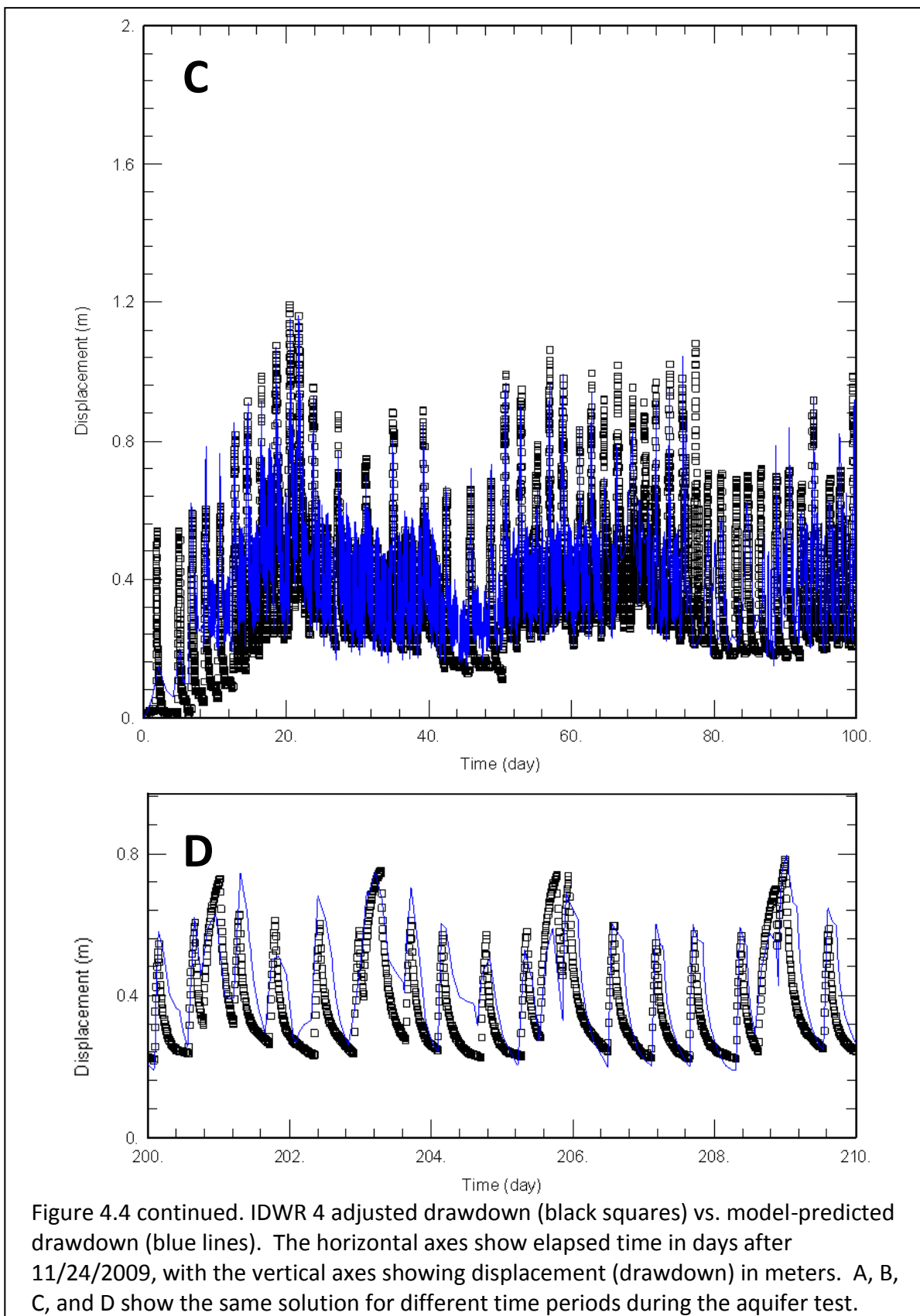
The analytical model appears to slightly overestimate drawdown from zero to 150 days, and also overestimate the system recovery from approximately 300 days until the end; however, the intermediate-scale fluctuations discussed in section 3.3 appear to be well represented by the simulated type curve. Several short-term features are evident in both the adjusted and predicted drawdowns. Some of these were identified earlier as being caused by pumping of Palouse 1 and Palouse 3 (section 3.3). Other, less obvious fluctuations observed in the Palouse 3 record could not be traced directly to any individual pumping well through comparison to HOB0 data, but were simulated to some degree by the model type curve (Figure 4.3 B, D). This suggests that these lower-magnitude fluctuations may be due to pumping of a combination of other basin wells. The drawdown caused by scheduled pumping of the Palouse 3 well (high outliers shown in Figure 4.3 A) was underestimated by the model because it does not account for well loss, a process in which drawdown in a pumping well increases beyond predicted values due to turbulence within and near the pumped well. These large drawdown values continue past 150 days, for the full period of the test, but are not shown in Figure 4.3 A due to the scale of the figure.

#### IDWR 4

Analytical modeling yielded a visual match to adjusted drawdown for IDWR 4 with an estimated aquifer transmissivity (T) of  $6050 \text{ m}^2/\text{day}$ , storativity (S) of  $7.7 \times 10^{-5}$ , and leakage parameter (B) of  $7.8 \times 10^4 \text{ m}$ . Generated plots are shown in Figure 4.4.

Similarly to Palouse 3, the model results over predict system recovery after 290 days into the test (Figure 4.4 A), but closely simulate intermediate-scale ups and downs in the record (Figure 4.4 C). Short-term drawdown from UI 4 and Moscow 9 pumping is also predicted. The model predicts drawdown due to pumping of Moscow 6 and Moscow 8 (Figure 4.4 B, 7 to 13 days elapsed time), which does not exist in the real, measured data. The prediction of significant drawdown due to pumping in Moscow 6 and 8, which does not exist in the observed data, is an example of the failure of the analytical model to account for significant local heterogeneities.





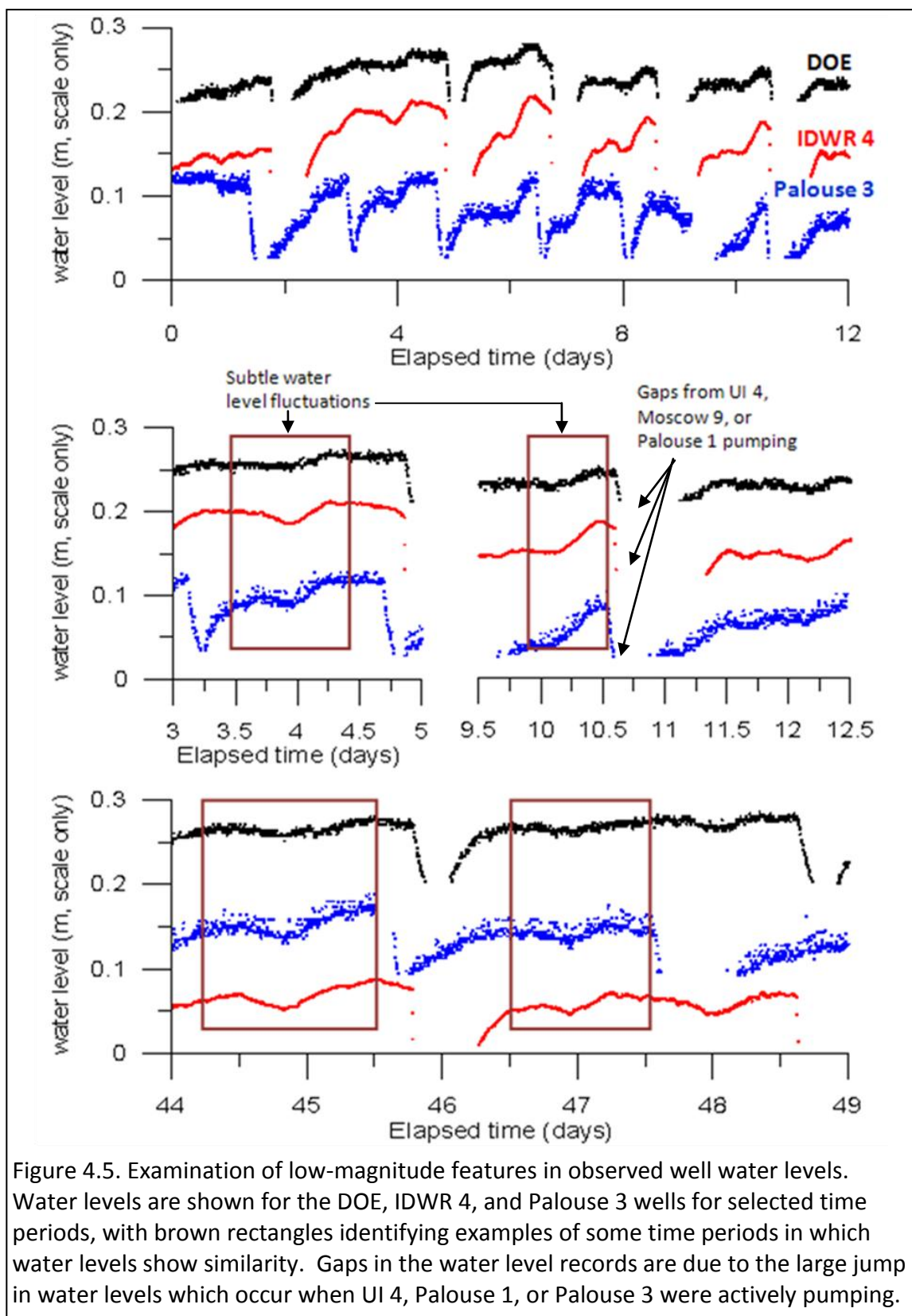
### Discussion of analytical modeling of 372-day period

Results of analytical modeling suggest that the Hantush-Jacob leaky-aquifer model as used in this investigation is capable of estimating long-term and short-term drawdown in IDWR 4 and Palouse 3. However, this does not exclude the possibility that another mathematical solution or model may also provide an equally acceptable match to observed water levels.

Several of the discrepancies between the model results and observed responses in Palouse 3 and IDWR 4 are assumed to be caused by heterogeneities and the required simplification of complex boundaries within the model. Specific responses to known heterogeneities include these: IDWR 4 does not respond as predicted to pumping in nearby wells Moscow 6 and Moscow 8, and the irregular boundaries and limited aquifer extent of Kamiak Gap likely exert a large influence on drawdown in Palouse. The analytical model over predicts aquifer recovery after the period of summertime pumping, between approximately 280 and 372 days elapsed time, for both wells. Two possible explanations for this discrepancy could be related to the assumption in the Hantush-Jacob (1955) method that water levels in the unpumped source aquifer are constant, or that the logarithmic correction applied to the original data is not accurate at late time. The sensitivity of boundary placement was not evaluated as part of this thesis investigation; however, these results do not indicate that the inclusion of Palouse within the boundaries of the aquifer is incorrect.

#### 4.4 Investigation of low-level water level features in DOE, IDWR 4, and Palouse 3

Numerous low-magnitude fluctuations were identified in the water level records for IDWR 4, DOE, Palouse 1, and Palouse 3. These features could not be traced to any individual pumping well, but were predicted to some degree by the Hantush-Jacob solution with superposition for Palouse 3 (Figure 4.3 B, 6 to 10 days elapsed time) and to a lesser extent for IDWR 4. Close examination of these features reveals that they occur at approximately the same time in each well, and at similar magnitudes in Palouse and



IDWR 4, but are slightly attenuated in DOE (Figure 4.5). These features are only visible during periods when UI 4 and Moscow 9 are not pumping (for DOE and IDWR 4), or Palouse 1 and Palouse 3 are not pumping (for Palouse 3).

These features suggest that DOE, IDWR 4, and Palouse 3 water levels are responding to pumping of the same specific well or a combination of wells. The AQTESOLV-generated type curves (Figure 4.3 B, D) indicate that the pumping wells which create these subtle drawdown features are among those included in the analysis. This in turn implies that a hydraulic connection exists between Moscow or Pullman and Palouse. To rule out the possibility that these features could have been caused by imprecise barometric correction of water levels, these fluctuations were directly compared to corresponding pressure changes. Based on this examination, it does not appear that barometric pressure is the source of these features; in fact, these fluctuations were concealed in the original data by larger-magnitude barometric pressure-induced changes, until these were removed through barometric correction of water levels.

Analysis of drawdown data collected early during the test gives additional evidence that IDWR 4 and Palouse 3 respond to pumping of Pullman area wells, as shown in Figure 4.6. Fluctuations in the adjusted drawdown data shown for Palouse 3 and IDWR 4 are roughly predicted by the Hantush-Jacob solution with superposition for multiple pumping wells using the same aquifer parameter values identified during analysis of the complete record (section 4.3). The first Moscow-area well to pump was UI 4, which began pumping at 1.74 days into the test. The only Grande Ronde wells which began pumping during the first 1.3 days of the test were WSU 4 (0.0 days elapsed time), Pullman 7 (0.5 days), Pullman 5 (0.5 days), and WSU 8 (0.14 days); these wells then turned on and off several times during the time periods shown in Figure 4.6 (Table 4.1). The large drawdowns shown in Figure 4.6 are due to pumping in Palouse 1 and UI 4; these pumping wells are known to cause significant drawdown in Palouse 3 and IDWR 4, respectively.

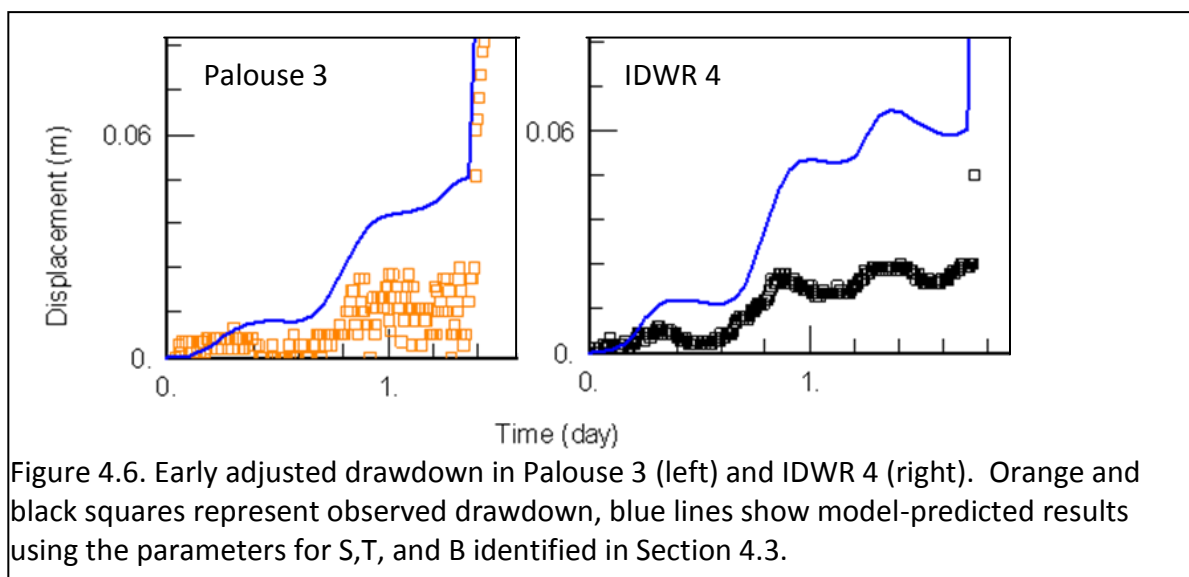


Table 4.1 Early-test pumping periods, through 1.6 days elapsed time

Elapsed time at pump on (days)	Well ID	Time on (hrs)	Total pumped (gal)
0.00	WSU 4	4.46	385000
0.14	WSU 8	0.37	54000
0.49	Pullman 5	6.55	661000
0.53	Pullman 7	6.57	690000
0.65	WSU 8	1.47	211000
0.94	Pullman 5	0.82	82000
1.00	WSU 4	3.43	296000
1.09	Pullman 7	2.24	236000
1.15	WSU 8	1.35	194000
1.28	Pullman 5	0.90	91000
1.38	Palouse 1	5.44	230000
1.55	Pullman 7	2.67	281000
	<b>Totals:</b>	<b>36.27</b>	<b>3.41 MGal</b>

Figure 4.7 presents the same adjusted drawdown data for Palouse 3 and IDWR 4 shown in Figure 4.6, but with different aquifer parameters determined by convergence of the Hantush-Jacob solution to early-time drawdown data (0 days through 1.3 for Palouse 3 and Palouse 1, and 0 days through 1.6 days for IDWR 4). Early-time adjusted drawdown data are also shown for Palouse 1; analysis of long-term drawdown in Palouse 1 was not performed due to a shorter length of water level record for this well.

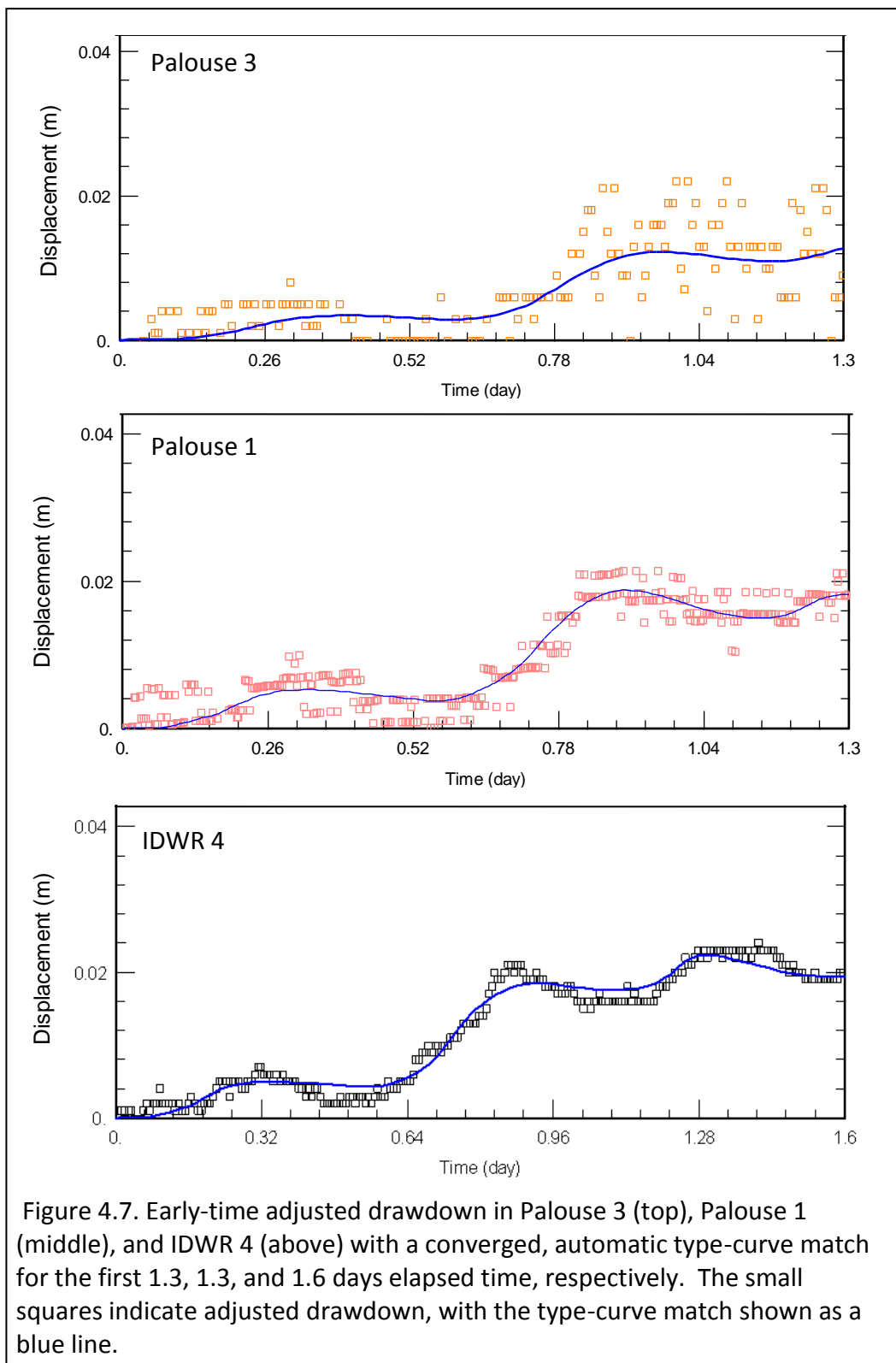


Figure 4.7. Early-time adjusted drawdown in Palouse 3 (top), Palouse 1 (middle), and IDWR 4 (above) with a converged, automatic type-curve match for the first 1.3, 1.3, and 1.6 days elapsed time, respectively. The small squares indicate adjusted drawdown, with the type-curve match shown as a blue line.

Figure 4.7 illustrates that IDWR 4 and Palouse 1 water levels clearly respond to pumping of Pullman-area wells, even if the total drawdown from pumping of these wells is small (<3 cm). Palouse 3 water levels also appear to respond to Pullman-area pumping; however, the amount of noise present in the Palouse 3 masks this evidence to some degree. It is possible that the adjustment procedure used to account for continued water level recovery may have exaggerated drawdown for the early test period; however, even without adjustment of water level data, water levels in Palouse 1 still showed measureable drawdown prior to 1.3 days elapsed time (Figure 4.1 B).

The solution shown for Palouse 3 converged for an aquifer transmissivity (T) of  $1.8 \times 10^4 \text{ m}^2/\text{day}$ , aquifer storativity (S) of  $7.2 \times 10^{-5}$ , and a leakage parameter (B) of  $1.0 \times 10^4 \text{ m}$ . The solution shown for IDWR 4 converged for an aquifer transmissivity (T) of  $3.8 \times 10^4 \text{ m}^2/\text{day}$ , an aquifer storativity (S) of  $2.7 \times 10^{-4}$ , and a leakage parameter (B) of  $1.1 \times 10^4 \text{ m}$ . The solution shown for Palouse 1 converged for an aquifer transmissivity (T) of  $3.4 \times 10^4 \text{ m}^2/\text{day}$ , an aquifer storativity (S) of  $6.7 \times 10^{-5}$ , and a leakage parameter (B) of  $1.4 \times 10^4 \text{ m}$ . As stated above, these aquifer parameters were obtained through convergence of the AQTESOLV automatic match of the Hantush-Jacob leaky-confined aquifer analytical solution (Gauss-Newton linearization method; HydroSOLVE, Inc, 2007) to a limited time period; while they provide a convincing match to early data, they do not accurately represent short-term drawdown resulting from pumping in nearby wells or annual drawdown.

Table 4.2. Estimated aquifer parameters

Well ID	Estimated Parameters			
	S	T ( $\text{m}^2/\text{day}$ )	B (m)	K'/b' (1/day)
IDWR 4 (372 days)	$7.7 \times 10^{-5}$	$6.1 \times 10^3$	$7.8 \times 10^4$	100
Palouse 3 (372 days)	$4.7 \times 10^{-5}$	$1.4 \times 10^4$	$1.8 \times 10^4$	43
IDWR 4 (early time)	$2.7 \times 10^{-4}$	$3.8 \times 10^4$	$1.1 \times 10^4$	314
Palouse 1 (early time)	$6.7 \times 10^{-5}$	$3.4 \times 10^4$	$1.4 \times 10^4$	170
Palouse 3 (early time)	$7.2 \times 10^{-5}$	$1.8 \times 10^4$	$1.0 \times 10^4$	180

The inability to obtain good type curve matches to the adjusted drawdown for all time periods may be due to the inadequacy of certain assumptions about the system in the model, specifically homogeneity, isotropy, and simplified, linear boundaries; however, the actual cause is unknown.

A potential source of error in this analysis is derived from the fact that AQTESOLV is unable to ignore any noise in the data, or distinguish between true drawdown and drawdown caused by “quantification error” of the data loggers for variations less than approximately 3 mm. Consequently, fluctuations in observed and adjusted drawdown on the order of approximately 0.003 m may be a result of data logger noise. Any errors in the removal of barometric effects or the “adjustment” process used to account for continued water level recovery would also affect the results of analysis of aquifer test data.

## Chapter 5 - Estimation of Basin Storativity

### 5.1 Introduction

A primary objective of this research was to estimate the storativity ( $S$ ) of the Grande Ronde aquifer system. Storativity is defined as the volume of water extracted per unit surface area of the aquifer, per unit change in head. In confined aquifers such as the Grande Ronde, the volume of water released from storage is controlled by two phenomena, the expansion of water, and the reduction of pore spaces by compression of the aquifer matrix. Consequently, storativities for confined aquifers can be orders of magnitude smaller than those for unconfined systems, generally falling within the range of  $10^{-3}$  to  $10^{-5}$ . Accurate aquifer storativity estimates are essential for proper groundwater resource evaluation and management.

This chapter presents three different approaches to estimating the storativity of the Grande Ronde: examination of previous research and models, estimation based on barometric efficiency, and parameter estimation based on analytical modeling. Also included in this chapter is a discussion of the implications of aquifer storativity with respect to determining the size of the basin and quantifying recharge to the Grande Ronde aquifer.

### 5.2 Previous research

Numerous local estimates of Grande Ronde aquifer storativity ( $S$ ) are available both regionally and locally from previous aquifer tests, well construction reports, and groundwater model calibrations. In the CRBG near Hanford, WA, La Sala and Doty (1971) reported  $S$  between  $6 \times 10^{-4}$  and  $1.4 \times 10^{-5}$  for aquifer tests. Most aquifer tests conducted in the Palouse Basin have predicted values of  $S$  between  $10^{-3}$  and  $10^{-5}$ , typically in the lower half of this range. Storativities used in groundwater models of the Grande Ronde aquifer are generally higher than those from aquifer testing, and towards the upper

bound for confined aquifers (Table 5.1). The larger values of  $S$  calculated through numerical modeling result from calibration in combination with other aquifer information; Barker (1979) indicated that decreasing the aquifer storage from the calibrated values “caused unacceptable differences between simulated and measured water levels.” Some recent research has attempted to model the Grande Ronde as a dual-storativity fractured rock system, with values of  $S$  of  $10^{-3}$  and 0.022 for short-term and long-term behavior, respectively (Fiedler, 2011).

Table 5.1. Grande Ronde aquifer storativity estimates from previous Palouse Basin investigations

Research	Storativity	Transmissivity (m <sup>2</sup> /day)	Basis
McVay (2007)	$7.5 \times 10^{-5}$	$1.8 \times 10^4$	DOE, responding to UI3 and M9 pumping
	$6.7 \times 10^{-5}$	$2.4 \times 10^4$	DOE, second test
	$2.2 \times 10^{-4}$	$2.1 \times 10^4$	Champion Electric, responding to UI3 and M9 pumping
	$2.4 \times 10^{-3}$	$2.8 \times 10^4$	Premix response
	$9.5 \times 10^{-4}$	$1.3 \times 10^5$	WSU Test
	$4.2 \times 10^{-3}$	$1.3 \times 10^5$	WSU Test, responding to Pullman pumping
	$5.4 \times 10^{-6}$	$6.5 \times 10^3$	Moscow 9
Owsley (2003)	$1.9 \times 10^{-5}$	$8.0 \times 10^2$	Moscow 6, responding to M8 pumping
Ralston (2000)	$1.0 \times 10^{-4}$	$2.7 \times 10^4$	Palouse 3, responding to Palouse 1 pumping
Golder (2001)	$7.9 \times 10^{-7}$ - $1.6 \times 10^{-6}$	$2.3 \times 10^4$ - $4.7 \times 10^4$	Pullman 7 pump test
Golder (2008)	0.006	$1.2 \times 10^5$	Pullman 8 pump test
Barker (1979)	0.005- 0.006	variable	MODFLOW Model calibrated values
Lum et al. (1990)	0.001		Model calibrated values
Smoot (1987)	0.0001		Model-calibrated values

### 5.3 Estimation of aquifer storativity ( $S$ ) from barometric efficiency ( $BE$ )

Barometric efficiency can be used as a tool to estimate  $S$ , based on the relationship between barometric efficiency and aquifer matrix compressibility. The equation derived by Jacob (1940) is shown below, where  $n$  is porosity,  $\gamma_w$  is the unit weight of water ( $9800 \text{ N/m}^3$ ),  $b$  is aquifer thickness,  $E_w$  is the elastic modulus of water ( $2.2 \times 10^9 \text{ Pa}$ ),  $BE$  is barometric efficiency, and  $S$  is aquifer storativity.

$$S = \frac{n\gamma_w b}{E_w BE}$$

eq. 5.1

Two of the input variables, thickness and porosity, are poorly defined for the Grande Ronde aquifer. Thickness was estimated from a sample of well construction reports based on the saturated thickness of the Grande Ronde with no significant head change vertically throughout. In the eastern part of the basin, thickness is relatively small, and is controlled by the contact with sloped, underlying basement rocks. The well Moscow 6 is bottomed in granite, and the approximate thickness of the Grande Ronde aquifer in this well is approximately 200 m (Fiedler, 2009). The deepest well in the Palouse Basin is WSU 7; no significant head change was encountered during well drilling from approximately 224 ft (69 m) bgs to 1850 ft (564 m) bgs, implying that vertical flow does not occur and that producing zones in this section of the Grande Ronde basalts are hydraulically connected, with a confined aquifer thickness of approximately 500 m (Ralston, 1987).

The porosity of basalt exhibits a large range of values due to the variability in structural characteristics between the dense, massive interiors of flows and the fractured and vesicular flow tops and bottoms. General ranges are identified as 5%-50% (Freeze and Cherry, 1979), or 3%-35% (Domenico and Schwartz, 1990). Additional site-specific investigations have been completed to better confine porosity estimates of the CRBG. Reidel et al. (2003) cites laboratory tests conducted by Loo et al. (1984), which measured porosities of 7%-30% in flow top core samples, but notes that these values may

overestimate true conditions. Abundant small fractures (one to 37 per meter) have been documented in CRBG basalts. However, these fractures are mostly filled with secondary minerals, with 2.5-6% of the original volume available for groundwater flow (US DOE, 1986). Davis (1969) identified a range of 0.8%-11.4% porosity for dense to porous massive basalt.

Table 5.2 displays estimated values of S for the Grande Ronde aquifer based on BE=1 for WSU 7, for a range of possible porosity and thickness values. The most likely ranges of thickness and porosity place S for the Grande Ronde aquifer within approximately one order of magnitude, between  $3 \times 10^{-5}$  and  $3 \times 10^{-4}$ .

Table 5.2. Sample Grande Ronde aquifer S estimated from BE, for selected values of thickness and porosity

	thickness (m)		
porosity	200	400	600
0.01	8.9E-06	1.8E-05	2.7E-05
0.05	4.5E-05	8.9E-05	1.3E-04
0.1	8.9E-05	1.8E-04	2.7E-04
0.15	1.3E-04	2.7E-04	4.0E-04

#### 5.4 Analytical modeling storativity (S) estimates

The primary goal of analytical modeling of aquifer test data is to calculate aquifer parameters, most importantly T and S. However, the particular circumstances surrounding aquifer testing in the Palouse Basin complicate estimation of S in particular. The most significant source of error in calculating S through analytical methods is related to the assumption of homogeneity. The validity of S estimates calculated from aquifer test data in spatially-heterogeneous environments has been addressed by numerous studies; the general consensus is that estimates of S derived from traditional analytical treatment of pumping and drawdown data represent some average of the true S over the area of interest, with certain limitations.

Schad and Teutsh (1994) described aquifer parameter estimates in heterogeneous settings as “semi-quantitative,” and advised the use of numerical

methods in environments with known heterogeneities. Sanchez-Vila et al. (1999) concluded that estimates of  $S$  can show large spatial variability in a well field even when the true storativity of the aquifer is constant, and that the geometric mean of  $S$  estimates from different observation wells was the closest approximation to the true  $S$  of the system. These observations were qualified by Wu et al. (2005), who indicated that spatially-variable  $S$  estimates are primarily an average of the true  $S$  within portions of the aquifer spatially located between the observation well and pumping wells, while estimates of transmissivity reflect the average value for the entire cone of depression. Wen et al. (2010) supported these conclusions with a field test, and showed that  $S$  estimates, while spatially-variable over as much as an order of magnitude, do not appear to change over time.

The methodology for this aquifer test was atypical, in that it included elements of traditional aquifer testing (short time intervals between measurements), with a focus on characterizing aquifer behavior for longer time scales. Transient water level responses linked to an evolving cone of depression from pumping are essential for estimating  $S$ ; averaging of pumping rates or water level responses collected over longer periods of time is insufficient to confine  $S$  estimates (Maurer and Halford, 2006). The leaky-confined Grande Ronde aquifer model used for data analysis (Hantush and Jacob, 1955) introduces a source of possible error, in that long-term variable rate tests are not sensitive to  $S$  at late time because leakage confounds estimates of this parameter. Constraining  $S$  in short-term tests in heterogeneous environments is subject to the duration of the test (Osiensky et al., 2000).

Despite the uncertainty associated with estimating  $S$  in heterogeneous environments, the aquifer system parameters ascertained in this study from application of the Hantush-Jacob leaky-confined aquifer solution fall within the expected ranges for describing the Grande Ronde aquifer. The long-term values shown in Table 5.3 were generated from a visual match to data for the full period of the aquifer test (described in section 4.3). The early-time values were generated from independent, converged, AQTESOLV automatic matches to the first 1.3 days (Palouse 1 and Palouse 3) and 1.6 days

(IDWR 4) of elapsed time. These values fall within the range of possible  $S$  values identified in section 5.3.

Table 5.3. Aquifer test estimated  $S$  values

Well ID	Estimated Storativity	
	Long-term (section 4.3)	Early-converged (section 4.4)
Palouse 1	N/A	$6.7 \times 10^{-5}$
Palouse 3	$4.7 \times 10^{-5}$	$7.2 \times 10^{-5}$
IDWR 4	$7.7 \times 10^{-5}$	$2.7 \times 10^{-4}$

### 5.5 Implications of estimated storativity ( $S$ ) values

A simple model of fluxes and storage in the Grande Ronde aquifer is useful for testing conceptual models and understanding how changing estimates for system parameters affects recharge estimates. Eq. 5.2 relates the volume of water pumped ( $PV$ ) to aquifer storativity ( $S$ ), basin size ( $A$ ), water level decline ( $\Delta h$ ), and recharge ( $R$ ):

$$PV = SA (\Delta h) + R$$

eq. 5.2

On an annual time scale, the values of two of these variables are known: the total volume pumped from the aquifer, and water level decline (2600 MGal and 0.38 m, respectively, for 2009; PBAC, 2010). With these variables held constant, and by setting  $S$  to  $1 \times 10^{-4}$  (within the range discussed earlier in the chapter), eq. 5.2 defines an explicit linear relationship between basin size and total recharge. Using the initial boundaries hypothesized by Bush, shown on the map of the Palouse Basin (Figure 1.1) with the corresponding basin size of 1300 km<sup>2</sup>, the total recharge to the Grande Ronde should be 2590.4 MGal (0.76 cm of areal recharge across the basin), only 9.6 MGal less than the total amount withdrawn. As basin size decreases, recharge volumes must increase, but areal recharge will still be small, even with a very small basin. For example, a hypothetical basin size of 270 km<sup>2</sup>, approximately  $1/5$  of the size of the basin as described by Bush, would require only 7.6 MGal more of annual recharge (a total of 2598), with an areal recharge rate of 3.6 cm/year. In addition, it is clear from eq. 5.2 that the overall

deficit between pumped volumes and recharge must be relatively small in order to keep basin size within a realistic range.

As stated above, eq. 5.2 is a very simple model of the system, and does not account for outflow or regional discharge or local variations in water level declines. However, the objective of this analysis is to emphasize that low values for  $S$  are not inconsistent with reasonable values for both basin size and recharge. Based on eq. 5.2, the following observations are significant:

- A low average storativity value for the Grande Ronde aquifer (in this case 0.0001) is reasonable in relation to estimates of areal recharge and basin size. Calculated areal recharge is reasonable even for relatively small possible basin sizes.
- The difference between outflow and inflow (annual deficit) is very small in comparison to total flows, meaning that recharge replaces most of the volume removed by pumping.

## Chapter 6 - Conclusions and Recommendations

### 6.1 Introduction

Analysis of water levels measurements and pumping data collected during a year-long aquifer test of the Grande Ronde aquifer in the Palouse Basin revealed important information about the hydrogeology of the area.

### 6.2 Specific conclusions

#### Barometric efficiency

- Barometric pressure changes can cause fluctuations in water level of up to 0.3 m. Removal of barometric effects on groundwater levels is imperative for identifying real changes in water level due to pumping, recharge, or other potential effects.
- Barometric efficiencies were calculated for each observation well monitored during the test using a variety of methods. Estimated barometric efficiencies of Grande Ronde wells range between 0.9 and 1.

#### Well connections

- Water levels in the WSU Test well respond to pumping of Pullman 7, Pullman 8, WSU 4, WSU 7, and WSU 8.
- WSU 7 water levels respond to pumping of Pullman 7, Pullman 8, WSU 4, and WSU 8.
- WSU 8 water levels respond to pumping of WSU 4, WSU 6, and WSU 7.
- Pullman 4 water levels respond to pumping of Pullman 7 and WSU 7.
- IDWR 4 water levels respond to pumping of Moscow 9 and UI 4, but do not appear to respond to pumping of Moscow 6 or Moscow 8.
- Water levels in the DOE well respond to pumping of Moscow 9 and UI 4, but do not exhibit measureable responses to pumping of individual Pullman-area wells.

- Combined pumping of Pullman-area wells (WSU 4, WSU 8, Pullman 5, and Pullman 7) causes measureable drawdown in IDWR 4, Palouse 1, and Palouse 3 water levels. Drawdown measured during the first 1.3 days of the aquifer test in these wells was predicted by the Hantush-Jacob leaky-aquifer solution with superposition for multiple pumping wells (independently for each observation well).
- Water levels in WSU 5 do not show measureable drawdown in response to pumping of individual wells for their usual durations of pumping; however, water levels in WSU 5 respond to overall fluctuations in combined basin pumping on a longer time scale (days-to-weeks).

#### Aquifer storativity

- Overall storativity of the Grande Ronde aquifer falls within the range of  $3 \times 10^{-5}$  to  $3 \times 10^{-4}$ , based on analysis of aquifer test data and estimation of storativity from barometric efficiencies.

### 6.3 General Conclusions

Interpretation of aquifer test results in the context of previous research and other hydrogeologic information available for the Palouse Basin yielded the following general conclusions related to area hydrogeology:

- Observed connections among wells located in Pullman, Moscow, and Palouse, as well as interpretation of groundwater elevation data and water level trends, indicate that these areas are hydraulically connected. The observed well responses preclude the existence of a hydraulic barrier between Moscow and Pullman, and demonstrate hydraulic connection of the pumping centers located in Moscow and Pullman through the Kamiak Gap to the city of Palouse.
- Water levels measured in the Colfax Clay Street well exhibit significantly smaller annual declines and long-term declines than water levels measured in Pullman, Moscow, and Palouse. This information, combined with groundwater elevation

data which show a steeper gradient between Pullman and Colfax, indicates a decrease in T between these cities.

- Direct assessment of the size of the Palouse Groundwater Basin was not possible with the data collected for this thesis investigation. Data derived from the aquifer test were also insufficient to delineate the location of any boundaries north of Palouse, or west of Pullman.
- Certain differences between adjusted drawdown and drawdown predicted by the analytical model (Hantush-Jacob with superposition) suggest that a significant degree of spatial heterogeneity exists within the Grande Ronde aquifer. These heterogeneities limit the applicability of aquifer-test-derived parameters in calculating complete system behavior from pumping data.
- Analysis of aquifer test data with the Hantush-Jacob solution with superposition for multiple pumping wells demonstrates that the Grande Ronde aquifer responds to pumping stresses as a leaky-confined aquifer system.
- Results from analytical modeling suggest that vertical leakage has a significant effect on water levels in the Grande Ronde aquifer. In addition, inflow/outflow calculations indicate that a substantial amount of recharge reaches the Grande Ronde aquifer annually.

#### 6.4 Review of methodology and recommendations for future work

##### Evaluation of methodology

Collection of observation well data on a 5-minute increment for a period of a full year was helpful for investigating small-scale responses over time, but there were also significant disadvantages associated with the substantial amounts of time and resources required for collecting, processing, and manipulating such a large volume of monitoring data. It is difficult with any project to determine the level of detail that is required; while it is true that an even smaller time increment would have provided additional information for delineating transient responses, five-minute data appears to have been sufficient for the

analyses performed as part of this thesis. HOBO® on/off motor-monitoring devices proved to be a valuable and convenient source of accurate pumping data.

Analytical modeling of the Grande Ronde aquifer test data with the Hantush-Jacob solution with superposition for multiple pumping wells was instrumental for making generalized conclusions concerning the Grande Ronde. However, analytical models are limited in their ability to represent heterogeneities such as the Kamiak gap and the high-T zone that appears to extend from DOE to Moscow 9 and UI 4. In addition, the spatial distribution of Grande Ronde wells within the Palouse Basin was a major limitation. With the exception of the DOE well, existing monitoring wells are predominantly clustered in populated areas. This in turn requires the qualification of conclusions from the aquifer test, in that observed conditions may only be valid for the areas expressly monitored.

#### Recommendations for further study

While traditional aquifer testing has been important for delineating aquifer connections and estimating local aquifer properties, continuation of aquifer testing and subsequent analytical modeling of test results in the future is not likely to yield any additional useful information except in estimating aquifer parameters for new observation or pumping wells. Further refinement of transmissivity and storativity values is possible with continued aquifer testing, but these new values will be subject to the same heterogeneity-based uncertainties that affect current estimates. Obtaining slightly better T and S estimates is not critical for long-term basin management because of greater uncertainty in other parameters which cannot be resolved through analytical modeling, such as recharge rates and basin extent. Numerical modeling is probably a better alternative for future study due to its ability to accommodate complex boundaries, and could utilize information gathered by past aquifer tests (including this one) in attempting to delineate boundaries within the basin, identify the scale and placement of heterogeneities which are known to exist, and quantify recharge into the Grande Ronde. Any projects that use previously-collected water level and pumping data

to refine the hydrogeologic conceptual model of the Palouse Basin would be valuable as well as inexpensive.

The most important priorities for future work include extending the monitoring network with observation wells located in uncharacterized areas, and analyzing data which have already been collected. Hydrologic data, specifically groundwater elevations and seasonal and long term water level trends, must be obtained for the area between Pullman and Colfax. The areas north and west of Palouse are also not characterized. Hypotheses about aquifer boundaries to the west and north need to be validated or refuted by high-quality observation well data.

In addition to any new initiatives, the existing observation well network and HOBO® on/off pump monitoring devices should be maintained in order to continue to evaluate annual responses across the basin; characterizing annual water level declines is likely to yield more important information for future groundwater management in the basin than any other focus area.

## References

- Barker, R.A. 1979. Computer simulation and hydrogeology of a basalt aquifer system in the Pullman-Moscow Basin, Washington and Idaho. Washington DOE, Water Supply Bulletin No. 48.
- Brown, W.G. 1976. Well construction and stratigraphic information: Pullman test and observation well, Pullman, Washington. 76/15-6, Washington State University: Pullman, WA.
- Bush, J.H., D.L. Garwood, W.L. Oakley, and T.W. Erdwam. 2001. Geologic report, Pullman city well no. seven, report for the city of Pullman. Latah Institute of Geologic Studies: Moscow, ID.
- Bush, J.H., and D.L. Garwood. 2004. Geologic cross-section, Moscow-Pullman, Idaho-Washington.
- Bush, J.H. 2005. The Columbia River basalt group of the Palouse Basin with hydrological interpretations, western Latah County, Idaho, and eastern Whitman County, Washington.
- Bush, J.H. 2006. Geologic report on Moscow monitoring wells.
- Bush, J.H., and D.L. Garwood. 2006. Bedrock geologic map of the Pullman 7<sup>1/2</sup> minute quadrangle, Whitman County, Washington.
- Butler, J.J. 2008. Pumping tests for aquifer evaluation- time for a change? Ground Water, 47:615-617.
- Butler, J.J., and M. Tsou. 2003. Pumping-induced leakage in a bounded aquifer: An example of a scale-invariant phenomenon. Water Resources Research, 39: TNN 2-1:2-8.
- Clark, W.E. 1967. Computing the barometric efficiency of a well. Journal of the Hydraulics Division Proceedings of the American Society of Civil Engineers, 93(HY 4): 93-98.
- Crosby III, J.W., and R.M. Chatters. 1965. Water dating techniques as applied to the Pullman-Moscow ground-water basin. Washington State University, College of Engineering Research Division, Bulletin 296: Pullman, WA.
- Davis, S.N. 1969. Porosity and permeability of natural materials, pp. 53-89 in Flow Through Porous Media, ed. De Weist R.J.M. Academic Press: New York, NY.

Domenico, P.A., and F.W Schwartz. 1990. Physical and Chemical Hydrogeology. John Wiley and Sons; New York, NY.

Douglas, A.A. 2004. Radiocarbon dating as a tool for hydrogeological investigations in the Palouse Basin. MS thesis, University of Idaho: Moscow, ID.

Fairley, J.P., M.D. Solomon, J.J Hinds, G.W. Grader, J.H. Bush, and A.L. Rand. 2006. Latah County hydrologic characterization project, final report. Idaho Department of Water Resources: Boise, ID.

Fiedler, A. 2009. Well interference effects in the Grande Ronde aquifer system in the Moscow-Pullman area of Idaho and Washington. MS Thesis, University of Idaho: Moscow, ID.

Fiedler, F. 2011. Personal communication. Moscow, ID.

Freeze, R.A., and J.A. Cherry. 1979. Groundwater. Prentice-Hall, Inc: Englewood Cliffs, New Jersey.

Golder Associates, Inc. 2001. Pullman well no. 7 drilling and testing results. City of Pullman: Pullman, WA.

Golder Associates, Inc. 2008. Pullman well no. 8 drilling and testing results. City of Pullman: Pullman, WA.

Maurer, D., and K.J. Halford. 2006. Analysis of a multiple-well, aquifer test, Carson Valley, Nevada. USGS: Sacramento, CA.

Hantush, M.S., and C.E. Jacob. 1955. Non-steady radial flow in an infinite leaky aquifer. Transactions American Geophysical Union, 46: 95-100.

HOBO® U9 motor on/off data logger product manual. Onset Computer Corporation. Doc #9622-B, MAN-U9-004.

Holom, D. 2006. Ground water flow conditions related to the pre-basalt basement geometry delineated by gravity measurements near Kamiak Butte, Eastern Washington. MS Thesis, University of Idaho: Moscow, ID.

HydroSOLVE, Inc. 2007. AQTESOLV for Windows, v.4.5.

Jacob, C.E. 1940. On the flow of water in an elastic artesian aquifer. American Geophysical Union, 22:574-586.

Janczak, L.L. 2001. Relationships between spring discharge and aquifer water levels in the thousand springs region, Idaho. MS Thesis, University of Idaho: Moscow, Idaho.

Klein, D.P., R.A. Sneddon, and J.L. Smoot. 1987. Magnetotelluric study of the thickness of volcanic and sedimentary rock in the Pullman-Moscow Basin of eastern Washington. USGS Open-File Report, 87-140.

Larson, K.R. 2000. Water resource implications of 18O and 2H distributions in a basalt aquifer system. MS thesis, Washington State University: Pullman, WA.

La Sala, A.M., and G.C. Doty. 1971. Preliminary evaluation of hydrologic factors related to radioactive waste storage in basaltic rocks at the Hanford reservation, Washington. U.S. Atomic Energy Commission: Richland, WA.

Loo, W.W., R.C. Arnett, L.S. Leonhart, S.P. Luttrell, I.S. Wang, and W.R McSpadden. 1984. Effective porosities of basalt: a technical basis for values and probability distributions used in preliminary performance assessments. SD-BWI-TI-254, Rockwell Hanford Operations: Richland, WA.

Lum, W.E.I., J.L. Smoot, and D.R. Ralston. 1990. Geohydrology and numerical analysis of ground-water flow in the Pullman-Moscow area, Washington and Idaho. USGS Water-Resources Investigation report 89-4103.

McVay, M. 2010. Personal Communication. Moscow, ID.

McVay, M. 2007. Grande Ronde aquifer characterization in the Palouse Basin. MS Hydrology Thesis, University of Idaho: Moscow, ID.

Owsley, D. 2003. Characterization of Grande Ronde aquifers in the Palouse Basin using large-scale aquifer tests. MS Hydrology thesis, University of Idaho: Moscow, ID.

Merritt, M.L. 2004. Estimating hydraulic properties of the floridan aquifer system by analysis of earth-tide, ocean-tide, and barometric effects, Collier and Hendry Counties, Florida. USGS Water-resources Investigations Report 03-4267.

Moench, A.F. 1984. Double-porosity models for a fissured groundwater reservoir with fracture skin. Water Resources Research, 20(7):831-846.

Neuman, S.P., and P.A. Witherspoon. 1969. Applicability of current theories of flow in leaky aquifers. Water Resources Research, 5(4):817-829.

Osiensky, J.L., R.E. Williams, B. Williams, and G. Johnson. 2000. Evaluation of drawdown curves derived from multiple well aquifer tests in heterogeneous environments. *Mine Water and the Environment*, 19(1):30-55.

Osiensky, J.L. 2011. Personal communication. Moscow, ID.

Palouse Basin Aquifer Committee. 2010. 2009 Palouse ground water basin water use report.

Price, M. 2009. Barometric water-level fluctuations and their measurement using vented and non-vented pressure transducers. *Quarterly Journal of Engineering Geology and Hydrogeology*, 42:245-250.

Ralston, D.R. 1987. Construction Report for the WSU No. 7 Production/Test Well. Washington State University, Pullman, WA

Ralston, D.R. 2000. Report of construction and testing of a new well for the city of Palouse, Washington. Ralston Hydrologic Services.

Rasmussen, T.C., and L.A. Crawford. 1997. Identifying and removing barometric pressure effects in confined and unconfined aquifers. *Ground Water*, 35:502-511.

Reidel, S.P., V.G. Johnson, F.A. Spane. 2003. Natural gas storage in basalt aquifers of the Columbia Basin: a guide to site characterization. Pacific Northwest National Lab: Hanford, WA.

Robischon, S. 2007. Utilizing barometric efficiency to estimate aquifer storativity in the Palouse Basin ground water system. Unpublished term paper submitted for HYDR 509, Quantitative Hydrology, taught by Johnson, G., University of Idaho.

Robischon, S. 2010. Personal communication. Moscow, ID.

Sanchez-Vila, X., P.M. Meier, and J. Carrera. 1999. Pumping tests in heterogeneous aquifers: an analytical study of what can be obtained from their interpretation using Jacob's method. *Water Resources Research*, 35(4): 943-952.

Schad, H., and G. Teutsh. 1994. Effects of the investigation scale on pumping test results in heterogeneous porous aquifers. *Journal of Hydrology*, 159: 61-77.

Smoot, J.L., and D.R. Ralston. 1987. Hydrogeology and mathematical model of ground-water flow in the Pullman-Moscow region, Washington and Idaho. Idaho Water Resources Research Institute.

- Sokol, D. 1966. Interpretation of short term water level fluctuations in the Moscow Basin, Latah County, Idaho. Pamphlet 137, Idaho Bureau of Mines and Geology; Moscow, ID.
- Solinst 3001 Levellogger Manual. 2010. Solinst Canada Ltd.: Georgetown, Ontario, Canada.
- Spane, F.A. 2002. Considering barometric pressure in groundwater flow investigations. *Water Resources Research*, 38(6): 1-18.
- TerraGraphics, Inc. 2011. Palouse Ground Water Basin framework project final Report. Palouse Basin Aquifer Committee, Moscow, ID.
- Toll, N.J. 2005. Barometric fluctuation removal in water level records and solutions to flow in aquifers during sinusoidal aquifer pumping tests. M.S. Thesis, University of Georgia, Athens, GA.
- Toll, N.J, and T.C Rasmussen. 2007. Removal of barometric pressure effects and earth tides from observed water levels. *Ground Water*, 45: 101-105.
- US DOE. 1986. Environmental assessment: reference repository location, Hanford site, Washington, Vol. 1. Office of Civilian Radioactive Waste Management; Washington, DC.
- Wen, J.C., C.M. Wu, T.C. Yeh, and C.M. Tseng. 2010. Estimation of effective aquifer hydraulic properties from an aquifer test with multi-well observations. *Hydrogeology Journal*, 18: 1143-1155.
- Wu, C.M., T.C. Yeh, J. Zhu, T.H. Lee, N.S. Hsu, C.H. Chen, and A.F. Sancho. 2005. Traditional analysis of aquifer tests: comparing apples to oranges? *Water Resources Research*, 41: W09402.

## **Appendix A**

### **Water Level Data**

Information on attached CD includes:

Well water level data

Manual water level measurements

## **Appendix B**

### **HOBO Data and Other Pumping Data**

Included on CD

## **Appendix C**

### **Well Location Data**

Included on CD

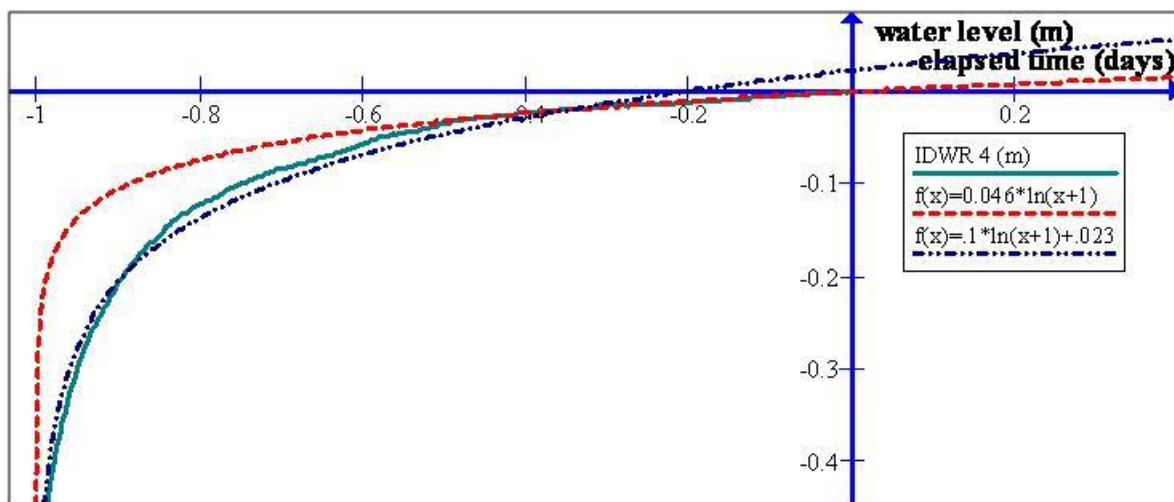
## Appendix D

### Recovery Trend Estimation and Removal

Logarithmic curves were generated from pre-test aquifer test water levels to account for the effects of pre-test pumping and approximate continued water level recovery for the period of the aquifer test. These curves were fit individually for each well based on the water levels measured during the 24-hour pumping shutdown preceding the start of the aquifer test, as described in section 4.2.

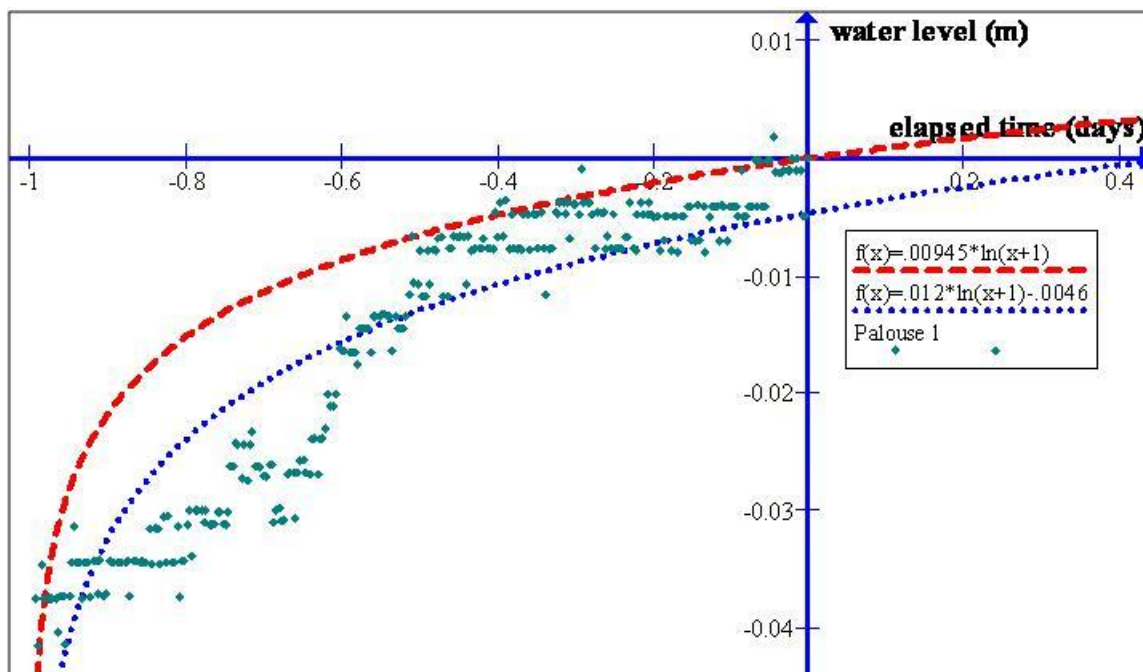
#### IDWR 4

The logarithmic function fit to the IDWR 4 pre-test data and used for water level adjustment is  $f(x)=0.046*\ln(t+1)$ , for units of meters and days (t). The best-fit logarithmic curve to the pre-test data is  $f(x)=0.10*\ln(t+1)$ ; this function was replaced since it does not cross at the origin. The best-fit logarithmic functions were calculated by converting the water level data to semi-log data and calculating the line with the minimum sum-of-squares. The function  $f(x) 0.046*\ln(t+1)$  was the best-fit line to the pretest data from  $t=-0.5$  to  $t=0$ ; this function appeared to be a much better fit to late time data (slope change due to possible boundary effects) and resulted in a smaller adjustment to the original data. Adjusted water levels were calculated by subtracting the logarithmic function from the measured water levels; these values were multiplied by -1 to create drawdown.



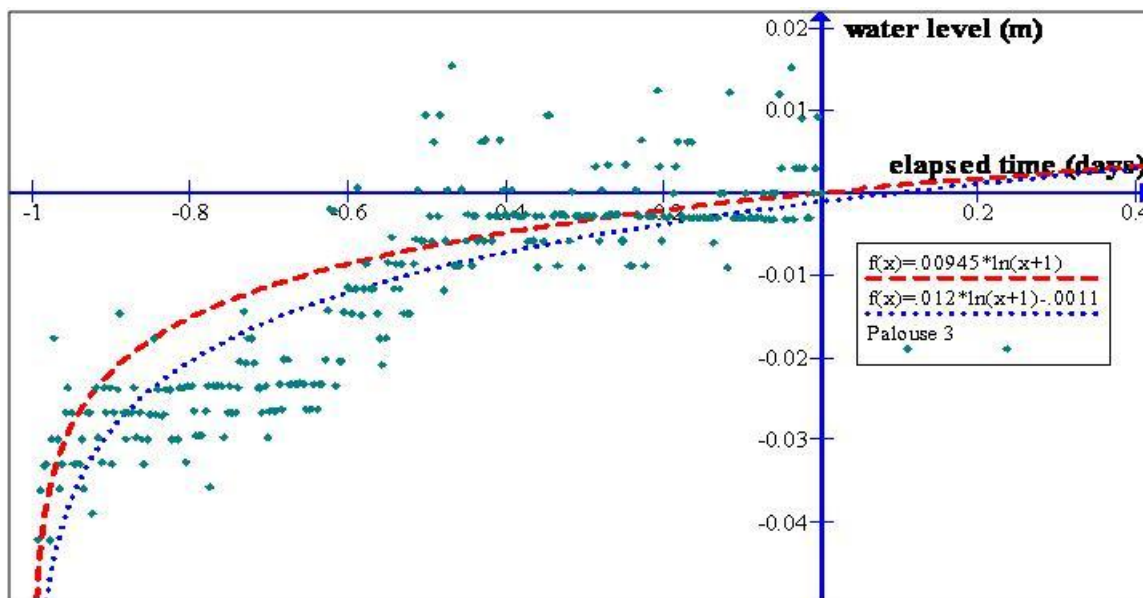
### Palouse 1

The logarithmic function fit to the Palouse 1 pre-test data and used for water level adjustment is  $f(x)=0.00945*\ln(t+1)$ , for units of meters and days (t). The best-fit logarithmic curve to the pre-test data is  $f(x)=0.012*\ln(t+1)-0.0046$ ; this function was modified since it does not cross at the origin. Adjusted water levels were calculated by subtracting the logarithmic function from the measured water levels; these values were multiplied by -1 to create drawdown.



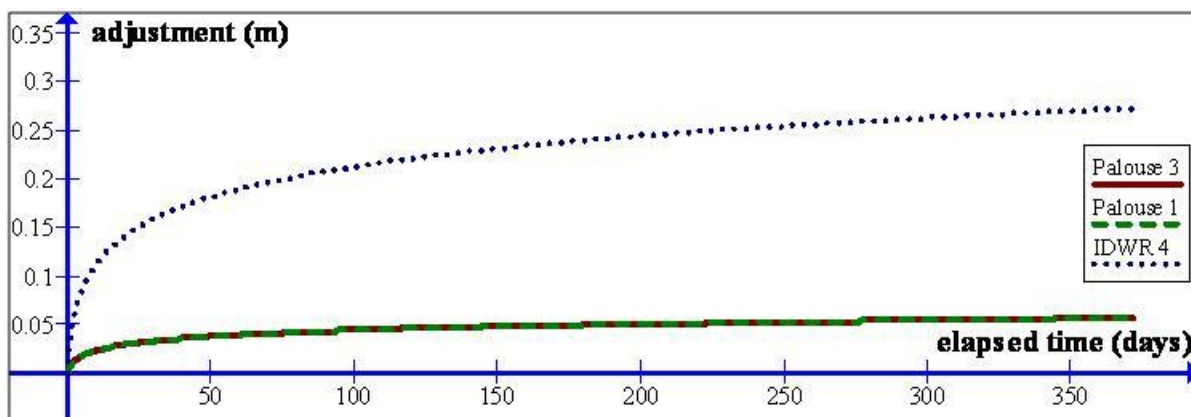
### Palouse 3

The logarithmic function fit to the Palouse 3 pre-test data and used for water level adjustment is  $f(x)=0.00945*\ln(t+1)$ , for units of meters and days (t). The best-fit logarithmic curve to the pre-test data is  $f(x)=0.012*\ln(t+1)-0.0011$ ; this function was modified since it does not cross at the origin. Adjusted water levels were calculated by subtracting the logarithmic function from the measured water levels; these values were multiplied by -1 to create drawdown.

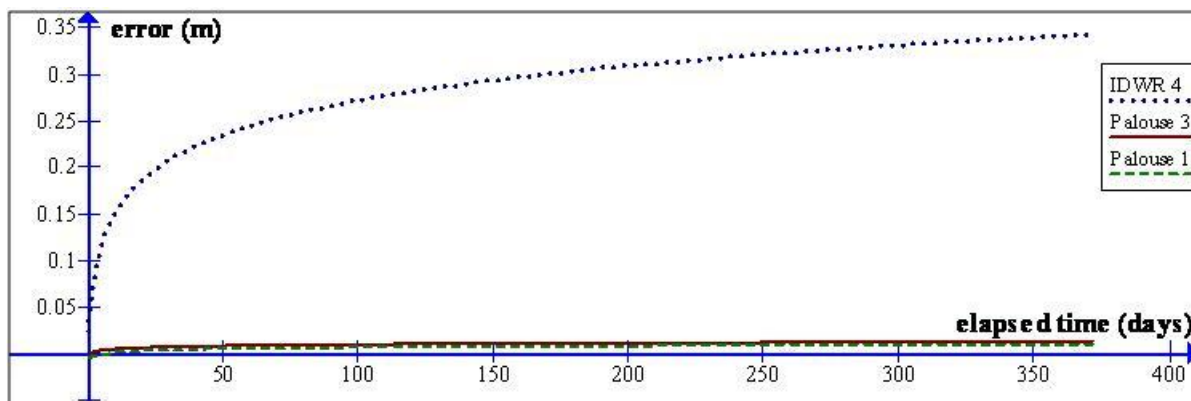


### Comparison of selected logarithmic functions to “best-fit” logarithmic functions.

The logarithmic functions used to approximate water level recovery and to adjust the water level data are shown in the plot below.



The logarithmic functions used to adjust water level data for each of the three wells are not equal to the best-fit logarithmic functions for water level data from  $t=-1$  to  $t=0$ , as discussed above. The differences between the best-fit functions and the logarithmic functions used for the data adjustment are shown below (the best-fit values minus the logarithmic curve used for correction).



## Appendix E

### AQTESOLV Methods and Solution Description

The following description of the Hantush-Jacob (1955) aquifer test solution and information on the procedure for automatic matching in AQTESOLV are taken directly from the help files included within the software (HydroSOLVE, Inc. 2007. AQTESOLV for Windows, v.4.5.).

### **Hantush-Jacob (1955)/Hantush (1964) Solution for a Pumping Test in a Leaky Aquifer**

Hantush and Jacob (1955) derived a solution for unsteady flow to a fully penetrating well in a homogeneous, isotropic leaky confined aquifer. The solution assumes a line source for the pumped well and therefore neglects wellbore storage.

Hantush (1964) extended the method to correct for partially penetrating wells and anisotropy. When you choose the Hantush-Jacob solution in AQTESOLV, you may analyze data for fully or partially penetrating wells.

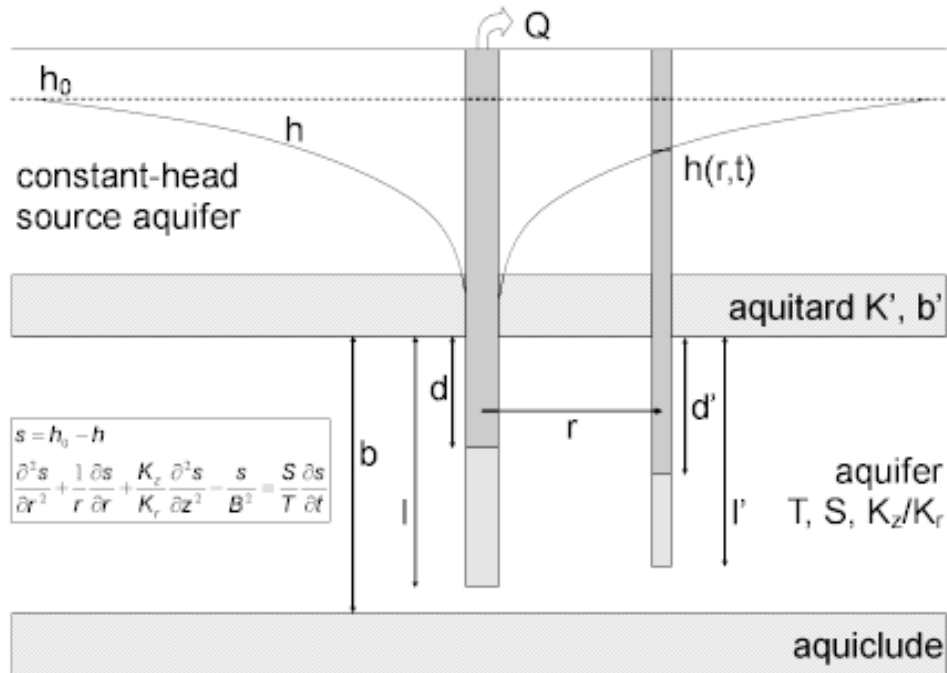
The Hantush-Jacob solution can simulate variable-rate tests including recovery through the application of the principle of superposition in time. Use this solution to analyze both pumping and recovery data from constant- or variable-rate pumping tests.

Walton (1962) developed a manual curve-fitting procedure based on the Hantush-Jacob solution. To apply Walton's method in AQTESOLV, choose the Hantush-Jacob solution. For a well performance test, you may choose the Hantush-Jacob (1955) solution for a step-drawdown test in a leaky confined aquifer.

Vandenberg (1977) presented a solution for evaluating drawdown a leaky confined aquifer bounded by two parallel no-flow boundaries (i.e., a leaky strip aquifer). In AQTESOLV, you may use the Hantush-Jacob solution in conjunction with aquifer boundaries to evaluate the same leaky strip aquifer problem as the Vandenberg method. Unlike Vandenberg's method, however, you may use AQTESOLV to evaluate partially

penetrating wells and observation wells may be located at any radial distance from the pumped well.

○ Illustration



○ Equations

Hantush and Jacob (1955) derived an analytical solution for predicting water-level changes in response to pumping in a homogeneous, isotropic leaky confined aquifer assuming steady flow (no storage) in the aquitard(s):

$$s = \frac{Q}{4\pi T} \int_u^{\infty} e^{-y-r^2/4B^2y} \frac{dy}{y}$$

$$u = \frac{r^2 S}{4Tt}$$

$$B = \sqrt{\frac{Tb'}{K'}}$$

$$s_D = \frac{4\pi T}{Q} s$$

$$t_D = \frac{Tt}{r^2 S}$$

where

- $b'$  is aquitard thickness [L]
- $K'$  is vertical hydraulic conductivity in the aquitard [L/T]
- $Q$  is pumping rate [L<sup>3</sup>/T]
- $r$  is radial distance [L]
- $s$  is drawdown [L]
- $S$  is storativity [dimensionless]
- $t$  is time [T]
- $T$  is transmissivity [L<sup>2</sup>/T]

Hydrogeologists commonly refer to the integral expression in the drawdown equation as the Hantush well function for leaky aquifers, abbreviated as  $w(u,r/B)$ . Therefore, we can write the Hantush drawdown equation in compact notation as follows:

$$s = \frac{Q}{4\pi T} w(u, r/B)$$

Hantush (1964) derived equations for the effects of partial penetration and anisotropy in a leaky aquifer. The partial penetration correction for a piezometer is as follows:

$$s = \frac{Q}{4\pi T} \left( w(u, r/B) + \frac{2b}{\pi(l-d)} \sum_{n=1}^{\infty} \frac{1}{n} \left[ \sin\left(\frac{n\pi l}{b}\right) - \sin\left(\frac{n\pi d}{b}\right) \right] \cdot \cos\left(\frac{n\pi z}{b}\right) \cdot w\left(u, \sqrt{\left(\frac{r}{B}\right)^2 + \frac{K_z}{K_r} \left(\frac{n\pi}{b}\right)^2}\right) \right)$$

For an observation well, the following partial penetration correction applies:

$$s = \frac{Q}{4\pi T} \left( w(u, r/B) + \frac{2b^2}{\pi^2(l-d)(l'-d')} \sum_{n=1}^{\infty} \frac{1}{n^2} \left[ \sin\left(\frac{n\pi l}{b}\right) - \sin\left(\frac{n\pi d}{b}\right) \right] \cdot \left[ \sin\left(\frac{n\pi l'}{b}\right) - \sin\left(\frac{n\pi d'}{b}\right) \right] \cdot w\left(u, \sqrt{\left(\frac{r}{B}\right)^2 + \frac{K_z}{K_r} \left(\frac{n\pi}{b}\right)^2}\right) \right)$$

where

- $b$  is aquifer thickness [L]
- $d$  is depth to top of pumping well screen [L]
- $d'$  is depth to top of observation well screen [L]
- $l$  is depth to bottom of pumping well screen [L]
- $l'$  is depth to bottom of observation well screen [L]
- $K_r$  is radial hydraulic conductivity [L/T]
- $K_z$  is vertical hydraulic conductivity [L/T]
- $z$  is depth to piezometer opening [L]

At large distances, the effect of partial penetration becomes negligible when:

$$r > 1.5b / \sqrt{K_z / K_r}$$

○ Assumptions

- aquifer has infinite areal extent
- aquifer is homogeneous and of uniform thickness
- pumping well is fully or partially penetrating
- flow to pumping well is horizontal when pumping well is fully penetrating

- aquifer is leaky confined
  - flow is unsteady
  - water is released instantaneously from storage with decline of hydraulic head
  - diameter of pumping well is very small so that storage in the well can be neglected
  - confining bed(s) has infinite areal extent, uniform vertical hydraulic conductivity and uniform thickness
  - confining bed(s) is overlain or underlain by an infinite constant-head plane source
  - flow is vertical in the aquitard(s)
- Data Requirements
- pumping and observation well locations
  - pumping rate(s)
  - observation well measurements (time and displacement)
  - partial penetration depths (optional)
  - saturated thickness (for partially penetrating wells)
  - hydraulic conductivity anisotropy ratio (for partially penetrating wells)
- Solution Options
- constant or variable pumping rate including recovery
  - multiple pumping wells
  - multiple observation wells
  - partially penetrating wells
  - boundaries
- Estimated Parameters
- T (transmissivity)
  - S (storativity)
  - $r/B$  (leakage parameter)
  - $Kz/Kr$  (hydraulic conductivity anisotropy ratio)
  - b (saturated thickness)

Partially penetrating wells are required to estimate  $Kz/Kr$  and b.

The Report also shows aquitard properties ( $K'/b'$  and  $K'$ ) computed from the leakage parameter ( $r/B$ ).

- References
1. Hantush, M.S. and C.E. Jacob, 1955. Non-steady radial flow in an infinite leaky aquifer, Am. Geophys. Union Trans., vol. 36, pp. 95-100.
  2. Hantush, M.S., 1961a. Drawdown around a partially penetrating well, Jour. of the Hyd. Div., Proc. of the Am. Soc. of Civil Eng., vol. 87, no. HY4, pp. 83-98.
  3. Hantush, M.S., 1961b. Aquifer tests on partially penetrating wells, Jour. of the Hyd. Div., Proc. of the Am. Soc. of Civil Eng., vol. 87, no. HY5, pp. 171-194.
  4. Hantush, M.S., 1964. Hydraulics of wells, in: Advances in Hydrosience, V.T. Chow (editor), Academic Press, New York, pp. 281-442.

## How Automatic Curve Matching Works

AQTESOLV performs nonlinear weighted least-squares parameter estimation (automatic curve matching) using the Gauss-Newton linearization method. To improve the convergence of the method from poor initial guesses for the unknown parameters, AQTESOLV includes the Marquardt damping parameter (Marquardt 1963).

In the Gauss-Newton method of parameter estimation, the parameter corrections necessary to minimize the difference between observed and estimated values of the response variable can be expressed as a Taylor series expanded about the current estimated value as follows:

$$y_i = \hat{y}_i + \frac{\partial y}{\partial b} \Delta b + \frac{\partial^2 y}{2! \partial^2 b} (\Delta b)^2 + \frac{\partial^3 y}{3! \partial^3 b} (\Delta b)^3 \dots$$

where:

$y_i$  =  $i$ th observed value of response variable

$\hat{y}_i$  = estimate of  $y_i$

$\Delta b$  = parameter correction,  $\hat{b}^1 - \hat{b}^0$

$\hat{b}^1$  = updated estimate of unknown parameter

$\hat{b}^0$  = previous estimate of unknown parameter

The previous equation can be linearized by truncating the Taylor series after the first derivative as follows:

$$y_i \cong \hat{y}_i + \frac{\partial y}{\partial b} \Delta b$$

Thus, for  $p$  unknown parameters, the general linearized equation for computing parameter corrections is written as follows:

$$y_i \cong \hat{y}_i + \sum_{k=1}^p \frac{\partial y_i}{\partial b_k} \Delta b_k$$

The previous equation is written for each observed value of the response variable. The partial derivatives of the response variable with respect to the unknown parameters are known as **sensitivity coefficients**. When a parameter is insensitive, its sensitivity coefficients will approach zero. You can choose a method for calculating the sensitivity coefficients in the advanced options for automatic estimation.

The resulting system of linearized equations is solved iteratively until convergence is obtained. The objective function for this minimization problem is the residual sum squares (RSS) given by the following expression:

$$RSS = \sum_{i=1}^n (y_i - \hat{y}_i)^2$$

where n is the total number of observed values of the response variable. In matrix form, the Gauss-Newton method computes parameter correction as follows:

$$\Delta B = (X^T X)^{-1} X^T \Delta Y$$

where:

$\Delta B$  = p x 1 vector of parameter corrections  
 $X$  = n x p matrix of sensitivity coefficients  
 $X^T$  = p x n transpose of  $X$   
 $X^T X$  = p x p variance-covariance matrix  
 $\Delta Y$  = n x 1 vector of residuals ( $y_i - \hat{y}_i$ )

To improve the conditioning of the  $X^T X$  variance-covariance matrix, AQTESOLV adds the Marquardt damping parameter to the previous equation:

$$\Delta B = (X^T X + \lambda \cdot I)^{-1} X^T \Delta Y$$

where:

$\lambda$  = Marquardt correction factor  
 $I$  = identity matrix

AQTESOLV also uses scaling of the variance-covariance matrix to improve the conditioning of the procedure (Bard 1970).

A well-conditioned variance-covariance matrix has a small condition number. Large condition numbers can result from poor starting guesses and lead to slow convergence, or even divergence, of the iterative parameter updating procedure; in these situations, **singular value decomposition**, an advanced estimation option, can improve convergence of the procedure.

AQTESOLV adds the Marquardt damping parameter when parameter corrections computed by the Gauss-Newton method fail to reduce the RSS. Iterations performed with the

Marquardt damping parameter start with a sufficiently small value of lambda; larger values of lambda are applied until the RSS is reduced. As iterations continue and the objective function approaches a minimum, AQTESOLV reduces lambda for faster convergence. You can control the lambda updating method in the advanced options for automatic estimation. The parameter estimation algorithm terminates when user-defined convergence criteria are met.

Weighted least-squares estimation is accomplished as follows:

$$\Delta B = (X^T W X)^{-1} X^T W \Delta Y$$

where:

$W = n \times n$  nonsingular symmetric matrix of weights obtained from  $\omega^T \omega$

$\omega = n \times n$  diagonal matrix of weights

In this implementation of the weighted least-squares algorithm, a larger weight assigned to a measurement results in greater influence by that measurement in the parameter estimation procedure.

AQTESOLV determines variances of the estimated parameters as follows:

$$\text{Var}(\hat{b}) = (X^T \omega X)^{-1} \sigma_e^2$$

The standard errors of the estimated parameters are given by the square root of the main diagonal elements of the  $(X^T \omega X)^{-1} \sigma_e^2$  matrix.

Correlations between the individual parameters are determined from the following equation:

$$r_{ij} = \frac{\text{Cov}(\hat{b}_i, \hat{b}_j)}{\sqrt{\text{Var}(\hat{b}_i) \text{Var}(\hat{b}_j)}}$$

where the variance and covariance terms are components of  $(X^T \omega X)^{-1} \sigma_e^2$ .